AD-A170 641 MILITARY HYDROLOGY; REPORT 13: COMPARATIVE EVALUATION OF DAM-BREACH FLOOD..(U) ARMY ENGINEER WATERWAYS EXPERIMENT STATION VICKSBURG MS ENVIR.. R A WURBS

1/2

UNCLASSIFIED JUN 86 WES/MP/EL/79-6 F/G 13/2 NL

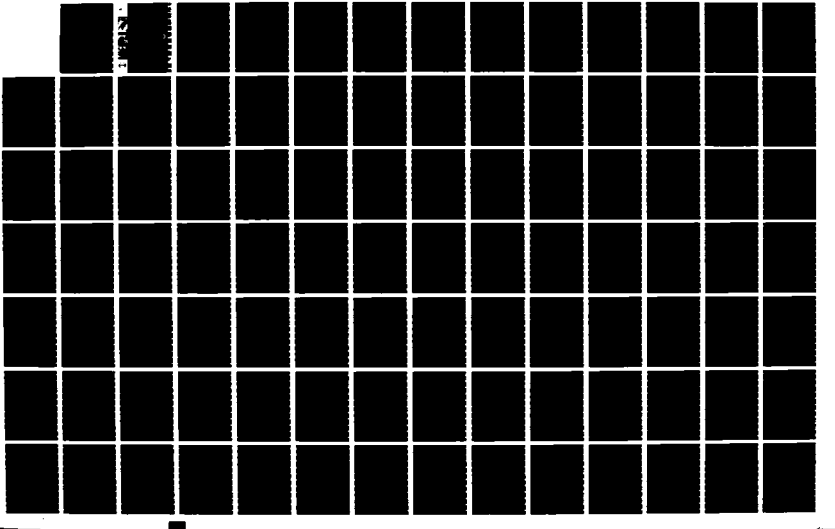

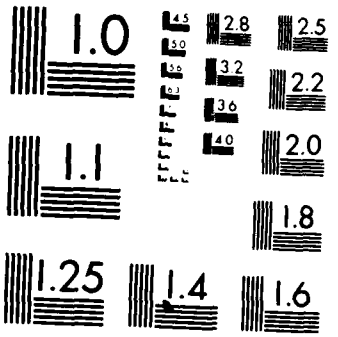

US Army Corps of Engineers

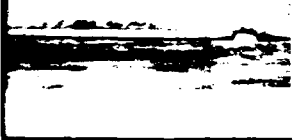

ENVIRONMENTAL LABORATORY

MISCELLANEOUS PAPER EL-79-6

(12)

MILITARY HYDROLOGY

Report 13

COMPARATIVE EVALUATION OF DAM-BREACH FLOOD FORECASTING METHODS

by

Ralph A. Wurbs

Environmental Laboratory

DEPARTMENT OF THE ARMY
Waterways Experiment Station, Corps of Engineers
PO Box 631, Vicksburg, Mississippi 39180-0631

June 1986

Report 13 of a Series

Prepared for DEPARTMENT OF THE ARMY
US Army Corps of Engineers
Washington, DC 20314-1000

Under DA Project No. 4A762719AT40
Task Area BO, Work Unit 052

MILITARY HYDROLOGY REPORTS

Report No.	No. in Series	Title	Date
TR EL-79-2	-	Proceedings of the Military Hydrology Workshop, 17-19 May 1978, Vicksburg, Mississippi	May 1979
MP EL-79-6 (Military Hydrology Series)	1	Status and Research Requirements	Dec 1979
	2	Formulation of a Long-Range Concept for Streamflow Prediction Capability	Jul 1980
	3	A Review of Army Doctrine on Military Hydrology	Jun 1981
	4	Evaluation of an Automated Water Data Base for Support to the Rapid Deployment Joint Task Force (RDJTF)	Nov 1981
	5	A Quantitative Summary of Groundwater Yield, Depth, and Quality Data for Selected Mideast Areas (U)	Mar 1982
	6	Assessment of Two Currently "Fieldable" Geophysical Methods for Military Ground-Water Detection	Oct 1984
	7	A Statistical Summary of Ground-Water Yield, Depth, and Quality Data for Selected Areas in the CENTCOM Theatre of Operations (U)	Oct 1984
	8	Feasibility of Using Satellite and Radar Data in Hydrologic Forecasting	Sep 1985
	9	State-of-the-Art Review and Annotated Bibliography of Dam-Breach Flood Forecasting	Feb 1985
	10	Assessment and Field Examples of Continuous Wave Electromagnetic Surveying for Ground Water	Jun 1986
	11	Identification of Ground-Water Resources in Arid Environments Using Remote Sensing Imagery	
	12	Case Study Evaluation of Alternative Dam-Breach Flood Wave Models	
	13	Comparative Evaluation of Dam-Breach Flood Forecasting Methods	Jun 1986
Unnumbered		Proceedings of the Ground-Water Detection Workshop, 12-14 January 1982, Vicksburg, Mississippi	Dec 1984

Destroy this report when no longer needed. Do not return it to the originator.

The findings in this report are not to be construed as an official Department of the Army position unless so designated by other authorized documents.

The contents of this report are not to be used for advertising, publication, or promotional purposes. Citation of trade names does not constitute an official endorsement or approval of the use of such commercial products.

Unclassified

SECURITY CLASSIFICATION OF THIS PAGE (When Data Entered)

REPORT DOCUMENTATION PAGE		READ INSTRUCTIONS BEFORE COMPLETING FORM
1. REPORT NUMBER Miscellaneous Paper EL-79-6	2. GOVT ACCESSION NO.	3. RECIPIENT'S CATALOG NUMBER
4. TITLE (and Subtitle) MILITARY HYDROLOGY; Report 13: COMPARATIVE EVALUATION OF DAM-BREACH FLOOD FORECASTING METHODS		5. TYPE OF REPORT & PERIOD COVERED Report 13 of a series 6. PERFORMING ORG. REPORT NUMBER
7. AUTHOR(s) Ralph A. Wurbs		8. CONTRACT OR GRANT NUMBER(s)
9. PERFORMING ORGANIZATION NAME AND ADDRESS US Army Engineer Waterways Experiment Station Environmental Laboratory PO Box 631, Vicksburg, Mississippi 39180-0631		10. PROGRAM ELEMENT, PROJECT, TASK AREA & WORK UNIT NUMBERS DA Project No. 4A762719AT40, Task Area BO, Work Unit 052
11. CONTROLLING OFFICE NAME AND ADDRESS DEPARTMENT OF THE ARMY US Army Corps of Engineers Washington, DC 20314-1000		12. REPORT DATE June 1986 13. NUMBER OF PAGES 117
14. MONITORING AGENCY NAME & ADDRESS(if different from Controlling Office)		15. SECURITY CLASS. (of this report) Unclassified 15a. DECLASSIFICATION/DOWNGRADING SCHEDULE

16. DISTRIBUTION STATEMENT (of this Report)

Approved for public release; distribution unlimited.

17. DISTRIBUTION STATEMENT (of the abstract entered in Block 20, if different from Report)

18. SUPPLEMENTARY NOTES

Available from National Technical Information Service, 5285 Port Royal Road, Springfield, Virginia 22161.

19. KEY WORDS (Continue on reverse side if necessary and identify by block number)

Dam breach
Flood routing
Military hydrology
Comparative evaluation

20. ABSTRACT (Continue on reverse side if necessary and identify by block number)

Several alternative dam-breach flood forecasting models are evaluated and compared based upon (a) consideration of the underlying concepts and theory incorporated into the models; (b) findings reported in the published and unpublished literature with respect to application, testing, evaluation, and comparison of various models; and (c) results obtained and experience gained in applying the models to several case study data sets. The objective is to

(Continued)

DD FORM 1 JAN 73 1473 EDITION OF 1 NOV 65 IS OBSOLETE

Unclassified

SECURITY CLASSIFICATION OF THIS PAGE (When Data Entered)

20. ABSTRACT (Continued).

provide an assessment of the state of the art of dam-breach flood forecasting which can serve as a basis for selecting and adapting specific models for military use.

The comparative evaluation focused on the following leading dam-breach flood wave models which are representative of the current state of the art: DAMBRK, FLOW SIM 1, FLOW SIM 2, HEC-1, SMPDBK, TR 66, and the HEC dimensionless graph procedure. A set of dam-breach flood forecasting methods developed during the 1950's and early 1960's were also reviewed, as was the recently developed Military Hydrology Model (MILHY). Although MILHY is a rainfall-runoff model with no special features for dam-breach modeling, a breach simulation routine could be added. DAMBRK and SMPDBK were determined to be the optimal models for military application.

PREFACE

The work reported herein was conducted under Department of the Army Project No. 4A762719AT40, "Mobility and Weapons Effects Technology," Task Area BO, "AirLand Battlefield Environment," Mission Area, "Combat Support," Work Unit 052, "Induced Floods as Linear/Area Obstacles." The study was sponsored by the Office, Chief of Engineers (OCE), US Army. MAJ Denton Brown was the OCE Technical Monitor.

The study was conducted by the US Army Engineer Waterways Experiment Station (WES) under the general supervision of Dr. John Harrison, Chief of the Environmental Laboratory, and Dr. L. E. Link, Chief of the Environmental Systems Division, and under the direct supervision of Mr. M. P. Keown, Chief of the Environmental Constraints Group (ECG), and Mr. J. C. Collins, ECG. Mr. M. R. Jourdan, ECG, Principal Investigator, Work Unit 052, provided technical assistance and review. This report was prepared by Dr. Ralph A. Wurbs, who is an Assistant Professor at Texas A&M University working under an Intergovernmental Personnel Act agreement as a Research Engineer, ECG. The Stillhouse case study and a portion of the Teton case study were performed by CPT David N. Buttery. At the time of the analyses, CPT Buttery was a graduate student at Texas A&M University under an Army educational assignment. The report was edited by Ms. Jessica S. Ruff of the WES Publications and Graphic Arts Division.

Director of WES was COL Allen F. Grum, USA. Technical Director was Dr. Robert W. Whalin.

This report should be cited as follows:

Wurbs, R. A. 1986. "Military Hydrology; Report 13: Comparative Evaluation of Dam-Breach Flood Forecasting Methods," Miscellaneous Paper EL-79-6, US Army Engineer Waterways Experiment Station, Vicksburg, Miss.

CONTENTS

CONVERSION FACTORS, NON-SI TO SI (METRIC)
UNITS OF MEASUREMENT

Non-SI units of measurement used in this report can be converted to SI (metric) units as follows:

Multiply	By	To Obtain
acres	4,046.873	square metres
acre-feet	1,233.489	cubic metres
cubic feet	0.02831685	cubic metres
feet	0.3048	metres
miles (US statute)	1.609347	kilometres
square miles	2.589998	square kilometres

MILITARY HYDROLOGY

COMPARATIVE EVALUATION OF DAM-BREACH FLOOD FORECASTING METHODS

PART I: INTRODUCTION

Background

1. Under the Meteorological/Environmental Plan for Action, Phase II, approved for implementation on 26 January 1983, the US Army Corps of Engineers (USACE) has been tasked to implement a Research, Development, Testing, and Evaluation program that will: (a) provide the Army with environmental effects information needed to operate in a realistic battlefield environment, and (b) provide the Army with the capability for near-real time environmental effects assessment on military materiel and operations in combat. In response to this tasking, the Directorate for Research and Development, USACE, initiated the AirLand Battlefield Environment (ALBE) Thrust program. This new initiative will develop the technologies to provide the field Army with the operational capability to perform and exploit battlefield effects assessments for tactical advantage.

2. Military hydrology, one facet of the ALBE Thrust, is a specialized field of study that deals with the effects of surface and subsurface water on planning and conducting military operations. In 1977, the Office, Chief of Engineers, approved a military hydrology research program. Management responsibility was subsequently assigned to the Environmental Laboratory, US Army Engineer Waterways Experiment Station (WES), Vicksburg, Miss.

3. The objective of military hydrology research is to develop an improved hydrologic capability for the Armed Forces with emphasis on applications in the tactical environment. To meet this overall objective, research is being conducted in four areas: (a) weather-hydrology interactions, (b) state of the ground, (c) streamflow, and (d) water supply.

4. Previously published Military Hydrology reports are listed inside the front cover. This report is the third which contributes to the streamflow modeling area. Streamflow modeling is oriented toward the development of procedures for rapidly forecasting streamflow parameters including discharge,

velocity, depth, width, and flooded area from natural and man-induced hydrologic events. Specific work efforts include: (a) the development of simple and objective streamflow forecasting procedures suitable for Army Terrain Team use, (b) the adaptation of procedures to automatic data processing equipment available to Terrain Teams, (c) the development of procedures for accessing and processing information included in digital terrain data bases, and (d) the development of streamflow analysis and display concepts.

Purpose and Scope

5. A major objective of the USACE Military Hydrology research is to provide the Armed Forces improved capabilities for forecasting the downstream flood flow impacts resulting from controlled or uncontrolled (dam-breach) releases from single or multiple dams. The objective of the study reported herein was to evaluate and compare available state-of-the-art dam-breach flood wave models to establish a basis for selecting and adapting models for military use.

6. This research was initiated with a comprehensive literature survey of dam-breach flood wave modeling supplemented by discussions with a number of model developers and users. This initial work was documented by Wurbs (1985a). Based on this state-of-the-art review, several models were selected for detailed study. The present investigation builds upon and extends the previous work through application of selected models using several case study data sets and further in-depth study of pertinent reference material. The models are evaluated and compared based on the experience gained through the case study applications and information available in the published and unpublished literature. The overall comparative evaluation, including a summary of the case study findings, is presented in this report. The quantitative results of the case study analyses have been documented in detail by Wurbs (1985b).

7. The case study analyses summarized in Part III of this report significantly contributed toward providing a basis for evaluating and comparing models. The case studies consisted of applying the models cited above to several data sets. Model accuracy was assessed by comparing model results with measured data and with results computed with alternative models. Experience

in dealing with modeling practicalities and difficulties was provided by the case studies.

8. The specific problem being addressed is that of predicting the flow characteristics of a flood wave resulting from the postulated breach of a dam. This problem can be divided into two modeling tasks: (a) computation of the reservoir outflow hydrograph for a given reservoir inflow hydrograph and set of breach characteristics (which involves breach simulation), and (b) computation of the discharges, velocities, and stages that occur at various locations and times as the flood wave moves through the downstream valley.

PART II: DAM-BREACH FLOOD FORECASTING MODELS

State-of-the-Art Models

9. Dam-breach flood wave analysis is a classic problem of unsteady open-channel flow which has been of theoretical interest to hydraulic engineers for well over a century. Military concerns provided a major impetus for the development of practical dam-breach flood forecasting capabilities, particularly during the 1940's and 1950's. An intensified public and governmental concern over dam safety has motivated a greatly increased civilian sector interest in dam-breach flood forecasting during the past decade. Recent dam safety programs being conducted by Federal and State water resources development agencies and the flash flood warning program of the National Weather Service demonstrated a critical need for greatly expanded dam-breach flood forecasting capabilities. Generalized mathematical models have been and continue to be developed to meet this need. Essentially all present state-of-the-art dam-breach flood wave models were developed within the last 10 years. These models provide major improvements over modeling capabilities of a decade ago. A number of significant revisions to the models have occurred within the last 3 or 4 years. The present Military Hydrology program effort in developing an improved dam-breach flood forecasting capability for the Armed Forces is very timely from the perspective of applying recent advances in the state of the art.

10. Numerous dam-breach flood wave models have been reported in the literature. Based on the comprehensive state-of-the-art review presented in Military Hydrology Report 9 (Wurbs 1985a), DAMBRK, FLOW SIM 1 and 2, HEC-1, SMPDBK, Dimensionless Graphs, and TR 66 were selected for in-depth study. These seven models are considered to be representative of the current state-of-the-art of dam-breach flood wave modeling. The models were developed within the last decade for civilian application and are readily available from Federal agencies in the United States. The comparative evaluation of dam-breach flood wave models presented in this report focuses on these seven leading state-of-the-art models.

11. The recently developed Military Hydrology model (MILHY) computes the streamflow hydrograph that would result from a given rainstorm over a watershed. Unlike the models cited above, MILHY has no special features for

dam-breach flood forecasting and has not been used for this purpose. However, with the addition of a breach simulation routine, MILHY could be used for dam-breach flood forecasting. The flood routing component of MILHY is also included in the comparative evaluation.

12. Military Hydrology Bulletins 9 and 10 (US Army Engineer District (USAED), Washington 1957a, 1957b) and the Defense Intelligence Agency (DIA 1963) outflow hydrograph computation procedure were developed during the 1950's and early 1960's for military use. These are the most recent models developed specifically for military dam-breach flood forecasting applications. These methods are outdated due to recent developments incorporated in more advanced models; however, they were considered to a limited extent in the present study.

Description of Selected Models

13. The models selected for inclusion in the case study analyses are briefly described below, and references providing detailed documentation are cited.

NWS Dam-Break Flood Forecasting Model (DAMBRK)

14. Computer program DAMBRK was developed by Dr. Danny L. Fread of the National Weather Service (NWS) Hydrologic Research Laboratory in Silver Spring, Md. An initial version of the model presented by Fread (1977) was subsequently expanded. The DAMBRK version A, dated 30 January 1982, was used in the case studies discussed later in this report. The most recent version is dated 18 July 1984. DAMBRK is described in detail by Fread (1984) and is discussed by a number of others, including Land (1980a), McMahon (1981), and Singh and Snorrason (1982). The US Army Engineer Hydrologic Engineering Center (HEC) is responsible for maintaining current versions of the program for use by CE personnel. The US Geological Survey (USGS) made minor modifications in DAMBRK to emphasize general-purpose applications and developed a user's manual for their version of the model (Land 1981). Several short courses on the use of DAMBRK have been sponsored by the NWS, HEC, and various universities.

15. DAMBRK simulates the failure of the dam, computes the resultant outflow hydrograph, and simulates the movement of the flood wave through the

downstream river valley. An inflow hydrograph is routed through a reservoir using either hydrologic storage routing or dynamic routing. The type of reservoir routing is a user option. Two types of breaching may be simulated. An overtopping failure is simulated as a rectangular-, triangular-, or trapezoidal-shaped opening that grows progressively downward from the dam crest with time. Flow through the breach at any instant is calculated using a broad-crested weir equation. A piping failure is simulated as a rectangular orifice that grows with time and can be centered at any specified elevation through the dam. Instantaneous flow through the breach is calculated with either orifice or weir equations, depending on the relation between the elevation of the water surface and the top of the orifice. Weir and orifice flows include corrections that account for tailwater submergence. The pool elevation at which breaching begins, the time required for breach formation, and the geometric parameters of the breach must be specified by the user.

16. The outflow hydrograph from the reservoir is routed downstream by a weighted four-point implicit nonlinear finite difference solution of the St. Venant equations. Variable time and distance steps are used. The Newton-Raphson method is used to solve the systems of equations generated by the procedure. Dynamic routing is the only method provided for propagating the wave through the downstream valley. The same dynamic routing algorithm is one of two options provided for reservoir routing. The input data for valley cross sections can specify inactive as well as active flow areas. The inactive portion of a cross section is intended to account for an area where water ponds and/or does not have a significant velocity component in the direction of flow. Inactive areas are considered in the continuity equation but not in the momentum equation.

17. A river can be treated as a single channel. Alternatively, the river can be represented by three components: left overbank, main channel, and right overbank. Flows are computed for each component separately and summarized to obtain the total flow. The water surface is still assumed horizontal perpendicular to the direction of flow.

18. The DAMBRK program can simulate the progression of a dam-break wave through a downstream valley containing one or more additional dams that may or may not fail. However, the multiple dams have to be in series. The model cannot simulate failure of dams on different tributaries. Downstream bridges are simulated in essentially the same way as a dam.

19. DAMBRK can accommodate supercritical flow either for the entire channel or for only an upstream portion of the channel. The supercritical flow regime is assumed to be applicable throughout the duration of the flow.

20. The Operational Dynamic Wave Model (DWOPER) was also developed by Dr. Fread of the NWS during the 1970's. The general-purpose unsteady flow computer program is described by Fread (1978) and is in operational service at the NWS river forecast centers. Computations are based on the same implicit finite difference solution of the St. Venant equations used in DAMBRK. DAMBRK is actually a specific-purpose dam-breach model that stemmed from the general-purpose DWOPER. DWOPER has wide applicability to rivers of varying physical features, such as irregular geometry, variable roughness parameters, lateral inflows, flow diversions, off-channel storage, local head losses such as bridge contractions-expansions, lock and dam operations, and wind effects. Unlike DAMBRK, DWOPER is suited for efficient application to dendritic (treelike) river systems or to channel networks consisting of bifurcations with weir-type flow into the bifurcated channel. An automatic calibration feature allows determination of the optimum roughness coefficients for either a single channel or a system of interacting channels. Data management programming features allow the model to be used in a day-to-day operational forecasting environment with minimal data coding required. The model is equally applicable for simulating unsteady flows for purposes of engineering planning and design.

21. DWOPER does not contain either the dam-breach simulation or hydrologic reservoir routing routines contained in DAMBRK. DAMBRK does not have the DWOPER capability to analyze dendritic river systems. DWOPER can be a useful supplement to DAMBRK in a multiple dam-breach situation in which the breached dams are located on different tributaries (in parallel) and backwater effects are not important. Each dam can be breached with separate runs of DAMBRK (or another dam-breach forecasting model). Hydrographs downstream of the breached dams can then be furnished as input to DWOPER. DWOPER routes the hydrographs through the tributary confluences and on downstream. However, this scheme does not allow backwater effects from the stream reaches analyzed by DWOPER to be transmitted to the reaches analyzed by DAMBRK, which could be a significant problem in some situations.

Flow Simulation Models (FLOW SIM 1 and 2)

22. The FLOW SIM 1 and 2 computer programs were developed by B. R. Bodine of the US Army Engineer Division, Southwestern, in Dallas, Tex. Several District offices of the Southwestern Division have been routinely using the models in their dam safety studies. A user's manual (Bodine, undated) provides instructions for using the programs. The computer programs are generalized models for simulating unsteady and spatially varied flow in rivers and for simulating dam failures. Both versions provide dynamic routing and use identical input data. The difference between the models is that FLOW SIM 1 uses an explicit solution scheme for solving the St. Venant equations and FLOW SIM 2 uses an implicit solution scheme. The December 1983 edition of both models was used in the case study analyses.

23. A user option provides for reservoir routing to be either hydrologic or dynamic. Two breach routines are provided. A breach routine similar to DAMBRK and HEC-1, in which break dimensions vary linearly with time, is provided. The other option is an erosion-type breaching technique in which the rate of growth of a trapezoidal-shaped breach is estimated using the Schoklitsch erosion formula. Dynamic routing is the only option for downstream valley routing. Inactive as well as active flow areas can be included in the cross-section data.

24. The models can account for bridges and other constrictions. Allowance is made for a dry stream to flood and dry up again after the passage of the flood. The models have no special provisions for supercritical flow. Multiple-tributary, branching stream systems can be simulated. Multiple dam failures can be simulated with the dams located on different tributaries as well as in series.

HEC Flood Hydrograph Package (HEC-1)

25. The widely used HEC-1 computer program was originally released by the Hydrologic Engineering Center in 1967. The program has been subsequently expanded and revised several times. A dam safety analysis capability was added to HEC-1 in 1978 for use in dam safety studies. A user's manual (HEC 1981) documents the current version of the model. HEC-1 was run on a mainframe computer for the case study analyses discussed in Part III of this report. However, the program has recently been coded to run on an IBM PC.

26. The HEC-1 flood hydrograph package models the precipitation-runoff process and routes flood hydrographs through channels and reservoirs. The package has economic flood damage analysis, flood control system optimization, and dam safety analysis capabilities. The dam safety analysis capability can be used to evaluate the overtopping potential of a dam and to analyze the flood wave that would result from an assumed structural failure of a dam. In regard to dam failure analysis, the model performs the following tasks: (a) development of an inflow hydrograph to the reservoir, (b) routing of the inflow hydrograph through the reservoir, (c) development of a failure hydrograph based on user-specified breach criteria and normal reservoir outflow, and (d) routing of the failure hydrograph to desired downstream locations. The results provide estimates of the peak discharge, time to peak, and maximum water surface elevation at each specified location.

27. The reservoir inflow hydrograph can be provided as input data or can be computed by the model from rainfall data using standard watershed modeling techniques. The hydrograph is routed through the reservoir using storage routing assuming a level water surface. HEC-1 contains a breach simulation methodology similar to that of DAMBRK and FLOW SIM 1 and 2 in which breach dimensions grow linearly with time, assuming an overtopping failure.

28. Channel routing options include Muskingum, modified Puls, working R&D, average-lag, and kinematic wave. Two options are provided for handling the storage versus outflow relationships used in modified Puls channel routing. The storage versus outflow relationships can be derived from water surface profile studies or other hydraulic analysis and supplied as input data to HEC-1. Alternatively, a cross section representative of a routing reach can be furnished as input data. Outflows and storages are computed by the model, assuming the representative cross section is constant throughout the reach and assuming uniform flow.

NWS Simplified Dam Breach
Flood Forecasting Model (SMPDBK)

29. Jonathan N. Wetmore and Dr. Fread of the Hydrologic Research Laboratory, NWS, developed the SMPDBK model for use in dam failure analyses when analytical time is limited or where mainframe computer facilities are unavailable to the user. The model was first presented by Wetmore and Fread (1981). Wetmore and Fread (1983) present a brief outline of the model's conceptual

basis, a step-by-step guide and examples of the computations involved in the model, and listings of FORTRAN and BASIC computer codes.

30. The objective in developing SMPDBK was to retain the critical aspects of the DAMBRK model while eliminating the need for large computer facilities. This is accomplished by assuming the downstream channel to be prismatic; neglecting the effects of off-channel storage; determining only the peak flows, stages, and travel times; neglecting the effects of backwater from downstream bridges and dams; and utilizing dimensionless peak-flow routing graphs developed using DAMBRK. The SMPDBK procedure entails three steps: (a) approximation of the channel downstream of the dam as a prismatic channel, (b) calculation of the peak outflow at the dam using the temporal and geometric description of the breach and the reservoir volume, and (c) calculation of dimensionless routing parameters used with dimensionless routing curves to determine the peak flow at specified cross sections downstream of the dam. The computations can be completed manually using graphs developed by Wetmore and Fread; also, several microcomputer versions are available.

Military Hydrology Model (MILHY)

31. The MILHY model was developed as a part of the Military Hydrology Research Program at the WES. The microcomputer program is documented in a user's manual (US Army Engineer WES 1985). MILHY was developed for use by Army Terrain Teams in forecasting streamflows that would result from a given rainfall event over a watershed. Rainfall can be input for a hypothetical storm or as measured data from precipitation gages or radar. The following methods are incorporated in the model: SCS curve number procedure for computing losses; two-parameter gamma function unit hydrograph; variable storage coefficient channel routing; modified Puls reservoir routing; and standard step water surface profile computations.

32. MILHY has no special features for dam-breach flood forecasting. However, a breach simulation routine could be added to the reservoir routing component of the model. The variable storage coefficient channel routing would be the same regardless of whether the hydrograph is generated by rainfall runoff or a breached dam.

HEC dimensionless graphs

33. Dimensionless graphs were developed by Dr. John G. Sakkas, Consulting Engineer, Davis, Calif., for the HEC. The graphs are documented in a 1974

report prepared by Dr. Sakkas, which was subsequently published as HEC Research Note No. 8 (Sakkas 1980).

34. A computational procedure based on the method of characteristics was used to solve the St. Venant equations. The graphs were developed for a dry prismatic channel assuming instantaneous, complete removal of the dam. Graphs were prepared for several of the parameters involved to cover a practical range of conditions.

35. The graphs can be used to estimate time of wave front arrival, maximum flood depth, and time of maximum flood depth at selected distances downstream of the dam. A procedure is provided for transforming irregular natural cross sections into one representative prismatic section of rectangular, triangular, or parabolic cross-sectional shape. Characteristics of the channel section and the water depth behind the dam are used to compute the parameters required to use the graphs.

Simplified Dam-
Breach Routing Procedure

36. Soil Conservation Service (SCS) Technical Release (TR) No. 66 (SCS 1979, revised December 1981) was developed by John A. Brevard and Fred D. Theurer of the Engineering Division in Glenn Dale, Md. The attenuation-kinematic routing model used to develop the routing graph incorporated into the procedure is described by Comer, Theurer, and Richardson (1982).

37. TR 66 is a simplified step-by-step manual computational procedure, based on graphs, for routing a dam-breach flood wave. Input data required to use the procedure consist of valley cross sections with depth versus discharge and depth versus area curves at each section, reservoir storage volume, and depth of water behind the dam. The procedure is used to compute peak discharges and associated stages of each valley section.

38. An instantaneous breach is assumed. A standard triangular or curvilinear breach hydrograph shape is assumed, depending on whether the flow in the channel reach immediately below the dam is supercritical or subcritical, respectively. The maximum discharge at the dam is determined from a curve of maximum discharge versus reservoir depth developed on the basis of information from actual dam failures. The downstream routing is a simplified version of the attenuation-kinematic model, which is a simultaneous storage routing-kinematic routing method. The model reflects attenuation due to

valley storage characteristics and the timing and distortion of the flood wave due to kinematic translation.

Military Hydrology Bulletins 9 and 10

39. The Military Hydrology Research and Development Branch of the USAED, Washington, investigated dam-breach flood forecasting methods during the 1950's. Several reports were prepared, including Military Hydrology Bulletins 9 and 10 (USACE 1957a, 1957b). Bulletin 9 outlines step-by-step graphical procedures for determining the outflow hydrograph from a breached dam using empirical weir and orifice formulas and hydrologic storage routing. Bulletin 10 presents similar procedures for determining the reservoir outflow hydrograph but also includes step-by-step procedures for downstream routing using the Muskingum method. These simplified methods were developed to permit rapid flood wave analysis with a degree of accuracy acceptable for military applications.

DIA outflow hydrograph computation method

40. A report published by the Defense Intelligence Agency (1963) updated Military Hydrology Bulletins 9 and 10 to better account for tailwater effects and a negative wave in the reservoir. The manual step-by-step procedure is designed for use by military engineers in expeditiously computing the outflow hydrograph from a breached dam. An instantaneous rectangular breach is assumed. Downstream routing is not included in the method.

Breach Simulation and Outflow Hydrograph Computation Methods

41. Analysis of the flood wave resulting from a dam breach involves two problems that can be considered jointly or separately: (a) determining the outflow hydrograph from the reservoir, and (b) routing the flood wave downstream through the river channel and floodplain. The reservoir outflow hydrograph may be influenced by tailwater conditions. Tailwater conditions are often neglected or estimated without considering downstream backwater effects. In this case, the outflow hydrograph determination and downstream routing can be handled separately as two distinct phases of the flood wave analysis. However, if downstream backwater effects are to be reflected in determining tailwater conditions, the flood wave analysis requires simultaneous interconnected reservoir and downstream routing.

42. The determination of the reservoir outflow hydrograph can be further divided into two tasks: (a) simulating the dam breach, and (b) routing the reservoir inflow and water stored in the reservoir through the breach and outlet structures.

Breach simulation

43. The outflow hydrograph from a dam breach is governed largely by the geometry of the breach and the development of the breach with time. Determination of breach characteristics is typically the aspect of dam-breach flood forecasting that involves the most uncertainty. The breach characteristics depend upon numerous factors, including the configuration and materials of the dam; reservoir depth, volume, and inflow; downstream tailwater conditions; and the situation or action that caused the dam failure. Breaches are of two main types: (a) surface openings with free-surface flow, such as overtopping failures, and (b) deep openings with flow under pressure, such as piping failures.

44. Different breach characteristics are generally associated with various types of dams. Earthen embankments have been involved in the largest number of failures. This is to be expected because earthen dams are the most common type, and earthen embankments are obviously more susceptible to erosion than concrete or masonry structures. Erosion of a breach through an earthen dam may be relatively slow at first, accelerating as flow velocities increase, and then decreasing again as the tailwater increases. Flow overtopping the embankment will probably first erode the downstream face of the dam, particularly near the dam toe where velocities are greatest. The breach will grow upstream from the dam toe, as well as downward from the top of the dam and laterally outward. The erosion may be gradual for periods of time and then accelerate, as portions of the embankment collapse into the breach. An entire embankment could fail, but most likely the breach will affect only a portion of the structure.

45. Concrete gravity dams are characteristically stable and may collapse only in the section that is overstressed. One or several monoliths may break away and be pushed downstream while the remainder of the dam remains in place. Slab and multiple-arch buttress dams may disintegrate as the buttresses fail in succession. Single-arch dams may collapse almost instantaneously and completely. A dam with water ponded behind a large release structure, such as a spillway with multiple tainter gates, could be effectively "breached" by destroying or simply opening the gates.

46. Since the reservoir outflow hydrograph characteristics are determined largely by breach characteristics, breach simulation is an important aspect of dam-breach flood forecasting. A dam-breach flood wave analysis model must include some mechanism for representing the flow of water from the breached dam. However, the models addressed herein do not have capabilities for predicting breach characteristics. Rather, the user must determine the breach characteristics independently of the model. The breach simulation mechanism provided in the model allows the user to represent the breach through input data furnished to the model. Predicting the response of a dam to a detrimental action or event is a complex problem involving geotechnical, structural, hydraulic and, in military applications, weapons effects considerations.

47. The breach simulation methods listed below are incorporated in the previously described selected models as well as in the other models reported in the literature.

a. Assume an instantaneous, complete removal of the dam.

b. Assume an instantaneous, partial breach of the dam.

c. Assume a breach of a fixed shape initiates when the reservoir water surface reaches a given elevation and then breach dimensions grow linearly with time.

d. Predict the growth of a breach through an earthen embankment using an erosion model.

e. Relate outflow hydrograph characteristics to data from past dam failures.

48. In order to simplify the analysis, early attempts to predict downstream flooding due to dam failure were usually based on the assumption of complete instantaneous removal of the dam. The HEC dimensionless graph procedure uses this approach. The DIA outflow hydrograph computation procedure and Military Hydrology Bulletins 9 and 10 are based on the other common approach of assuming the instantaneous removal of a portion of the dam. Complete instantaneous failure is conservative in the sense of simulating the worst possible downstream flooding conditions, but in most cases is unrealistic. Observations of past dam failures have indicated that earthen dams do not fail instantaneously or completely. Failure of a concrete arch dam is the case for which the assumption of complete, instantaneous removal is most likely to approximate reality. An assumption of instantaneous, partial breach might be most appropriate for a concrete gravity dam.

49. DAMBRK, FLOW SIM 1 and 2, and HEC-1 include similar breach simulation routines in which the breach begins at the top of dam and grows uniformly downward and outward. A breach of a fixed shape is initiated when the reservoir water surface reaches a given elevation, and then breach dimensions grow linearly with time. The user must input the water surface elevation at which failure begins and the breach formation time. A trapezoidal-, rectangular-, or triangular-shaped breach is specified by inputting the breach side slopes and terminal breach bottom width and elevation. DAMBRK also has an additional similar option for simulating a piping failure. A rectangular breach grows outward from a point linearly over the time to failure. The elevation of the center of the breach must be specified by the user.

50. With this approach, the model does not provide assistance to the user in determining the breach characteristics which would result from a detrimental action or event. However, this type of breach simulation routine provides a generalized, easy-to-use computational framework consistent with present capabilities for estimating breach parameters. This is the most flexible of the alternative breach simulation approaches. However, the basic simplifying assumptions are not necessarily realistic, particularly the assumptions of linear growth of the breach dimensions and a horizontal breach bottom profile along the direction of flow.

51. The process of erosion of a breach in an earthen embankment can be modeled using empirical sediment transport algorithms. The rate of erosion depends upon the embankment materials and the characteristics of flow as it occurs through the open . The FLOW SIM 1 and 2 models contain an optional routine in which the rate of growth of a trapezoidal-shaped breach is computed using the Schoklitsch bed load formula.

52. Fread (1985) developed the model BREACH, which considers the following complexities: (a) core material having properties which differ from those of the downstream face of the dam, (b) the necessity of forming an eroded ditch along the downstream face of the dam prior to the actual breach formation by the overtopping water, (c) enlargement of the breach through the mechanism of one or more sudden structural collapses due to the hydrostatic pressure force exceeding the resisting shear and cohesive forces, (d) enlargement of the breach width by slope stability theory, and (e) initiation of the breach via piping with subsequent progression to a free surface breach flow.

The Meyer-Peter and Muller and the duBoys sediment transport equations are used to predict the erosion capacity of the breach flow.

53. The SCS TR 66 provides the following relation:

$$Q_{max} = 65H^{1.85}$$

where Q_{max} is the maximum discharge in cubic feet per second and H, in feet, is the height of the dam if overtopped or the depth of water at time of failure if the dam is not overtopped. This relation was developed from data from actual past dam failures. Similar equations are presented by the Bureau of Reclamation (1983). The TR 66 procedure assumes an instantaneous breach with the maximum discharge occurring at time zero. The procedure computes only peak discharges, not the entire hydrograph. Since military applications will involve intentionally caused dam breaches significantly different from the actual past dam failures used to develop the above relationship, the usefulness of this method for military purposes is limited. However the TR 66 technique for computing the peak breach outflow is independent of the remainder of the computations. Therefore, the TR 66 valley routing can be performed with a peak breach discharge determined by another method.

Outflow hydrograph computation

54. The sudden removal of a part of a dam changes the pressure in the water body surrounding the opening and causes the water to accelerate. For sudden releases, a distinct, steep negative wave may propagate upstream through the reservoir. The magnitude and celerity of the negative wave depend upon the breach size, shape, and position; the reservoir characteristics; and the flow through the reservoir before the breach. The outflow hydrograph may or may not be affected by a negative wave in the reservoir. For purposes of flood wave analysis, breach outflow hydrographs can be categorized as being associated with small, medium, or large breach openings, depending on whether the outflow is affected by a negative wave in the reservoir and tailwater conditions below the dam (DIA 1963, Yevjevich 1975). By definition, the outflow hydrograph through a small breach is not affected by either a negative wave or tailwater. The outflow through a medium breach is not affected by tailwater but is affected by a negative wave. A large breach involves both negative wave and tailwater effects. The complexity of analysis procedures depends

upon whether and in what way the effects of negative waves and tailwater are handled.

55. Discharges through spillway and outlet works structures and dam breaches are typically computed as a function of reservoir water surface elevation using empirical weir and orifice equations. These equations may include corrections for tailwater effects. Weir and orifice equations are widely used in other hydraulic engineering applications and are described in hydraulics textbooks and various manuals. The discharge versus water-surface elevation relationships developed using weir and orifice equations are used in reservoir routing.

56. Reservoir routing is typically accomplished by either hydrologic storage or dynamic routing methods. Hydrologic reservoir routing is based on an assumed level water surface. The reservoir geometry is described by a storage versus elevation relationship. Hydrologic routing is applicable for wide, flat reservoirs with gradual changes in water surface levels. Dynamic routing methods are most advantageous for long, narrow reservoirs with rapid water-level changes at the breached dam. Dynamic routing handles the negative waves that may be caused by sudden reservoir drawdowns and positive waves produced by large reservoir inflows. Water surface profiles through and upstream of a reservoir can be developed as well as the outflow hydrograph. In dynamic routing, the reservoir geometry is described by cross sections and Manning roughness coefficients, as is the downstream valley. Hydrologic reservoir routing is generally easier to use than dynamic routing and, in many typical situations for which the basic assumptions are valid, is about as accurate. Dynamic routing is more accurate when the slope of the reservoir water surface is significant. Continued use of both methods in dam-breach flood forecasting can be expected.

Flood-Routing Methods

57. Flood routing entails mathematically predicting the changing magnitude (discharge and/or stage) and celerity of a flood wave propagating through a river system as a function of time and location. Techniques used for modeling dam-breach flood waves are essentially the same as for precipitation runoff flood waves. However, the dam-breach flood wave does have certain distinctive characteristics that complicate modeling. The dam-breach flood is

usually many times larger than the precipitation runoff flood of record. Consequently, measured discharge and stage data are generally not available for model calibration. The dam-breach flood has a very short time base, particularly from the beginning of rise to the peak. The rapidly occurring, large magnitude peak discharge results in the dam-breach flood wave having acceleration components of a far greater significance than those associated with a runoff-generated flood wave.

58. An overview of flood routing is presented here with a focus on those methods which have been incorporated into state-of-the-art dam-breach flood forecasting models. The flood-routing options contained in each of the previously described dam-breach models are listed in Table 1. The scheme for classifying flood-routing methods (shown after Table 1) provides an outline for the discussion that follows.

Table 1

Routing Methods Incorporated in Selected Dam-Breach Models

Dam-Breach Model	Routing Method	
	Reservoir Routing	Valley Routing
DAMBRK	Dynamic or modified Puls	Dynamic
FLOW SIM 1	Dynamic or modified Puls	Dynamic
FLOW SIM 2	Dynamic or modified Puls	Dynamic
SMPDBK	--	Generalized relationship
Dimensionless graphs	--	Generalized relationship
TR 66	--	Attenuation-kinematic
HEC-1	Modified Puls	Modified Puls or kinematic*
MILHY	Modified Puls	Variable storage coefficient
Bulletins 9 and 10	Modified Puls	Muskingum
DIA outflow hydrograph	Modified Puls	--

* HEC-1 also includes Muskingum, working R&D, and average lag valley routing options.

I. Two- and three-dimensional models

II. One-dimensional models

- A. Dynamic routing
- B. Generalized dimensionless relationships
- C. Simplified hydraulic routing methods
  1. Kinematic and diffusion wave models
  2. Linearization of the St. Venant equations
- D. Hydrologic storage routing
  1. Modified Puls and variations
  2. Muskingum and variations
  3. Variable storage coefficient
  4. Modified attenuation-kinematic routing
- E. Purely empirical methods

Two- and Three-Dimensional Models

59. The flow characteristics of a flood wave actually vary in three dimensions. Floodplain irregularities such as abrupt contractions and expansions in valley topography, tributaries, bridges, control structures, and overtopped levees cause accelerations with horizontal and vertical components perpendicular to the flow axis. Water may flow laterally outward from the river channel to fill overbank floodplain storage as the stage rises and then laterally back toward the channel as the stage falls. Significant three-dimensional accelerations can be expected near the dam in the case of a dam-breach flood wave.

60. Unsteady flow equations can be expressed in various forms which reflect components of flow in the three directions of a cartesian coordinate system. Two-dimensional flow modeling is much more common than three-dimensional modeling. The few fully three-dimensional models that now exist are in a developmental stage. In two-dimensional modeling, acceleration in the vertical direction is typically assumed to be negligible so that the equations can be written for flow components in the two horizontal directions. The state of the art of two-dimensional flow modeling has advanced considerably during the past decade due in part to advances in computer technology. However, the progress in two-dimensional flow modeling has been primarily in coastal and estuarine applications. Application of two-dimensional methods to flood routing in rivers and reservoirs has been much more limited. Military

Hydrology Report 9 cites a number of references which report the development and application of two-dimensional flood-routing models.

61. The current state of the art of dam-breach flood forecasting is one-dimensional modeling. Multidimensional modeling is much more complex and difficult to apply than one-dimensional modeling. The dam-breach flood forecasting models selected for the detailed case study analyses reported herein are all one-dimensional. Two-dimensional models that are competitive with one-dimensional models from the perspective of practical military application are not presently available. The availability of three-dimensional models is much more limited than two-dimensional models. The one-dimensional models are widely accepted as being accurate enough for practical applications. However, little, if any, work has been reported in regard to the significance of any improvements over one-dimensional models that could be achieved with multidimensional models in various dam-breach flood forecasting situations.

One-Dimensional Models

62. One-dimensional flow is a fundamental assumption of all the flood-routing methods discussed herein. Velocity variations are assumed to occur only in the one-dimensional direction of flow, with no vertical or lateral accelerations. The water surface is assumed level perpendicular to the direction of flow. The pressure distribution over any vertical section is assumed hydrostatic. Without vertical accelerations, changes in water-surface elevation occur over relatively large horizontal distances; thus, the flow is gradually varied. Computation of friction slope is based on the assumption that frictional resistance in unsteady flow is the same as in steady flow. Fluid density is assumed to be constant.

63. Past dam failures have demonstrated the tremendous amount of erosion and sediment transport capability of a dam-breach flood wave. The downstream valley geometry and roughness can be significantly changed by the flood wave. However, all the dam-breach flood wave models are based on the fundamental assumption of a fixed streambed without erosion or sedimentation.

64. One-dimensional flood-routing models can be categorized as (a) dynamic routing, (b) generalized dimensionless relationships, (c) simplified hydraulic routing methods, (d) hydrologic storage routing, and (e) purely empirical methods. The first three categories consist of hydraulic routing

methods based on the St. Venant equations, which are two partial differential equations expressing the physical laws of conservation of mass and conservation of momentum. Dynamic routing involves solution of the complete St. Venant equations. Numerous simplified hydraulic routing techniques have been developed based on neglecting certain terms or otherwise simplifying the St. Venant equations. Another approach for providing simplified routing capabilities has been to precompute generalized dimensionless curves using a dynamic routing model. Hydrologic routing methods are based upon the storage form of the continuity equation, which is an alternative way of expressing the concept of conservation of mass, and a relationship between storage and either outflow and/or inflow. The last category includes purely empirical methods, methods based strictly on intuition and observations of past floods.

Dynamic routing

65. A flood wave analysis model based on the complete St. Venant equations is called a dynamic wave (or dynamic routing) model. Dynamic routing is theoretically the most accurate of the numerous one-dimensional flood-routing methods. Dynamic routing is the only method that accounts for the acceleration effects of a flood wave and the backwater effects caused by channel constrictions, tributary inflows, dams, and bridges. Improvements in accuracy provided by dynamic routing over simpler hydraulic and hydrologic methods are most pronounced in situations where wave acceleration effects are significant compared to the effects of gravity and channel friction. Consequently, dynamic routing is particularly relevant to modeling dam-breach floods as compared to more gradually varied precipitation floods. Dynamic routing is also particularly advantageous for flat slopes where backwater effects are more pronounced. Steep slopes with supercritical flow can cause computational problems in dynamic routing solution schemes.

66. Unsteady flow equations. The basic theory for one-dimension gradually varied flow consists of two partial differential equations originally derived by Barre De Saint Venant in 1871. The St. Venant equations consist of a conservation of mass (continuity) equation:

$$\frac{\partial Q}{\partial x} + \frac{\partial Q}{\partial t} + q = 0$$

and a conservation of momentum (dynamic) equation:

$$\frac{\partial V}{\partial t} + V \frac{\partial V}{\partial x} + g \frac{\partial h}{\partial x} + gS_f + \frac{Vq}{A} = 0$$

where

Q = discharge

x = distance along the waterway

t = time

q = lateral outflow (lateral inflow negative) per unit length of waterway

V = mean velocity = Q/A

g = gravitational acceleration constant

h = water-surface elevation above a datum

S_f = friction slope

A = cross-sectional area

67. A number of references, including Chow (1959) and Cunge, Holley, and Verway (1980), contain derivations of the one-dimensional unsteady flow equations. The conservation of mass equation expresses the fundamental principle that inflow minus outflow equals change in storage over time. The conservation of momentum equation is derived from Newton's second law of motion, which states that the sum of all the external forces acting on a system of particles is equal to the time rate of change of linear momentum of the system. The terms in the conservation of momentum equation are expressions of local acceleration $\left(\frac{\partial V}{\partial t}\right)$, convective acceleration $\left(V \frac{\partial V}{\partial x}\right)$, pressure and gravity forces $\left(g \frac{\partial h}{\partial x}\right)$, frictional forces (gS_f), and acceleration of lateral inflow $\left(\frac{Vq}{A}\right)$. The last term is usually omitted, assuming the momentum of lateral inflows to be negligible.

68. The friction slope (S_f) is estimated using a steady-flow empirical formula such as the Chezy or Manning equation. The Manning equation is:

$$S_f = \frac{n^2 Q^2}{C A^2 R^{4/3}}$$

where

n = Manning roughness coefficient

C = constant (1.0 for SI (metric) units and 2.21 for non-SI units)

R = hydraulic radius

69. The St. Venant equations are found in the literature in a variety of equivalent forms. Some variations merely represent mathematical transformations or manipulations, while others result from assumptions made with regard to channel geometry or boundary resistance.

70. The St. Venant equations are a system of two simultaneous, first-order, nonlinear, hyperbolic partial differential equations involving functions of two dependent and two independent variables. The two dependent variables are: (a) the discharge Q or the average velocity V and (b) the water-surface elevation h or the depth of flow y. The independent variables are the distance x and time t. The equations are nonlinear because several coefficients of derivative terms involve the dependent variable V, and also because V appears to the second power in the expression for friction slope. However, these equations are sometimes called quasi-linear because no derivative occurs to a power higher than the first. The solution of hyperbolic equations, such as the St. Venant equations, is referred to mathematically as a propagation or initial-boundary-value problem. A general characteristic of this type problem is that the physical conditions imposed as initial and boundary values do not influence the complete solution instantaneously but are involved only as the solution proceeds through time and distance.

71. Numerical solution techniques. The St. Venant equations have no known general analytical solution. The equations have been solved analytically but only under very restrictive and simplifying conditions, with the solutions generally not acceptable for practical problems. However, during the last two decades, solution of the complete St. Venant equations has become practical using numerical methods and high-speed computers.

72. Numerical solution techniques convert the differential equations into algebraic difference equations that may be solved for Q (or V) and h (or y) at finite incremental values of x and t, given initial and boundary conditions. Various numerical techniques can be used, but all involve replacing the derivatives in the equations by finite difference approximations of some form. The differential equations are approximated with finite difference algebraic equations which are solved through a series of algebraic operations proceeding stepwise through time and distance.

In obtaining a numerical solution of the equations by finite-difference techniques, the domain of the independent variables x and t is replaced by a finite set of points called grid or mesh points. At each of these points, approximate values of the dependent variables Q and h (or V and y) are determined by the solution procedure. The pattern and spacing of the grid points vary with different solution procedures.

73. Explicit and implicit methods. Dynamic flood-routing methods can be classified as either explicit or implicit, depending on how the finite difference scheme is formulated. Explicit methods advance the solution point-by-point in an x-t grid from one time line to the next. After all the unknowns associated with one time line are evaluated, the procedure advances to the next time line. Two linear algebraic equations are generated at each grid point. Each equation gives one of the unknowns at an advanced point in terms of known quantities on the preceding time line, or lines. The known quantities are known from previous calculations or from initial and boundary conditions. The unknown is determined directly (explicitly) from the equation. A number of variations of explicit schemes have been developed, including the four-point, diffusing, leap-frog, Lax-Wendroff, and Dronkers methods, which are reviewed by Liggett and Cunge (1975) and Miller (1971).

74. Explicit models are generally much simpler than implicit models. However, due to numerical stability problems, explicit models have a restriction in the size of the time step used in the computations. For most explicit models, the restriction in Δt is given by the lesser of the following two inequalities (Fread 1982).

$$\Delta t \leq \frac{\Delta x}{V + \sqrt{g\ A/B}}$$

$$\Delta t \leq \frac{C_1\ R^{4/3}}{g\ n^2\ |V|}$$

where B is the water top width, C_1 is 1.0 in SI units and 2.21 in non-SI units, and the other terms are as previously defined. The first equation is known as the Courant condition and is derived for a frictionless flow. The

second equation is an added restriction when friction is considered.

75. Inspection of the Courant condition equation indicates that the computational time step is significantly reduced as the hydraulic depth (A/B) increases. In large rivers, time steps on the order of a few minutes or even seconds may be required even though the flood wave may be very gradual, having a duration in the order of weeks (Fread 1982). Such small time steps cause the explicit method to be very inefficient in the use of computer time.

76. Explicit schemes are usually based on equal distance (Δx) steps. Although this can be relaxed somewhat by using weighting factors, the requirement of equal distance steps can be very disadvantageous in modeling flows in natural waterways.

77. Implicit finite difference schemes advance the solution from one time line to the next simultaneously for all points. There are as many finite difference equations as unknowns, provided that boundary conditions are known at either end of the reach or two conditions are given at one end. The equations are solved simultaneously, such that the unknowns are determined implicitly (not independently). The system of algebraic equations generated may be either linear or nonlinear depending upon the type of implicit difference scheme used. Nonlinear simultaneous equations must be solved iteratively.

78. Implicit models were developed primarily because of the limitations on the size of the time step required for numerical stability of explicit models. Time steps are also restricted in size in implicit models for reasons of stability and accuracy, but the restrictions are less severe than for explicit models. Implicit models are generally much more stable than explicit models. Implicit solutions of linearized versions of the St. Venant equations are numerically stable, regardless of the size of the time and distance steps. However, implicit instability problems can occur with nonlinear models when modeling rapidly varying transients or very irregular channel geometry.

79. Implicit models require more extensive computations than explicit models. If the implicit scheme is linear, the system of equations is solved once at each step. Nonlinear implicit schemes require an iterative solution, which involves one or more solutions of the system of equations at each time step. The Newton-Raphson method is often used for solving the nonlinear system of equations generated by an implicit scheme. The double-sweep method developed in Europe and described by Liggett and Cunge (1975) is an efficient method for solving a linear system of equations. Fread (1971) describes a

compact quad-diagonal elimination method that makes use of the banded structure of the coefficient matrix of the system of equations generated by an implicit scheme.

80. Fread (1982), Liggett and Cunge (1975), and Miller (1971) review implicit models that have appeared in the literature and cite numerous research studies with implicit schemes that have been reported. Implicit schemes have generally been four-point, such that the conservation of mass and momentum equations are applied to the flow between two adjacent cross sections. Fread (1974) studied the numerical properties of implicit four-point finite difference schemes for solving the St. Venant equations. Price (1974) compared the four-point implicit method with two alternative explicit methods and with a characteristic method by comparing each to the exact analytical solution for a monoclinal wave.

81. The literature appears to support the conclusion that implicit models are the most efficient and versatile, although the most complex, of the models that solve the complete St. Venant equations and tend to be the optimum choice for flood-routing applications.

82. Method of characteristics. The St. Venant equations can be solved directly using explicit or implicit schemes, as discussed above. An alternative approach, called the method of characteristics, is based on transforming the two partial differential St. Venant equations into four ordinary differential equations, called the characteristic equations. The characteristic equations can be solved using various explicit and implicit schemes or other techniques. Since numerous techniques for solving the characteristic equations have been developed, the method of characteristics is actually a general group of solution methods. The characteristic equations are derived from and are equivalent to the St. Venant equations. Derivation of the four basic equations and detailed explanations of the overall concepts and specific solution techniques are presented by Abbott (1979), Chow (1959), and Miller (1971).

83. The characteristic equations are as follows:

$$\frac{dx}{dt} = V + c$$

$$d(v + 2c) = g(S_o - S_f)\, dt$$

$$\frac{dx}{dt} = V - c$$

$$d(V - 2c) = g(S_o - S_f)\, dt$$

where c is the wave celerity ($c = \sqrt{gy}$), S_o is the channel slope, and the other terms are as previously defined.

84. Models based on the method of characteristics can have either a curvilinear or rectangular distance-time grid. A curvilinear scheme is not practical for application in natural waterways of irregular geometry. Use of a rectangular characteristic grid, known as the Hartree method, requires interpolation formulas meshed within the finite difference solution procedure. Using the method of characteristics, it is nearly impossible to model irregular-shaped channels. These restrictions have tended to discourage the application of characteristic models for flood routing (Fread 1982).

85. Initial and boundary conditions. Initial conditions are required in the solution of hyperbolic partial differential equations, such as the St. Venant equations. For unsteady flow in a river, stage (or depth) and velocity (or discharge) must be known at the selected initial time at each distance interval throughout the length of the river. The initial (time zero) conditions may consist of: a steady-flow condition, which may be determined by backwater computations; a zero-flow condition, which would represent still water or a dry channel; or a condition of unsteady flow, which may be known from measurements or previous computations.

86. Boundary conditions must also be known. Boundary conditions usually take the form of a relationship between one of the dependent variables and time, such as depth versus time or discharge versus time, or between the two dependent variables, such as depth versus discharge. The geometric and resistance properties of the channel may also be considered boundary conditions. If the flow is subcritical, one condition is needed at the upstream boundary and one condition at the downstream boundary. Supercritical flow requires two conditions at the upstream boundary and no conditions at the downstream boundary. The proper specification of boundary conditions may change during the course of a solution in time if the flow changes from subcritical to supercritical or vice versa.

87. Accuracy and robustness. As previously indicated, analytical

(exact) solutions of the St. Venant equations are not possible unless the equations are first simplified in some way. Numerical techniques approximate the partial differential equations with finite difference algebraic equations. Numerical solutions of the complete equations usually correspond more closely to the real physical phenomena than analytical solutions of simplified equations. However, finite difference approximations involve inaccuracies. The validity of the results of a numerical model depends upon how well the:

a. Differential equations represent the physical phenomena.

b. Parameters provided as input data to the model describe the real situation.

c. Finite difference equations approximate the differential equations.

d. Solution technique solves the finite difference equations.

88. The finite difference solution is often discussed in terms of the convergence and stability of the difference scheme. A difference scheme is convergent if the solution of the difference equations approaches the solution of the partial differential equations as the time-distance grid mesh size is made smaller and smaller. A difference scheme is stable if errors introduced at any stage of the computation process do not grow with time and distance and make the solution meaningless. When a numerical method is unstable, a small perturbation (such as a truncation error) of the exact solution will grow with time, often being amplified beyond any reasonable limit after a few time steps. The effects of instability often show up as oscillations in the computed values of the dependent variables. Convergence and stability are generally related, so that the attainment of one usually, but not always, assures attainment of the other. Convergence tendencies and stability can often, but not always, be improved by refining the time and distance increments of the finite difference grid. Stability is often related to the relative size of the time step as compared with the distance step.

89. Convergence and stability are complex but important considerations in developing and applying numerical methods. For most practical problems, theory related to convergence, stability, and approximation is incomplete or lacking. Convergence and stability properties and other accuracy considerations for various numerical techniques are addressed by Liggett and Cunge (1975) and Miller (1971). Fread (1974) discusses convergence and stability

properties of the implicit four-point technique that is most often used in flood routing.

90. DAMBRK. The NWS DAMBRK model expresses the St. Venant equations in the following form for conservation of mass

$$\frac{\partial Q}{\partial x} + \frac{\partial (A + Ao)}{\partial t} - q = 0$$

and conservation of momentum

$$\frac{\partial Q}{\partial t} + \frac{\partial (Q^2/A)}{\partial x} + gA \frac{\partial h}{\partial x} + S_f + S_e = 0$$

where the cross-sectional area is divided between an active flow area A, and an inactive off-channel storage area A_o (Fread 1984). The conservation of momentum equation reflects only the active flow area, while the conservation of mass equation considers both active and inactive flow. The term S_e is defined as

$$S_e = \frac{k\Delta(Q/A)^2}{2g\Delta x}$$

where k is an expansion-contraction coefficient varying from 0.0 to ±1.0 (plus if contraction and minus if expansion) and $\Delta(Q/A)^2$ is the difference in the term $(Q/A)^2$ at two adjacent cross sections separated by a distance Δx. The other terms are as previously defined. The term S_f is computed using the Manning equation.

91. DAMBRK solves the St. Venant equations using a weighted four-point implicit finite difference scheme first proposed by Preissman (1961). The continuous x-t region, in which solutions of h and Q are sought, is represented by a rectangular grid of discrete points (Fread 1984). Neither the distance steps (Δx) nor the time steps (Δt) need to be constant. Each point in the rectangular grid can be identified by a subscript i which designates the distance (x) position and a superscript j which designates the time (t) position.

92. The time derivatives are approximated by a forward difference quotient centered between the i and $i+1$ points along the x axis as follows:

$$\frac{\partial K}{\partial t} = \frac{K_i^{j+1} + K_{i+1}^{j+1} - K_i^j - K_{i+1}^j}{2\Delta t_j}$$

where K represents any variable.

93. The spatial derivatives are approximated by a forward difference quotient positioned between two adjacent time lines according to weighting factors of θ and $1-\theta$, i.e.,

$$\frac{\partial K}{\partial x} = \theta \left[\frac{K_{i+1}^{j+1} - K_i^{j+1}}{\Delta x_i}\right] + (1-\theta) \left[\frac{K_{i+1}^j - K_i^j}{\Delta x_i}\right]$$

94. Variables other than derivatives are approximated at the time level where the spatial derivatives are evaluated by using the same weighting factors, i.e.,

$$K = \theta \left[\frac{K_i^{j+1} + K_{i+1}^{j+1}}{2}\right] + (1-\theta) \left[\frac{K_i^j + K_{i+1}^j}{2}\right]$$

A weighting factor θ value of 1.0 yields a fully implicit or backward difference scheme. A weighting factor of 0.5 is sometimes termed a box scheme. Fread (1974) found that maximum accuracy with a four-point implicit scheme is achieved with a θ of 0.5. However, due to instability problems, a value of about 0.6 is typically used. DAMBRK allows the user to specify θ, but a default value of 0.6 is provided.

95. When the derivatives and other variables in the St. Venant equations are replaced with the finite difference operators defined above, the following weighted four-point implicit difference equations are obtained.

$$\theta \frac{Q_{i+1}^{j+1} - Q_i^{j+1}}{\Delta x_i} - \theta\, q_i^{j+1} + (1-\theta) \frac{Q_{i+1}^j - Q_i^j}{\Delta x_i} - (1-\theta)\, q_i^j$$

$$+ \frac{(A + A_o)_i^{j+1} + (A + A_o)_{i+1}^{j+1} - (A + A_o)_i^j - (A + A_o)_{i+1}^j}{2\Delta t_j} = 0$$

and

$$\frac{Q_i^{j+1} + Q_{i+1}^{j+1} - Q_i^j - Q_{i+1}^j}{2\Delta t_j} + \theta \frac{(Q^2/A)_{i+1}^{j+1} - (Q^2/A)_i^{j+1}}{\Delta x_i}$$

$$+ g \bar{A}^{j+1} \frac{h_{i+1}^{j+1} + h_i^{j+1}}{\Delta x_i} + \bar{S}_f^{j+1} + S_{ce}^{j+1} + (1-\theta) \frac{(Q^2/A)_{i+1}^j - (Q^2/A)_i^j}{\Delta x_i}$$

$$+ g \bar{A}^j \frac{h_{i+1}^j - h_i^j}{\Delta x_i} + \bar{S}_f^j + S_{ce}^j = 0$$

where

$$\bar{A} = (A_i + A_{i+1})/2$$

$$\bar{S}_f = n^2 \bar{Q}|\bar{Q}|/(2.2 \bar{A}^2 \bar{R}^{4/3})$$

$$\bar{Q} = (Q_i + Q_{i+1})/2$$

$$\bar{R} = \bar{A}/\bar{B}$$

$$\bar{B} = (B_i + B_{i+1})/2$$

96. With all variables on one time line known, the value for the unknowns on the next time line are computed. The above two equations are repeated between each pair of distance locations resulting in N-2 equations, where N is the number of nodes on a time line. Combining two additional equations specifying upstream and downstream boundary conditions with the above equations results in a system of 2N nonlinear equations with 2N unknowns. DAMBRK uses the iterative Newton-Raphson method to solve the equations.

97. DAMBRK has the option to use a modified set of equations in which the valley section is divided between the channel, left floodplain, and right floodplain. This option is particularly applicable when the channel is sufficiently large to carry a significant portion of the total flow and has a rather meandrous path through the downstream valley.

98. FLOW SIM 1 and 2. FLOW SIM 2 incorporates a weighted four-point implicit finite difference solution of the St. Venant equations similar to

that used in DAMBRK. FLOW SIM 1 uses an explicit finite difference scheme. FLOW SIM 1 and 2 use identical input data and have the same output format. The difference between the two model versions is the method used to solve the St. Venant equations.

Generalized dimensionless relationships

99. Significant expertise, time, and computer resources are required to apply dynamic routing models. One strategy for an expedient dam-breach flood wave analysis capability is to develop precomputed generalized relationships. The generalized routing model consists of a family of dimensionless curves which have been developed using a dynamic routing model. Users can quickly and easily apply the generalized dimensionless relationships to their particular problems. However, significant simplifications are required to develop a set of dimensionless curves which can be applied to a wide range of situations using a few parameters. The assumption of a prismatic channel of specified shape is one of the major simplifications made.

100. The previously described NWS SMPDBK model and HEC dimensionless graph procedure are based on generalized dimensionless relationships. Both of these flood-routing methods were developed specifically for analyzing dam-breach floods. Both of the methods require simplifying the valley geometry to a prismatic channel with a cross section defined by a power function of the form $B = kh^m$ where B is valley width, h is depth, and k and m are constants. In applying the curves, the constants k and m are determined by fitting to actual valley topwidth versus elevation data.

101. The HEC dimensionless graphs were developed using a dynamic routing model based on the method of characteristics (Sakkas 1980). An instantaneous complete removal of the dam is assumed. The family of dimensionless graphs provide the capability to compute time of wave front arrival and maximum flood depth at locations along the valley as a function of a dimensionless Froude number and the constants used to approximate the valley geometry. The following input data are required to use the model: water depth behind dam, channel bottom slope, Manning roughness coefficient, and channel topwidth versus elevation data. The required parameters are determined following a manual computation procedure. The time of wave front arrival and maximum flood depth are then read from the dimensionless graphs at desired locations along the valley.

102. The DAMBRK model was used to develop the dimensionless routing curves contained in SMPDBK (Wetmore and Fread 1981). SMPDBK computes the peak outflow through the dam breach as a function of reservoir and breach characteristics. Peak discharge, depth at peak discharge, and time to peak at locations along the valley are determined from a computational procedure which utilizes a family of dimensionless routing curves relating peak discharge to a dimensionless Froude number and volume parameter. Input data required to use the model include: dam crest elevation, final breach bottom elevation, reservoir storage volume and surface area, final breach width, time required for breach formation, constant flow through outlet structures, channel bottom slope, topwidth versus elevation data, and Manning roughness coefficient.

Simplified hydraulic routing methods

103. The broad range of applications and modeling complexities has resulted in the development of numerous routing methods. Various simplifications to the St. Venant equations have been made over the years to overcome difficulties in obtaining solutions. Simplified hydraulic routing methods are based on neglecting or linearizing certain terms in the St. Venant equations.

104. Kinematic and diffusion wave models. Diffusion and kinematic routing are based on the St. Venant equation for conservation of mass and a simplified form of the conservation of momentum equation in which certain terms are neglected.

105. In kinematic routing, the momentum of the unsteady flow is assumed to be the same as that of steady uniform flow. The friction slope (S_f) is equal to normal slope $S_o = \partial y/\partial x - \partial h/dx$ where h is water-surface elevation above a datum and y is flow depth. Thus, the conservation of momentum equation is simplified to $S_f - S_o = 0$. Discharge is a single-valued function of stage which can be expressed by a uniform flow formula such as the Manning equation in the form $A = \alpha Q^{\beta}$. Combining these expressions with the conservation of mass equation results in the following kinematic wave equation:

$$\frac{\partial Q}{\partial x} + \alpha\beta Q^{\beta-1} \frac{\partial Q}{\partial t} = 0$$

which can be solved analytically or by various finite difference techniques.

106. The kinematic wave model reflects only translation of the flood wave and the attendant distortion that is attributed to kinematic effects of wave movement. Errors inherent in finite difference solutions cause an attenuation and dispersion of the flood wave. However, this numerical attenuation merely mimics the actual physical phenomenon. The kinematic wave equation contains no mechanism to model attenuation. Also, downstream backwater effects are not reflected in the model.

107. The diffusion model is based on the St. Venant conservation of mass equation and the following simplified form of the momentum equation:

$$S_f - \partial h/\partial X = 0$$

Inclusion of the water slope term ($\partial h/\partial X$) provides a significant improvement over the kinematic model. This term allows the diffusion model to reflect the attenuation effect of the flood wave. It also allows the specification of a boundary condition at the downstream end of the routing reach to account for backwater effects. The diffusion model does not include the inertia terms $\left(\frac{\partial V}{\partial t}\right.$ and $\left.V\frac{\partial V}{\partial t}\right)$ of the St. Venant momentum equation. Therefore, diffusion routing is limited to relatively gradually rising flood waves in channels of fairly uniform geometry.

108. Linearization of the St. Venant equations. The mathematical complexity of the St. Venant equations is due largely to their nonlinearity. The equations can be solved analytically if simplified sufficiently through linearization. The equations have been linearized by ignoring the nonlinear terms, such as $V\frac{\partial V}{\partial X}$ in the momentum equations, by assuming that some of the coefficients involving dependent variables (such as cross-sectional area) are constant and by approximating the more important nonlinear terms (such as resistance) through the substitution of a combination of linear terms. Simplifications have been made for various circumstances. The most common simplifications that have been made to linearize the St. Venant equations are:

a. The channel has a constant prismatic cross section, usually rectangular.

b. The channel bottom slope is constant, often assumed horizontal.

c. Resistance is linearly related to velocity, instead of being proportional to velocity squared.

d. The average water-surface elevation is constant along the channel, permitting the analysis of wave motion as a series of small deviations from the underlying steady flow.

e. The flood wave has a simple shape that is amenable to analytical expression.

f. Lateral inflow does not occur.

g. Nonlinear acceleration terms in the equations can be neglected.

Fread (1982) provides a synopsis of linearized flood-routing models within the subcategories of classical wave models, impulse response models, complete linearized models, and multiple linearized models.

Hydrologic storage routing

109. Hydrologic routing is based on the conservation of mass or continuity equation

$$I - O = \frac{dS}{dt}$$

where I is inflow rate, O is outflow rate, and dS/dt is rate of change in storage with respect to time. The continuity equation can be written in finite difference form as

$$\frac{I_1 + I_2}{2} - \frac{O_1 + O_2}{2} = \frac{S_2 - S_1}{\Delta t}$$

A relationship between storage and discharge must be combined with the continuity equation to obtain a routing model. All hydrologic routing methods use the continuity equation. Variations between methods are due to the different ways of expressing the storage versus discharge relationship.

110. Modified Puls and variations. The modified Puls or storage indication method and its variations are based on the assumption that storage is a single-valued function of outflow. The continuity equation can be written as

$$\frac{2S_2}{\Delta t} + O_2 = I_1 + I_2 + \frac{2S_1}{\Delta t} - O_1$$

which can be solved step-by-step for the left-hand side, with the right-hand side of the equation known at each step of the computations. A relationship between the left-hand side of the equation and outflow must be developed from a known storage-outflow relationship. In dam-breach analysis, the storage-outflow relationship changes with time as the breach grows. The term modified Puls routing is broadly used herein to include level pool reservoir routing where the storage-outflow relationship is a function of breach size.

111. The assumption that storage is a unique function of outflow is valid for a reservoir that is short and deep enough for the water surface to be horizontal. A reservoir storage-outflow relationship is developed from a reservoir elevation-storage relationship and rating curves for the outlet structures. The modified Puls method, or variations thereof, is widely used for routing flood hydrographs through reservoirs. DAMBRK, FLOW SIM 1 and 2, HEC-1, and MILHY use variations of the modified Puls technique for reservoir routing.

112. Although most applicable for reservoirs, the method is also used for channel routing. For example, HEC-1 has an option for modified Puls channel routing which is typically used in dam-breach flood routing. Storage-discharge relationships for a channel reach can be approximated by assuming uniform flow and using a uniform flow formula such as the Manning equation with a cross section representative of the reach. A somewhat better storage-discharge approximation can be achieved using water-surface profiles computed assuming steady, gradually varied flow. The input data for both of these approaches are cross sections and roughness coefficients. A third approach is to develop a storage-discharge function for a reach from historical inflow and outflow hydrographs.

113. Using modified Puls routing for channels is complicated by the fact that the degree of flood wave attenuation varies with the reach length used in the computations. A routing reach is typically divided into subreaches for computational purposes. The number of subreaches can be used as a calibration parameter but is difficult to estimate precisely if historical flow data are not available for calibration.

114. Muskingum and variations. The Muskingum method is based on the assumption of a linear relationship between storage and a weighted combination of inflow and outflow

$$S = K(xI + (1-x)O)$$

where K is a storage time constant and x is a weighting factor that varies between 0 and 0.5 for a given reach. Combining this expression with the conservation of mass equation results in the Muskingum routing equation

$$O_2 = C_o I_2 + C_1 I_1 + C_2 O_1$$

where

$$C_o = \frac{-Kx + 0.5\Delta t}{K - Kx + 0.5\Delta t}$$

$$C_1 = \frac{Kx + 0.5\Delta t}{K - Kx + 0.5\Delta t}$$

$$C_2 = \frac{K - Kx - 0.5\Delta t}{K - Kx + 0.5\Delta t}$$

Values for the parameter K can be approximated as the travel time through the reach, and an average value of 0.2 can be assumed for x. Better values of K and x can be determined from observed inflow and outflow hydrographs for the reach of river.

115. A modified version of the Muskingum method developed by Cunge (1969) assumed a single-value depth-discharge relationship, which is equivalent to a kinematic wave model, and applied a four-point finite difference technique to derive expressions for the routing coefficients x and K. After the constants x and K are determined for a particular river reach, the routing computations are identical to the original Muskingum method. The Muskingum-Cunge method does not require observed inflow and outflow hydrographs to establish the routing coefficients as required in the Muskingum method, but best results are obtained if some actual flow data are available.

116. Numerous other variations of the Muskingum method have been developed, including the Kalinin-Miljukov, SSARR, and lag and route methods (Fread 1982). Muskingum type models provide best results when applied to slowly fluctuating rivers with negligible lateral inflows and backwater effects.

117. Variable storage coefficient. The variable storage coefficient routing method was developed by Williams (1969) and is included in the MILHY

model (US Army Engineer WES 1985). The following expression for travel time (T),

$$T = \frac{L}{V} = \frac{S}{Q}$$

where L is reach length, V is average velocity, S is storage in reach, and Q is average discharge, is combined with the conservation of mass equation to obtain the variable storage coefficient routing equation

$$O_2 = C_2\left[I_a + \left(\frac{1}{C_1} - 1\right) O_1\right]$$

$$C_1 = \frac{2\Delta t}{2T_1 + \Delta t}$$

$$C_2 = \frac{2\Delta t}{2T_2 + \Delta t}$$

$$I_a = \frac{I_1 + I_2}{2}$$

where subscripts 1 and 2 refer to the beginning and end of the routing interval Δt. Travel time is computed for an average of inflow and outlet velocities along with a correction for variation in water-surface slope.

118. Thus, the variable storage coefficient routing equation is similar in form to the Muskingum routing equation. Storage is related to both inflow and outflow. However, unlike the Muskingum method, the storage-outflow function is not constrained to be linear. Also, whereas the Muskingum K is a constant, the coefficients reflecting travel time vary with discharge in the variable coefficient routing procedure. The iterative solution required for the variable coefficient method requires more computational effort than the Muskingum or modified Puls methods. However, variable storage coefficient routing should more closely represent an actual flood wave than these methods.

119. Input data for the variable storage coefficient routing procedure consist of cross sections and roughness coefficients.

120. Modified attenuation-kinematic routing. The SCS recently developed the modified attenuation-kinematic (Att-Kin) valley routing method for use in their TR 66 Simplified Dam-Breach Routing Procedure and revised TR 20, Computer Program for Project Formulation-Hydrology. Development of the new routing method is described in TR 66 (SCS 1979) and by Comer, Theurer, and Richardson (1982).

121. The Att-Kin model could be categorized as both simplified hydraulic routing and hydrologic storage routing. The model combines features from both storage and kinematic routing. Storage routing reflects only attenuation and attendant distortion of the flood wave that is attributable to valley storage. Kinematic routing reflects only translation of the flood wave and the attendant distortion that is attributable to kinematic effects of wave movement. In the Att-Kin method, the inflow hydrograph is routed using a hydrologic storage routing method based on the continuity equation and a single-valued valley storage-discharge relationship. The resulting attenuated hydrograph is then translated and distorted by kinematic routing.

122. The TR 66 Simplified Dam-Breach Routing Procedure provides dimensionless curves to simplify valley routing. The dimensionless curves were developed with the Att-Kin model. The user must develop single-valued storage-discharge and depth-discharge relationships from uniform or gradually varied flow computations. The peak discharge at a specified location along the valley is determined from an Att-Kin dimensionless curve as a function of peak discharge at the dam, reservoir volume, and parameters reflecting the storage-discharge relationship for the valley reach. Peak flow depth is determined by relating peak discharge to the depth-discharge function for the given location.

Purely empirical methods

123. Some flood-routing methods are based strictly on intuition and observations of past floods. Lag methods, such as the average lag option in HEC-1, and gage relations are examples of purely empirical methods. The Bureau of Reclamation (1983) presented a method developed specifically for routing dam-breach flood waves in which the peak discharge at a specified distance below the dam is computed as a function of only reservoir storage and depth. These are generally the least accurate and least versatile of the various flood-routing methods.

Water-Surface Profile Computations

124. Flow depths as well as discharges are computed using hydraulic routing techniques. However, hydrologic storage routing methods typically result in discharge hydrographs. Flow depths are then computed for a given discharge using either a uniform flow formula, such as the Manning equation, or a steady, gradually varied water-surface profile procedure. Thus, additional approximations enter the model in converting discharges to flow depths.

125. Computation of water-surface profiles is based on an iterative solution of the one-dimensional energy equation

$$\alpha_1 \frac{V_1^2}{2g} + WS_1 = \alpha_2 \frac{V_2^2}{2g} + WS_2 + h_L$$

which reflects gradually varied steady flow. The subscripts 1 and 2 refer to downstream and upstream cross sections, respectively, V is average velocity, α is a velocity distribution coefficient, g is acceleration of gravity, WS is water-surface elevation, and h_L is head loss between the cross sections. Head loss is typically estimated using the Manning equation and expansion and contraction coefficients. Weir and orifice equations are used to determine flow and head losses through bridges and culverts. The iterative standard step method is usually used to solve the energy equation. For subcritical flow, the computations begin at a known or assumed water-surface elevation and proceed upstream. Water-surface profile computations for supercritical flow proceed downstream from a known or assumed upstream water-surface elevation.

126. MILHY contains a standard step-method algorithm for computing gradually varied steady-flow water-surface profiles for subcritical flow. The Manning equation, assuming uniform flow, is used whenever the flow is supercritical. Flood-routing and water-surface profile computations are performed in a single run of the MILHY mode'. HEC-1 has the capability for computing water-surface profiles using the Manning equation assuming uniform flow. Flood-routing and water-surface profile computations are performed in a single HEC-1 run. The case study analyses addressed later in this report followed this approach in applying HEC-1. HEC-1 and HEC-2 have traditionally been used in combination for many applications. The HEC-2 Water Surface Profile

computer program is a standard step-method solution of the energy equation, assuming gradually varied steady flow (HEC 1982). Water-surface profiles, for an assumed range of discharges, computed with HEC-2 can be used to develop storage versus outflow relationships for input to HEC-1 for use in the modified Puls channel routing. Upon completion of the HEC-1 routing, the resulting peak discharges are provided as input to HEC-2 for computing the corresponding water-surface profiles.

PART III: CASE STUDY ANALYSES

127. The selected dam-breach flood forecasting models described in Part II were applied to several case study data sets. The purpose of the case studies was to test the accuracy and practicality of the models. The experience gained and lessons learned from the case study applications significantly contribute to providing an objective basis for evaluating and comparing the models.

128. Most of the Stillhouse Hollow case study and a portion of the Teton case study were performed by CPT David N. Buttery working with the author. CPT Buttery developed a military applications comparative analysis of dam-breach flood-routing techniques which constituted his master of engineering technical report (Buttery 1984). The author performed the remainder of the case study modeling. The case study results summarized here are documented in detail by Wurbs (1985b).

Description of Case Studies

129. The dam-breach flood wave models were tested and compared by application to the following case studies: (a) Teton Dam, (b) hypothetical prismatic channel, (c) Laurel Run Dam, and (d) Stillhouse Hollow Dam. The Laurel Run and Teton case studies involved field data sets from actual dam failures. The hypothetical prismatic channel case study used the Teton reservoir and dam data but replaced the complex Teton valley geometry with a prismatic channel. Stillhouse Hollow is an existing dam that has not actually failed. The models used in each case study are listed in Table 2. Descriptions of the dams, reservoirs, and floods associated with each case study are provided below.

Teton Dam failure flood

130. The Teton Dam on the Teton River in Idaho failed in June 1976. Eleven lives were lost, and damages reportedly were about $400 million. The newly constructed Bureau of Reclamation project was being filled for the first time during the spring of 1976. The reservoir contained 251,700 acre-ft* of

---

* A table of factors for converting non-SI units of measurement to SI (metric) units is presented on page 3.

Table 2

Models Applied in Each Case Study

Model	Case Study				
			Teton		
	Laurel Run	Hypothetical Prismatic	Original Data	Test Data	Stillhouse Hollow
NWS Dam-Break Flood Forecasting Model (DAMBRK)	X	X	X		X
SWD Flow Simulation Model (FLOW SIM 1)	X	X	X		X
SWD Flow Simulation Model (FLOW SIM 2)	X	X	X		X
HEC Flood Hydrograph Package (HEC-1)	X	X	X	X	X
NWS Simplified Dam-Break Model (SMPDBK)	X	X	X	X	X
HEC Dimensionless Graphs Procedure	X	X		X	X
SCS Simplified Dam-Breach Routing (TR 66)		X		X	X
Military Hydrology Model (*MILHY*)	X	X	X		X
Military Hydrology Bulletins 9 and 10				X	X
DIA Outflow Hydrograph Computation Method			X		

water and was almost full when the 305-ft-high, 2,500-ft-long earthfill dam failed. Approximately 173,000 a e-ft of water drained through the breached dam within 143 min, resulting in a peak discharge of 2.3 million cfs. A total of about 240,000 acre-ft drained from the reservoir within an 8-hr period. In the 100 miles between Teton Dam and the downstream American Falls Reservoir, the peak discharge and flood volume attenuated to 53,500 cfs and 160,000 acre-ft, respectively. American Falls Reservoir stored the entire flood flow. The dam failure was not associated with any precipitation flooding on the river. The almost fully penetrating breach, approximately trapezoidal in shape, included about 40 percent of the dam. A breach time of 1.0 hr was used in the analyses. Detailed information compiled by the USGS (Ray and Kjelstrom 1978), including measured discharge data and high-water marks, was used in the case study.

131. A map of the river system is provided as Figure 1. The dam was located in a narrow steep-walled canyon of the Teton River. The canyon ends about 5 miles downstream of the damsite. The river then meanders through a wide flat plain and divides into two forks about 4 miles downstream from the end of the canyon. Both the North and South Forks of the Teton River meander broadly through alluvial deposits before emptying into Henrys Fork of the Snake River about 11 miles below the end of the canyon. Henrys Fork joins the Snake River at Menan Buttes. The steep walls at Menan Buttes form a narrow "bottleneck" or flow constriction. A flow constriction is also formed at Ferry Butte just upstream of American Falls Reservoir. The floodplain of the Snake River between Menan Buttes and Ferry Butte is flat agricultural land. American Falls Dam is located on the Snake River 123 miles downstream from the mouth of Henrys Fork. About 185 square miles of land was inundated by the dam failure flood. The flooded area in the vicinity of Rexburg was more than 6 miles wide. The Teton dam-breach flood wave is particularly difficult to model due to the complex downstream valley geometry.

132. The Teton case study involved two sets of data. Cross sections were developed from USGS 1:24,000-scale topographic maps whereas reservoir and dam data were taken from the USGS report. This data set is referred to as "original data" in the following discussions. A set of Teton data is also routinely provided by the NWS and the HEC as test data with the DAMBRK computer program. The DAMBRK Teton test data may not necessarily have been representative of the actual flood in all respects but provided a convenient

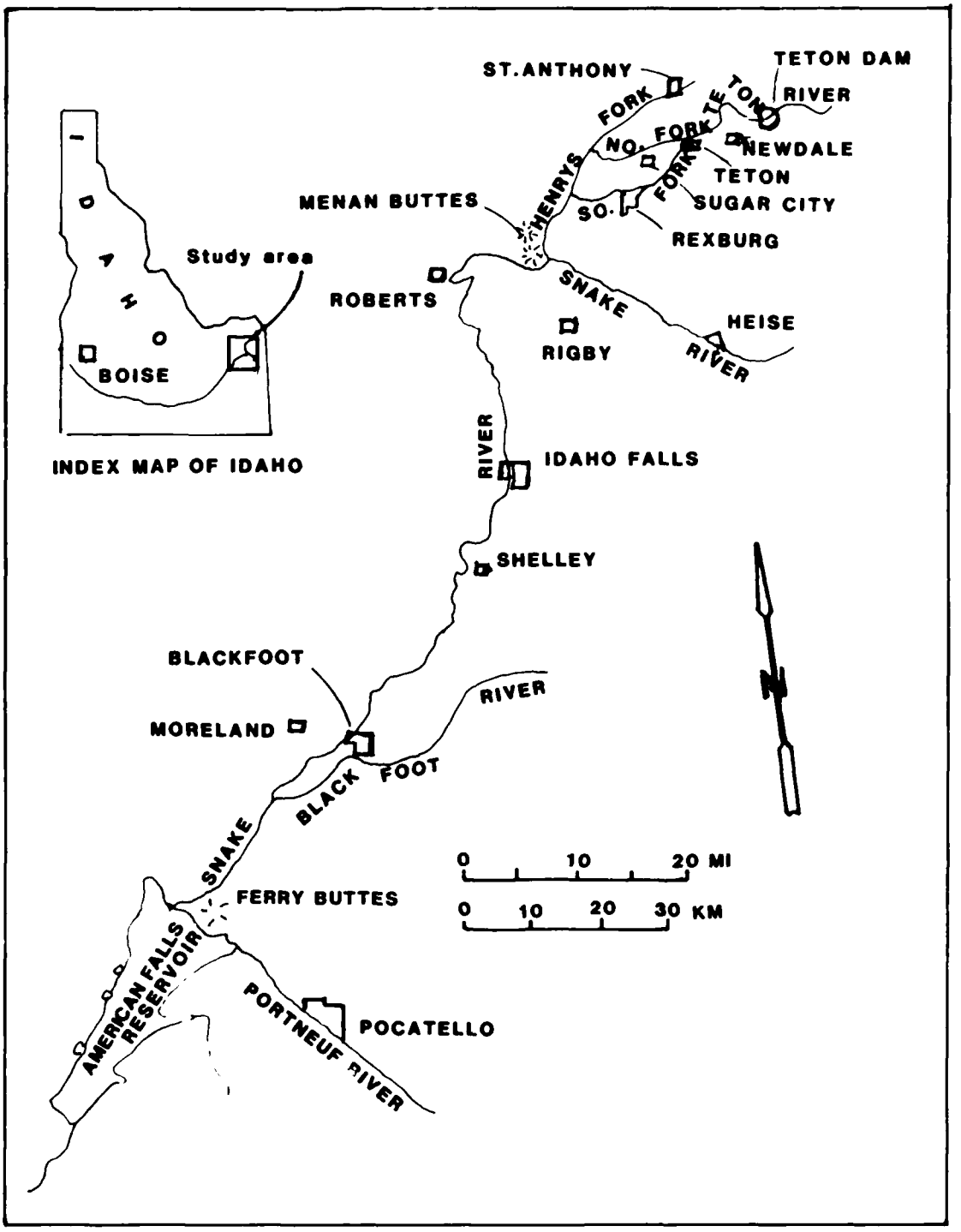

SOURCE : U.S.G.S. REPORT 77-765

Figure 1. Map of Teton-Snake River system

additional data set which was useful for various purposes in addition to getting DAMBRK running. Several simplified routing models were applied to the test data concurrently with development of the original test data set for application with the dynamic routing models.

Hypothetical prismatic channel

133. Computational difficulties associated with the complex valley geometry were the dominant consideration in the Teton case study. Irregular valley geometry was also an important complicating factor in the Laurel Run case study. The hypothetical prismatic channel case study was developed to test the models under conditions for which irregular valley geometry was not a major concern. The reservoir data for the Teton Reservoir was combined with a prismatic channel. The prismatic channel is essentially an extension of the 5-mile-long Teton Canyon to 50 miles.

134. The prismatic channel, as shown in Figure 2, consists of two reaches of constant cross section joined by a transition reach. The channel cross section from mile 0 to mile 5 is constant, and the reach between mile 10 and mile 50 has a slightly wider constant cross section. Miles 5 to 10 provide the transition between the two sections. The cross section for miles 0 to 5 approximates the geometry of the narrow, steep-walled Teton Canyon just below the dam. However, the remaining 45 miles of slightly wider prismatic channel does not approximate the wide, flat, abruptly changing topography of the valley of the Teton and Snake Rivers below the Teton Canyon. The prismatic channel has a constant bottom slope of 10 ft/mile and a constant Manning roughness coefficient of 0.040, which are representative of the Teton River canyon.

Laurel Run Dam failure flood

135. The failure of the dam on Laurel Run near Johnstown, Pa., resulted in the sudden release of 450 acre-ft of water into a stream that was already flooding from a severe rainstorm. Laurel Run has a drainage area of 14 square miles above its confluence with the Conemaugh River. The dam was located about 2.5 miles upstream of the confluence. On 19 and 20 July 1977, a severe rainstorm caused heavy flooding in many areas near Johnstown. Flooding in the Laurel Run Valley caused extensive property damage and loss of more than 40 lives. The Laurel Run Dam breached at about 2:35 a.m. on 20 July, significantly worsening flood flows.

136. The 45-ft-high earthen embankment had a crest elevation of

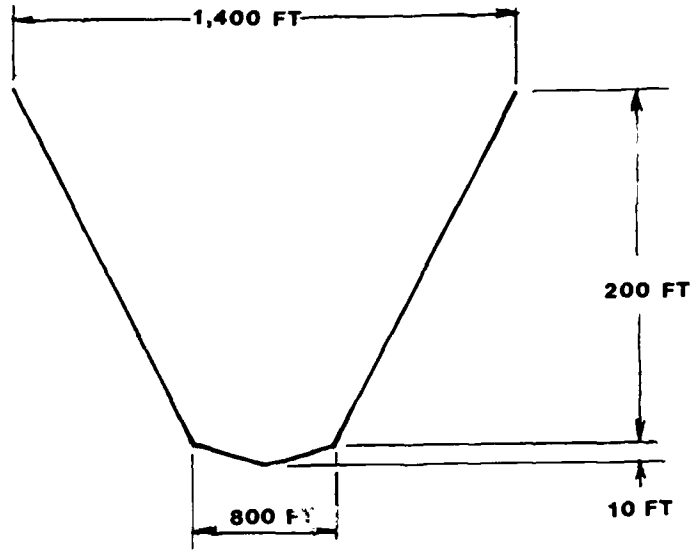

MILE 0 to 5

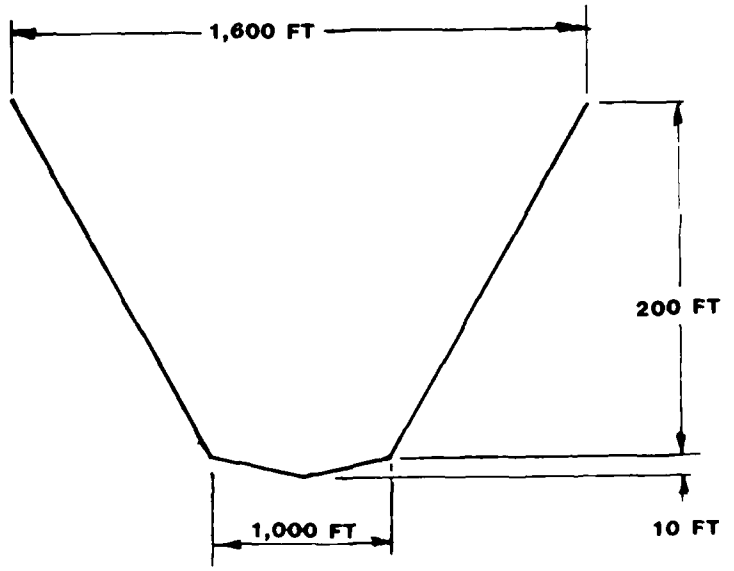

MILE 10 to 50

Figure 2. Prismatic channel cross section

1,436.5 ft with a spillway crest of 1,430 ft. The water surface is estimated to have reached an elevation of 1,437.2 ft at the time of failure. The breach was approximately triangular in shape and fully penetrated the dam with average side slopes of 2.45 horizontal to 1.0 vertical. The breach encompassed about one-third of the dam. A breach time of 15 min was used in the analyses. The reservoir was about 0.4 mile long and generally less than 600 ft wide. The steep walls of the downstream valley confined the flood to a width of less than 500 ft, often less than 200 ft. The channel slope is about 100 ft/mile. Red Run and Wildcat Run tributaries enter Laurel Run 1,100 ft and 9,700 ft below the dam, respectively. Figure 3 is a map of the stream system. The input data used in the analysis came primarily from a paper by Chen and Armbruster (1980) and a report by Land (1980a). The data included 15 surveyed cross sections covering a 13,400-ft reach below the dam and reservoir and tributary inflow hydrographs determined from rainfall-runoff modeling.

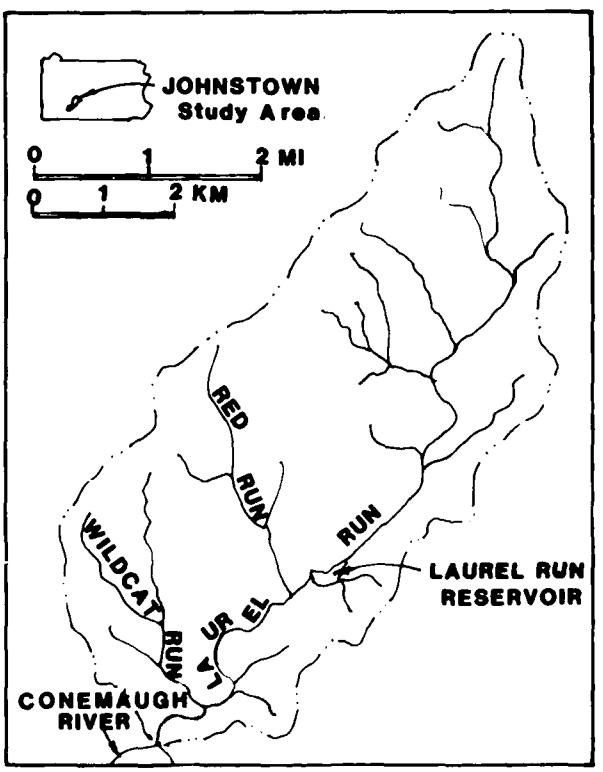

SOURCE: CHEN and ARMBRUSTER (1980)

Figure 3. Map of Laurel Run drainage basin

Stillhouse Hollow Dam

137. Stillhouse Hollow Dam is located on the Lampases River near Fort Hood in central Texas. The 200-ft-high earthfill embankment impounds a 204,900-acre-ft conservation pool and 396,600-acre-ft flood control pool. The hypothetical failure was assumed to occur with the water-surface elevation at top of flood control pool and a relatively small inflow to the reservoir. Stillhouse Hollow is an existing dam that has not failed. It was selected as a case study because of its well-defined, gently changing downstream valley topography and other characteristics which facilitate dam-breach flood wave modeling. The topography is significantly different from Teton and Laurel Run. The dam was constructed and is maintained by the USAED, Fort Worth. The necessary reservoir and dam data were provided by the District office.

Comparison of case studies

138. The four case studies represent a broad range of conditions. The Teton case study entailed extremely variable valley geometry which included a steep-walled canyon, wide flat floodplains, and abruptly changing steep-walled constrictions. Laurel Run is in a steep-walled valley with fairly irregular geometry in a mountainous area. The Stillhouse Hollow case study dealt with a relatively well-defined smoothly changing valley in an area of rolling hills topography. The hypothetical prismatic channel case study, of course, dealt with a prismatic channel.

139. Laurel Run has a steep channel bottom slope that causes supercritical flow. The other case studies involve relatively mild channel slopes. Laurel Run is also the only case study in which the dam breach occurred during a major rainstorm flood. The case study dams are further compared below.

Item	Teton	Laurel Run	Stillhouse Hollow
Type of dam	Earthen	Earthen	Earthen
Dam height, feet	305	45	200
Storage at time of failure, acre-feet	252,000	450	1,000,000
Channel slope, feet/mile	11	98	5.4
Length of valley modeled, miles	102	2.5	33

Comparative Summary of Model Results

140. The four case studies and 10 models are listed in Table 2. This table shows which of the models were applied in each case study. An original best-estimate set of input data was developed for each case study. A "base run" with each model was made with input data as close as possible to the best-estimate data set. The results from the base runs were used for comparisons with measured data and between models. Numerous other runs were made for purposes of sensitivity analysis and testing of the models. The models provide various types of information regarding the flood wave characteristics. The results are summarized in terms of peak discharges, peak water-surface elevations, maximum flow depths, and time to maximum depth at various distances from the dam.

141. The MILHY model does not have a breach simulation routine. Consequently, use of MILHY was limited to valley routing. Reservoir outflow hydrographs computed with DAMBRK were provided as input data to the MILHY model.

Computer resources

142. The four models requiring a mainframe computer were run on the Amdahl 470 computer system at Texas A&M University. Memory requirements for DAMBRK, FLOW SIM 1, FLOW SIM 2, and HEC-1 were 436K, 452K, 472K, and 556K bytes, respectively. As an indication of the relative magnitude of central processor unit (CPU) resources required by these programs, the Laurel Run base runs with DAMBRK, FLOW SIM 1, FLOW SIM 2, and HEC-1 had CPU times of 103, 248, 131, and 10 sec, respectively. The Teton base runs with DAMBRK, FLOW SIM 1, and HEC-1 had CPU times of 166, 106, and 18 sec, respectively. SMPDBK and MILHY were run on Apple and IBM microcomputers, with relatively short run times. The other models involved manual computations with graphs and a calculator.

Numerical computation problems

143. Most of the runs made with the three dynamic routing models (DAMBRK, FLOW SIM 1, and FLOW SIM 2) terminated without converging to a solution due to instability or other computational problems. Overcoming these dynamic routing computational problems was the most difficult and time-consuming aspect of the case studies. The modeling process consists essentially of first developing a best-estimate set of input data. The input data are then modified in a trial-and-error manner, with alternative combinations

of parameter values being tried until a solution is obtained. The objective is to obtain a solution with the input data being as close as possible to the best-estimate data.

144. The literature in general, as well as the experience with the case studies reported herein, indicates that rapidly rising hydrographs like those associated with dam breaches can be expected to cause computational problems, associated with numerical instability and nonconvergence of the iterative solution algorithm, when modeled using numerical approximations of the St. Venant equations. These problems are usually associated with the distance and time steps used in the computations, abruptly changing valley geometry, and/or changes between subcritical and supercritical flow. DAMBRK prints out a message that "nonconvergence occurred at certain cross sections" whenever the iterative Newton-Raphson technique does not converge to a solution. FLOW SIM 1 and 2 print out a message that "execution of the program is terminated because of an instability in the calculations."

145. Varying the distance and time steps and smoothing the valley geometry are the primary means for overcoming nonconvergence and instability problems. The flow in the channel at the beginning of the simulation can also be arbitrarily increased to prevent negative flow depths from occurring. Smoothing the valley geometry consists of removing abrupt changes either vertically or along the channel by altering topwidth elevation data or relocating or removing cross sections. Convergence and stability were also found in the case studies to be very sensitive to breach formation time and final breach width. If the water is allowed to flow from the reservoir relatively slowly (small breach dimensions and large breach time), the likelihood of obtaining a solution is better than for a large, rapidly formed breach.

146. Since flow characteristics are dependent upon downstream conditions in subcritical flow but not in supercritical flow, occurrence of supercritical flow is also a problem. Boundary conditions must be specified differently in the solution algorithm for subcritical and supercritical flow. DAMBRK can accommodate supercritical flow for either the entire channel or only an upstream reach of the channel, but the flow is assumed to be supercritical throughout the duration of the simulation. Changes between subcritical and supercritical flow as the flood wave passes a location cannot be modeled. FLOW SIM 1 and 2 have no special provisions for supercritical flow. Increasing the value of the Manning roughness coefficient, a strategy for

preventing simulated supercritical flow from occurring, was adopted in the case studies.

147. The valley downstream of Teton Dam required significant cross-sectional smoothing to obtain a solution. The initial attempt at modeling the Teton flood wave using DAMBRK was unsuccessful because convergence to a reasonable solution could not be obtained. Numerous runs with trial-and-error adjustments in input data terminated with messages that nonconvergence had occurred or negative areas had been computed. In some cases, solutions were obtained but were unreasonable. The adjustments included smoothing, relocating, or removing selected cross sections; increasing the base discharge; changing the θ weighting factor; and relaxing the convergence criterion. Finally, the initial data set was abandoned, and an essentially new data set was developed. The second data set had fewer cross sections, fewer topwidths per cross section, and different cross-section locations. Each cross section was smoothed. Initial runs with the second data set did not converge, but minor additional smoothing resulted in convergence to a reasonable solution. Although a solution was obtained with the base run (best-estimate) input data, solutions still could not be obtained for very large breach widths, very small breach times, or smaller Manning roughness coefficient values.

148. In regard to overcoming computational problems to obtain a reasonable solution, the performance of FLOW SIM 1 in the Teton case study was essentially the same as DAMBRK. A base run solution was obtained using the same smoothed valley geometry as used with DAMBRK. However, alternative runs with variations in breach parameters and other input data would terminate with a message indicating computational instability had occurred. The input data which ran successfully in FLOW SIM 1 would not run in FLOW SIM 2. Numerous unsuccessful runs were made with various combinations of input data. The best solution obtained included a breach time of 5 hr, which was not considered to be reasonably close to the 1-hr base-run breach time.

149. The hypothetical prismatic channel case study eliminated the abruptly changing valley geometry. Obtaining a solution with DAMBRK was not difficult under these conditions. However, computational instability was still a major problem with FLOW SIM 1 and 2. Trial-and-error runs were made with various combinations of values for the time and distance step sizes, breach characteristics, and Manning roughness coefficients. The distance and time step sizes did not seem to make much difference. Reasonable solutions

could be obtained with FLOW SIM 1 as long as the breach width was relatively small, the breach time was relatively large, and/or the Manning roughness coefficients were relatively large. Input data which resulted in solutions with FLOW SIM 1 terminated due to computational instability with FLOW SIM 2. The input parameters mentioned above had to have extremely favorable values to obtain a solution with FLOW SIM 2. Serious computational difficulties were not anticipated with the prismatic channel case study, and a satisfactory understanding of why the problems with FLOW SIM 1 and 2 were occurring was never reached. Difficulties could have been due to user error or lack of skill in applying the programs. The transition from a relatively flat canyon floor to steep canyon walls might have caused the computational problems. The right combination of distance and time step sizes might never have been obtained.

150. Although significant smoothing was still required, cross-section data for the Laurel Run valley were much easier to model than for the Teton valley. However, Laurel Run had the additional complication of a steep channel bottom slope of roughly 100 ft/mile. In order to obtain a solution with the dynamic routing models, the Manning roughness coefficients were increased enough to prevent supercritical flow from occurring. Significant time and effort involving numerous computer runs were required to overcome nonconvergence and instability problems. Cross-section data, distance and time steps, roughness coefficients, and other input data were varied in a trial-and-error manner in an attempt to obtain a solution with input data as close to the original best-estimate data as possible. The best runs obtained with DAMBRK and FLOW SIM 1 included Manning roughness coefficients that were double the actual values. A solution was obtained with FLOW SIM 2 with roughness coefficients that were 1.5 times the actual estimated values. For the Laurel Run case study, FLOW SIM 2 performed a little better than either FLOW SIM 1 or DAMBRK.

Case study results

151. The results obtained by applying the various models to the case study data sets are summarized in Tables 3-17 and Figures 4-17 in terms of peak discharge, peak flow depth, and time to peak flow depth at selected locations along the streams. The Teton and Laurel Run Dams actually failed, and field measurements of the resulting flood wave characteristics are available. Although the field measurements are not precise, an opportunity is provided to

Table 3

Peak Discharges for Teton

Model	Distance Below Dam, miles 2.5	8.8	55.7	67.5
	Peak Discharge in 1,000 cfs			
Measured	2,300	1,060	90.5	67.3
DAMBRK	1,890	1,020	203	200
FLOW SIM 1	1,670	950	150	150
HEC-1	1,760	1,200	245	220
SMPDBK	2,220	1,740	420	420
MILHY*	1,890	980	160	160
	Percent of Measured Peak Discharge			
Measured	100	100	100	100
DAMBRK	82	96	224	297
FLOW SIM 1	73	90	167	223
HEC-1	76	113	270	327
SMPDBK	97	164	464	620
MILHY*	100	92	177	238

* Valley routing was performed with the MILHY model with the reservoir outflow hydrograph computed with DAMBRK provided as input data.

Table 4

Peak Flow Depths for Teton

Model	Distance Below Dam, miles 2.5	8.9	20.0	35.5	53.8	67.5	90.0
	Peak Flow Depth, feet						
Measured	--	18	27	13	20	12	13
DAMBRK	64	22	23	17	28	29	17
FLOW SIM 1	63	21	22	16	25	27	11
HEC-1	78	40	37	29	38	72	30
SMPDBK	75	54	23	29	38	35	--
MILHY	78	14	10	10	25	27	20
	Deviation from High-Water Marks, feet						
Measured	--	0	0	0	0	0	0
DAMBRK	--	4	-4	4	8	17	4
FLOW SIM 1	--	3	-5	3	5	15	-2
HEC-1	--	22	10	16	18	60	17
SMPDBK	--	36	-4	16	18	23	--
MILHY	--	-4	-17	-3	5	15	7

Table 5

Time to Peak Flow Depth for Teton

Model	Distance Below Dam, miles						
	2.5	8.9	20.0	35.0	53.8	67.5	90.0
	Time to Peak Flow Depth, hours						
Measured	2.0	2.5	--	--	31	36	58
DAMBRK	1.1	2.7	6.0	12.6	25.0	27.7	36.0
FLOW SIM 1	4.0	5.9	9.2	15.4	29.1	31.6	41.2
HEC-1	1.2	1.8	4.5	8.5	12.9	16.0	21.0
SMPDBK	1.2	2.0	4.5	9.2	16.1	18.3	--
	Percent of Measured Time						
Measured	100	100	--	--	100	100	100
DAMBRK	55	108	--	--	81	77	62
FLOW SIM 1	200	236	--	--	94	88	71
HEC-1	60	72	--	--	42	44	36
SMPDBK	60	80	--	--	52	51	--

Table 6

Peak Discharges,

DAMBRK Test Data for Teton

Model	Distance Below Dam, miles							
	0.0	5.0	8.5	32.5	37.5	43.0	51.5	59.5
	Peak Discharge, 1,000 cfs							
DAMBRK	1,644	969	894	178	122	100	81	66
HEC-1	1,227	1,166	865	284	277	257	251	--
SMPDBK	1,632	1,318	1,022	226	196	189	200	205
TR 66	1,929	1,321	1,051	270	222	186	96	154
Bull. 9&10	1,648	1,135	1,046	786	778	8[illegible]	443	396
	Percent of DAMBRK Peak Discharge							
DAMBRK	100	100	100	100	100	100	100	100
HEC-1	75	120	97	160	227	257	310	--
SMPDBK	99	136	114	127	161	189	247	311
TR 66	117	136	118	152	182	186	205	233
Bull. 9&10	100	117	117	442	638	879	547	600

Table 7

Peak Flow Depths,

DAMBRK Test Data for Teton

Model	Distance Below Dam, miles							
	0.0	5.0	8.5	32.5	37.5	43.0	51.5	59.5
	Peak Flow Depth, feet							
DAMBRK	96.2	58.7	29.8	21.2	21.8	27.2	27.6	17.8
HEC-1	91.4	71.9	26.7	21.1	21.5	33.6	52.6	--
SMPDBK	103.2	66.0	31.4	21.9	26.2	34.5	42.4	33.0
TR 66	127.0	87.5	36.2	21.2	26.2	36.2	41.0	30.5
Bull. 9&10	103.3	73.1	35.8	26.1	31.5	67.6	53.3	38.5
	Deviation from DAMBRK Peak Depth, feet							
DAMBRK	0.0	0.0	0.0	0.0	0.0	0.0	0.0	0.0
HEC-1	-4.8	13.2	-3.1	-0.1	-0.3	6.4	25.0	--
SMPDBK	7.0	7.3	1.6	0.7	4.4	7.3	14.8	15.2
TR 66	30.8	28.8	6.4	0.0	4.4	9.0	13.4	12.7
Bull. 9&10	7.1	14.4	6.0	4.9	9.7	40.4	25.7	37.5

Table 8

Time to Peak Flow Depth,

DAMBRK Test Data for Teton

Model	Distance Below Dam, miles							
	0.0	5.0	8.5	32.5	37.5	43.0	51.5	59.5
	Time to Peak Flow Depth, hours							
DAMBRK	1.33	2.63	3.44	20.85	27.53	31.37	33.21	33.97
HEC-1	1.75	2.00	2.75	9.25	10.00	11.75	12.50	--
SMPDBK	1.3	1.7	2.4	8.4	10.1	11.4	12.7	14.2
Bull. 9&10	0.00	1.33	1.81	11.15	13.68	16.68	18.97	23.6
	Percent of DAMBRK Peak Discharge							
DAMBRK	100	100	100	100	100	100	100	100
HEC-1	132	76	80	44	36	37	38	--
SMPDBK	98	65	70	40	37	36	38	42
Bull. 9&10	0	51	53	53	50	53	57	69

Table 9

Peak Discharges for Prismatic Channel

Model	Distance Below Dam, miles 0	5	10	20	30	40	50
			Peak Discharge, 1,000 cfs				
DAMBRK	3,841	3,468	3,220	2,529	2,135	1,777	1,567
HEC-1	3,911	3,558	3,291	2,910	2,520	2,180	1,856
SMPDBK	4,016	3,235	3,212	3,880	2,620	2,410	2,216
TR 66*	3,841	2,996	2,612	1,950	1,540	1,300	1,044
MILHY	3,841	3,238	2,671	1,734	1,272	1,024	856
			Percent of DAMBRK Peak Discharge				
DAMBRK	100	100	100	100	100	100	100
HEC-1	102	103	102	115	118	123	118
SMPDBK	105	93	100	114	123	136	141
TR 66*	100	86	81	77	72	73	67
MILHY	100	93	83	69	60	58	55

* The TR 66 procedure resulted in a peak discharge at the dam of 1,931,000 cfs, which is much smaller than the values obtained with the other models. Consequently, the DAMBRK peak discharge at the dam of 3,841,000 cfs was used with all other computations performed with the TR 66 procedure.

Table 10

Peak Flow Depths for Prismatic Channel

Model	Distance Below Dam, miles 0	5	10	20	30	40	50
			Peak Flow Depth, feet				
DAMBRK	114.6	103.9	93.6	83.9	75.3	68.9	53.0
HEC-1	--	--	145.1	135.8	136.0	137.8	147.5
SMPDBK	112.6	100.2	89.5	84.0	79.9	76.7	73.0
TR 66	123.0	107.9	89.0	75.3	66.4	61.0	54.4
Graphs	119.5	101.6	95.8	87.7	81.3	78.1	72.8
MILHY	114.7	98.4	84.3	67.2	57.9	51.6	47.6
			Deviation from DAMBRK Peak Flow Depth, feet				
DAMBRK	0.0	0.0	0.0	0.0	0.0	0.0	0.0
HEC-1	--	--	51.5	51.9	60.7	68.9	94.5
SMPDBK	-2.0	-3.7	-4.1	0.1	4.6	7.8	20.0
TR 66	8.4	4.0	-4.6	-8.6	-8.9	-7.9	1.4
Graphs	4.9	-2.3	2.2	3.8	6.5	9.2	19.8
MILHY	0.1	-5.5	-9.3	-16.7	-17.4	-17.3	-5.4

Table 11

Time to Peak Flow Depth,

Prismatic Channel

Model	Distance Below Dam, miles 0	5	10	20	30	40	50
			Time to Peak Depth, hours				
DAMBRK	1.00	1.15	1.30	1.65	2.10	2.61	2.99
HEC-1	--	--	1.30	1.72	2.17	2.76	3.13
SMPDBK	1.00	1.20	1.50	1.97	2.45	2.98	3.50
Graphs	0.00	0.43	0.68	1.07	1.36	1.75	2.22
			Percent of DAMBRK Time to Peak Depth				
DAMBRK	100	100	100	100	100	100	100
HEC-1	--	--	100	104	103	105	105
SMPDBK	100	104	115	119	117	114	117
Graphs	0	37	52	65	65	67	74

Table 12

Peak Discharges for Laurel Run

Model	Peak Discharge, cfs 1 mile Below Dam	Percent of Measured
Measured	37,000	--
DAMBRK	36,500	99
FLOW SIM 1	34,800	94
FLOW SIM 2	32,900	89
HEC-1	37,800	102
SMPDBK	53,800	145
MILHY	27,800	75

Table 13

Peak Flow Depths for Laurel Run

Model	Distance Below Dam, feet						
	400	2,000	4,000	6,000	8,000	10,000	12,000
	Peak Flow Depth, feet						
Measured	11.0	16.0	17.5	18.5	15.0	14.0	17.0
DAMBRK	16.2	17.1	17.7	15.7	21.1	18.2	16.4
FLOW SIM 1	14.7	17.9	20.0	15.3	23.9	20.4	15.5
FLOW SIM 2	11.8	15.5	16.8	13.5	20.8	17.4	13.3
HEC-1	16.1	31.7	24.6	28.9	23.7	22.7	29.2
SMPDBK	10.7	17.4	17.8	16.6	16.3	15.3	25.4
Graphs	23.4	20.5	19.0	18.0	16.4	15.4	15.1
MILHY	14.7	13.5	13.8	11.2	20.8	9.2	10.4
	Deviation from High-Water Marks, feet						
Measured	0.0	0.0	0.0	0.0	0.0	0.0	0.0
DAMBRK	5.2	1.1	0.2	-2.8	6.1	4.2	-0.6
FLOW SIM 1	3.7	1.9	2.5	-3.2	8.9	6.4	-1.5
FLOW SIM 2	0.8	-0.5	-0.7	-5.0	5.8	3.4	-3.7
HEC-1	5.1	15.7	7.1	10.4	8.7	8.7	12.2
SMPDBK	-0.3	1.4	0.3	-1.9	1.3	1.3	8.4
Graphs	12.4	4.5	1.5	-0.5	1.4	1.4	-1.9
MILHY	3.7	-2.5	-3.7	-7.3	5.8	-4.8	-6.6

Table 14

Time to Peak Flow Depth for Laurel Run

Model	Distance Below Dam, miles						
	400	2,000	4,000	6,000	8,000	10,000	12,000
	Time to Peak Flow Depth, hours						
DAMBRK	0.26	0.28	0.33	0.35	0.41	0.44	0.49
FLOW SIM 1	0.35	0.37	0.41	0.44	0.50	0.53	0.60
FLOW SIM 2	0.36	0.38	0.41	0.43	0.48	0.50	0.55
HEC-1	0.25	0.27	0.28	0.32	0.33	0.35	0.38
SMPDBK	0.3	0.3	0.3	0.3	0.4	0.4	0.4
Graphs	0.01	0.03	0.06	0.09	0.12	0.15	0.18
MILHY							

Table 15

Peak Discharges for Stillhouse Hollow

Model	Distance Below Dam, miles							
	0.0	3.03	4.98	7.48	15.38	21.09	29.02	33.43
	Peak Discharge, 1,000 cfs							
DAMBRK	2,783	2,683	2,550	2,477	2,342	2,296	2,220	2,228
HEC-1	2,644	2,511	2,428	2,363	2,258	1,878	1,756	--
SMPDBK	3,827	2,826	2,872	2,870	2,888	2,554	2,203	2,038
TR 66	2,783	2,421	2,241	2,060	1,698	1,503	1,239	1,113
Bull. 9&10	3,000	2,505	2,376	2,240	1,854	1,695	1,521	1,413
MILHY	2,783	2,660	2,591	2,502	2,215	2,059	1,807	1,686
	Percent of DAMBRK Peak Discharge							
DAMBRK	100	100	100	100	100	100	100	100
HEC-1	95	94	95	95	96	82	79	--
SMPDBK	138	105	113	116	123	111	99	91
TR 66	100	90	88	83	73	65	56	50
Bull. 9&10	108	93	93	90	79	74	69	63
MILHY	100	99	102	101	95	90	81	76

Table 16

Peak Flow Depths for Stillhouse Hollow

Model	Distance Below Dam, miles							
	0.0	3.03	4.98	7.48	15.38	21.09	29.02	33.43
	Peak Flow Depth, feet							
DAMBRK	137.8	88.6	91.4	85.5	74.1	67.5	59.5	58.2
HEC-1	77.0	71.8	79.6	82.5	67.4	71.2	56.2	--
SMPDBK	131.2	103.1	93.4	99.0	78.0	82.1	73.6	79.2
TR 66	101.0	97.5	76.5	93.0	58.0	62.0	48.5	51.0
Graphs	142.3	132.5	129.2	125.2	116.7	112.1	107.4	105.1
Bull. 9&10	99.0	94.4	75.0	92.9	58.8	63.8	50.2	53.9
MILHY	76.9	79.0	83.7	84.3	75.6	66.0	64.0	55.0
	Deviation from DAMBRK Peak Depth, feet							
DAMBRK	0.0	0.0	0.0	0.0	0.0	0.0	0.0	0.0
HEC-1	-60.8	-16.8	-11.8	-3.0	-6.7	3.7	-3.3	--
SMPDBK	-6.6	14.5	2.0	13.5	3.9	14.6	14.1	21.0
TR 66	-36.8	8.9	-14.9	7.5	-16.1	-5.5	-11.0	-7.2
Graphs	4.5	43.9	37.8	39.7	42.6	44.6	47.9	46.9
Bull. 9&10	-38.8	5.8	-16.4	7.4	15.3	-3.7	-9.3	-4.3
MILHY	-60.9	-9.6	-7.7	-1.2	1.5	-1.5	4.5	-3.2

Table 17

Time to Peak Flow Depth for Stillhouse Hollow

Model	Distance Below Dam, miles							
	0.0	3.03	4.98	7.48	15.38	21.09	29.02	33.43
	Time to Peak Flow Depth, hours							
DAMBRK	4.2	4.6	4.8	5.0	6.2	6.6	7.6	7.2
HEC-1	4.2	4.6	5.0	5.6	6.4	8.6	9.6	--
SMPDBK	4.0	4.3	4.6	5.0	6.0	6.9	8.5	9.4
Graphs	0.0	0.6	0.9	1.0	1.8	2.4	3.2	3.7
Bull. 9&10	0.0	1.7	2.2	3.0	5.6	7.0	8.9	10.0
	Percent of DAMBRK Time to Peak Flow Depth							
DAMBRK	100	100	100	100	100	100	100	100
HEC-1	100	100	104	112	103	130	126	--
SMPDBK	95	93	96	100	97	105	112	131
Graphs	0	13	19	20	29	36	42	51
Bull. 9&10	0	37	46	60	90	106	117	139
MILHY	--	--	--	--	--	--	--	--

test the accuracy of the models. The tables compare computed to measured peak discharges and times to peak flow depth by expressing computed values as a percentage of measured values (computed value divided by measured value times 100 percent). Peak flow depths are expressed in terms of deviation from high-water marks in feet (computed depth minus measured depth). Although measured flood data do not exist for the Stillhouse Hollow and hypothetical prismatic channel case studies, comparison of results obtained with the alternative models still provides a meaningful analysis of model performance. For these case studies, the DAMBRK results are used as a basis for comparison. Results from the other models are expressed in the tables as a percentage of or deviation from the DAMBRK results.

152. Indirect measurements of peak discharges for the Teton flood at five locations and the one peak discharge indirect measurement for the Laurel Run flood are indicated in the tables and figures. Field measurements of high-water elevations were available at a number of locations for both the Teton and Laurel Run floods. The field measurements were interpolated as necessary to obtain the high-water elevations at the locations indicated in the tables. The various models have different schemes for determining the

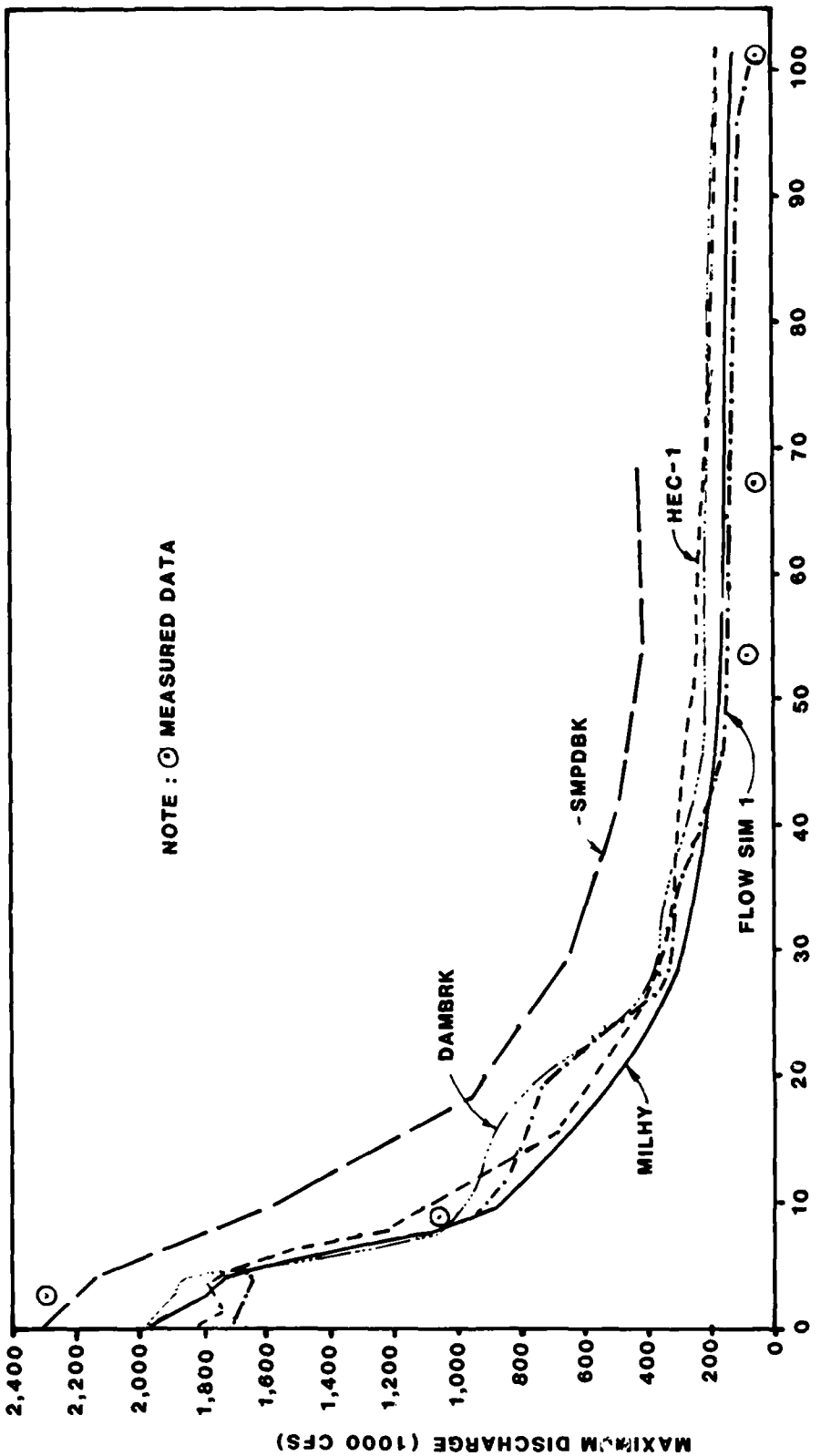

Figure 4. Peak discharges for Teton

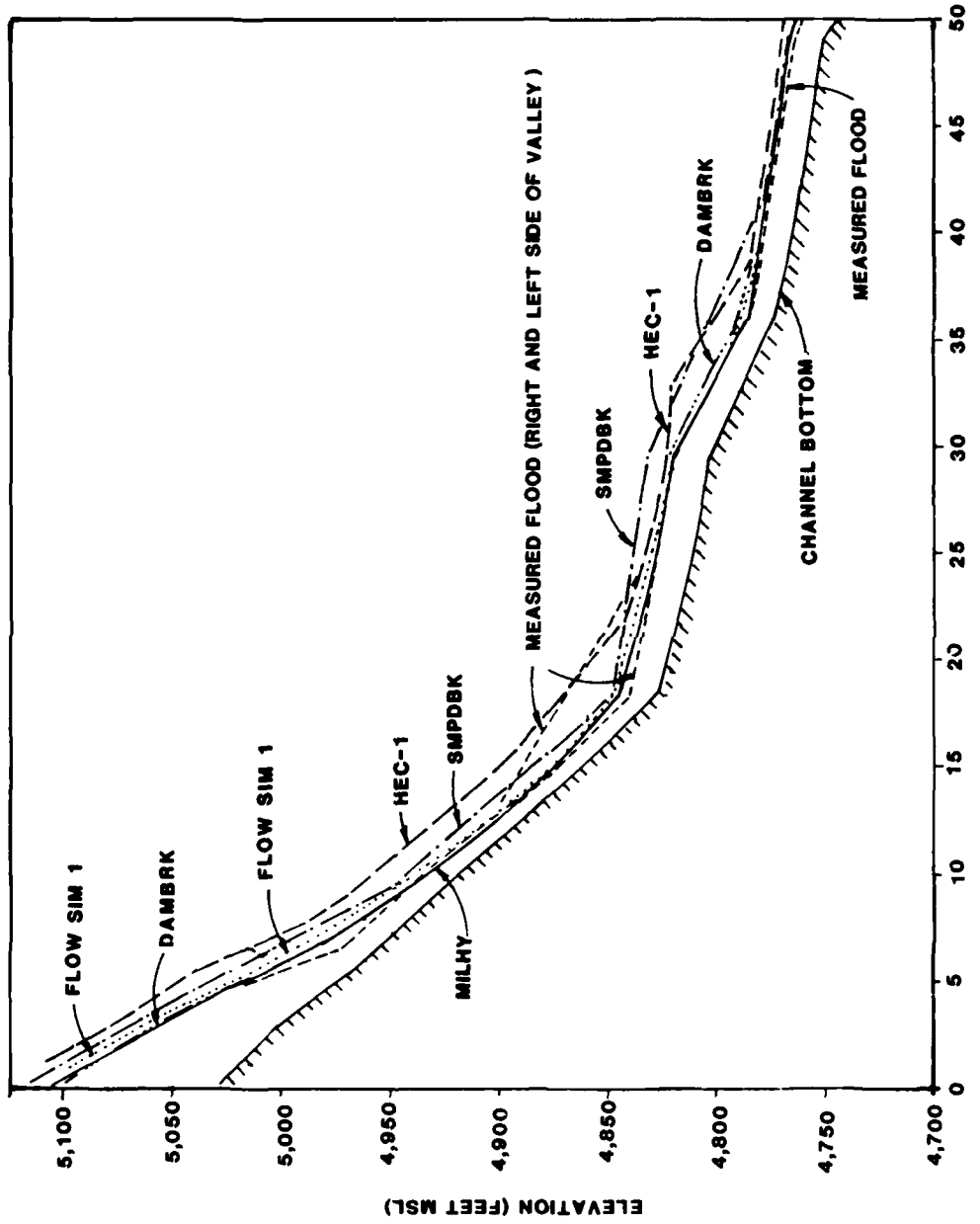

Figure 5. Peak water surface profiles for Teton (Continued)

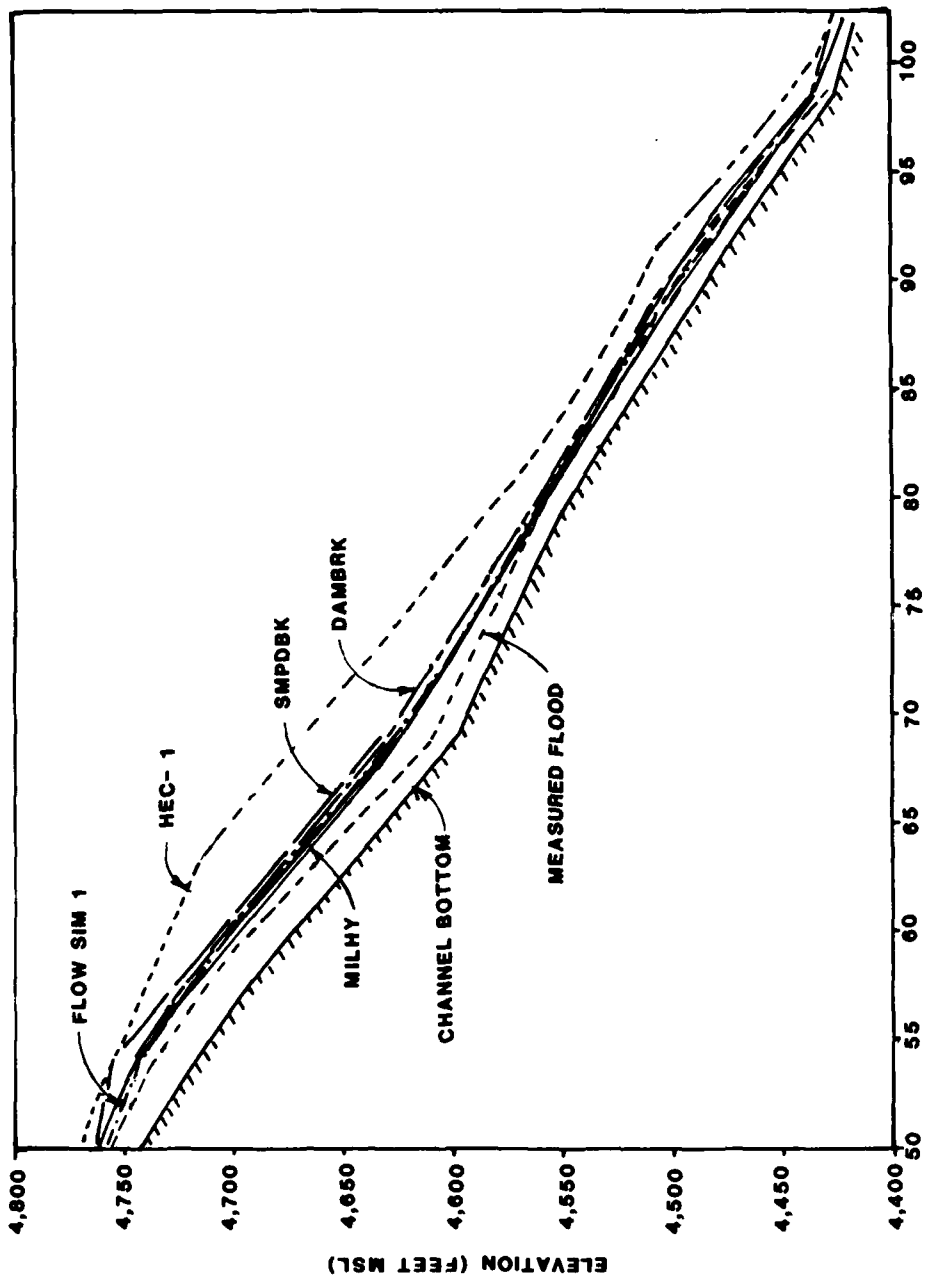

Figure 5. (Concluded)

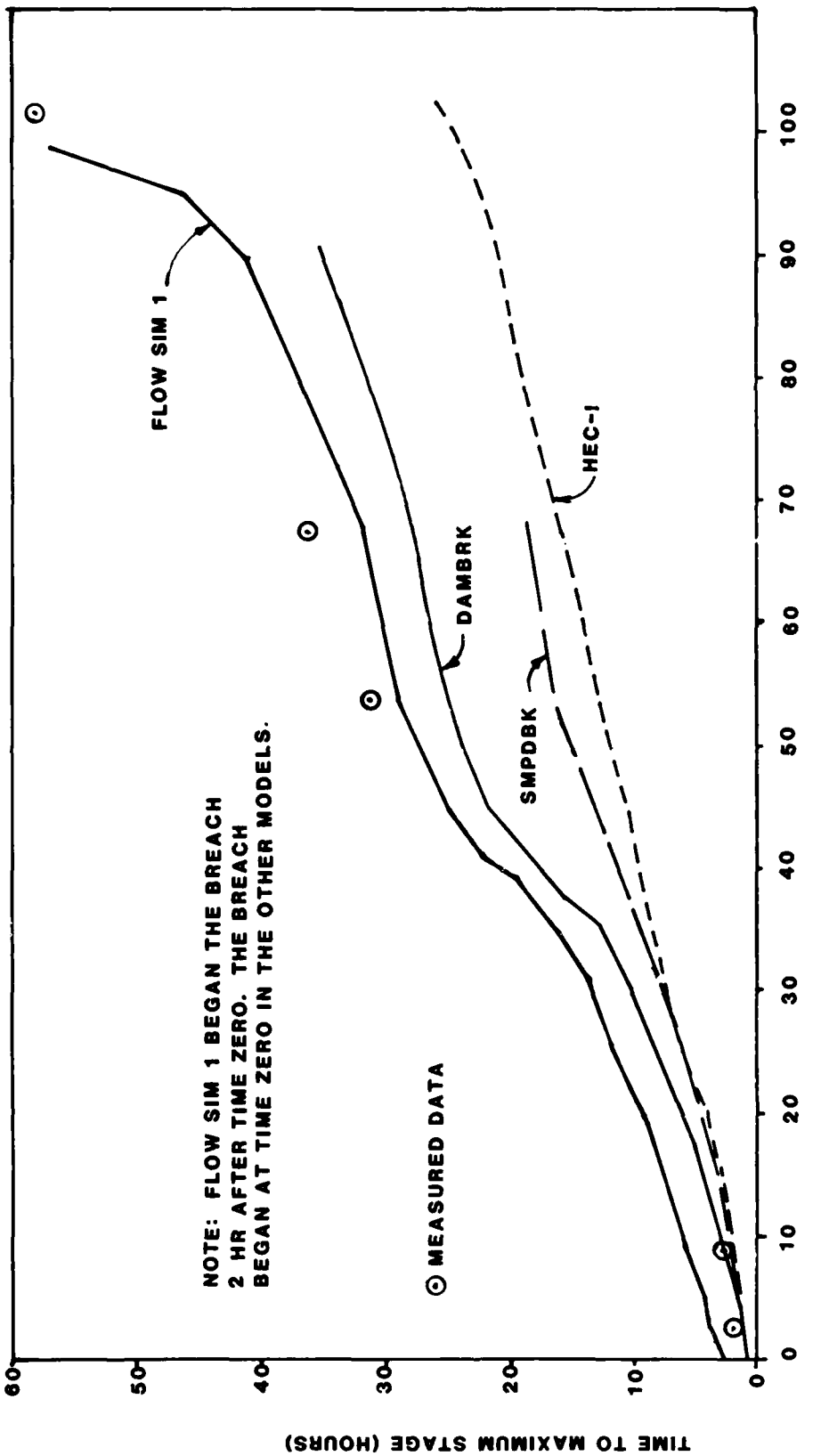

Figure 6. Time to peak depth for Teton

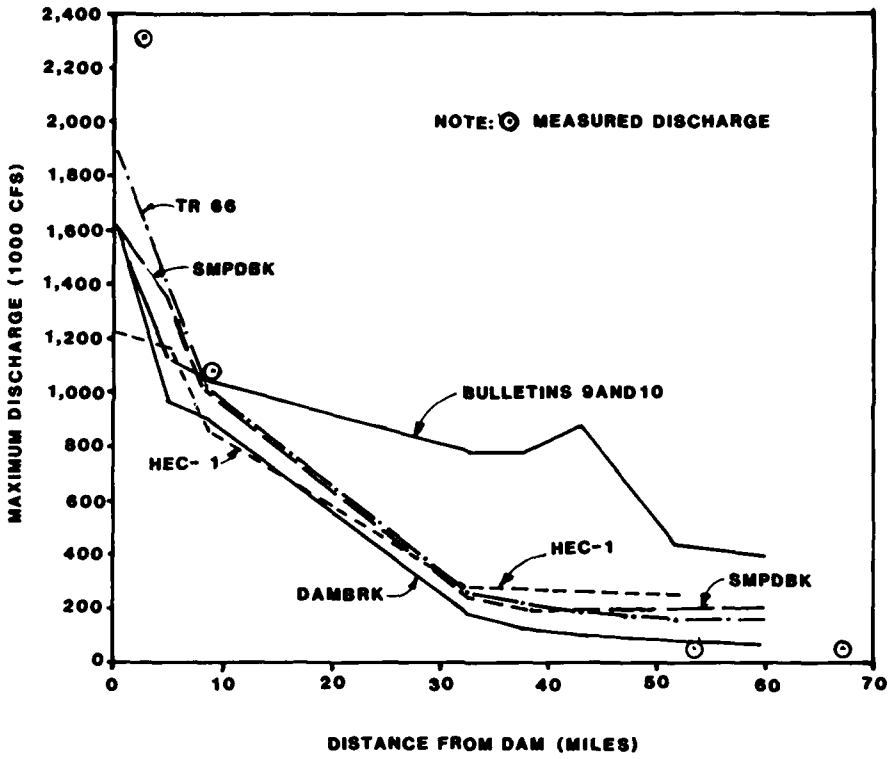

Figure 7. Peak discharges for DAMBRK test data for Teton

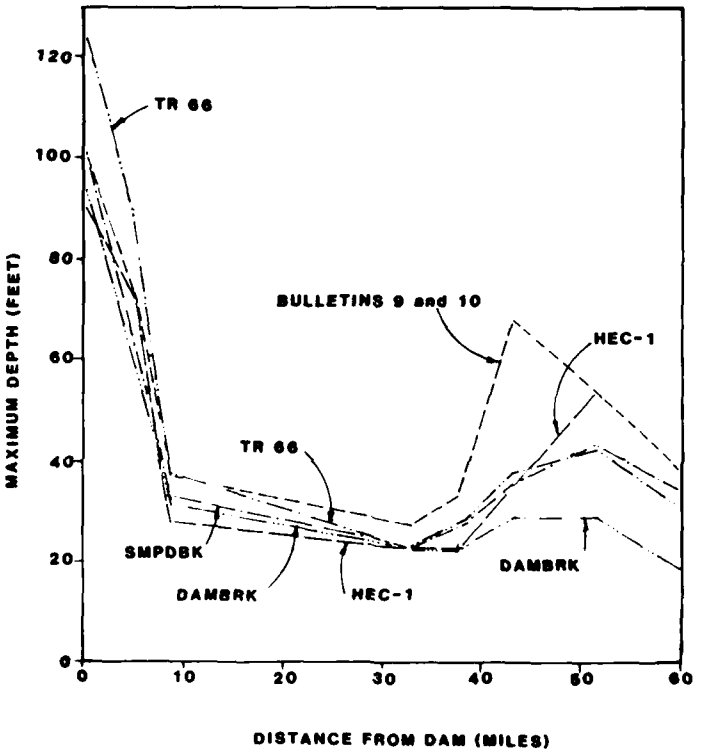

Figure 8. Peak flow depths for DAMBRK test data for Teton

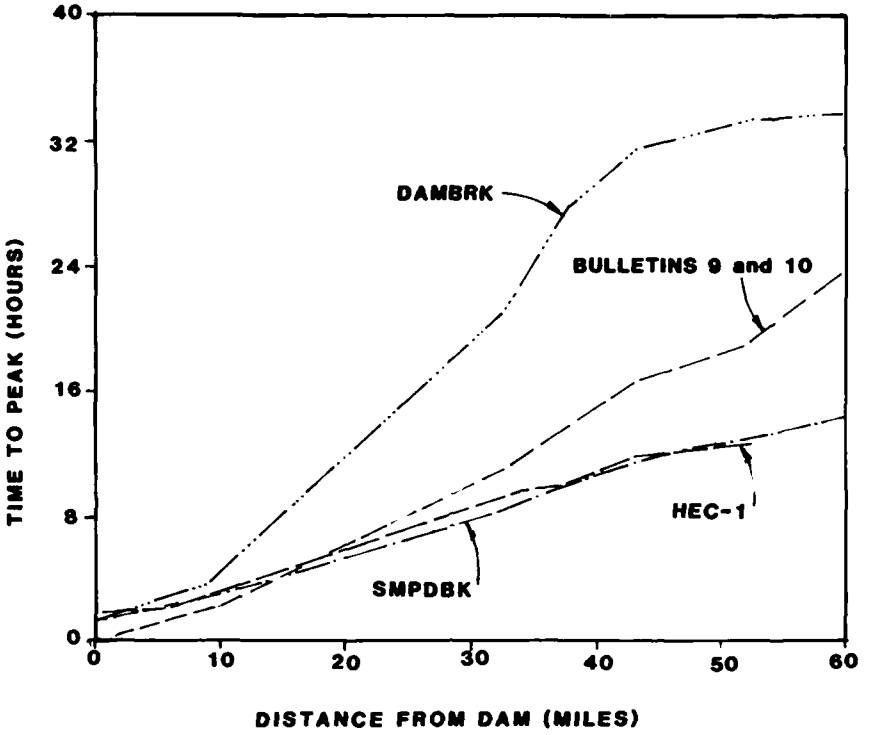

Figure 9. Time to peak for DAMBRK test data for Teton

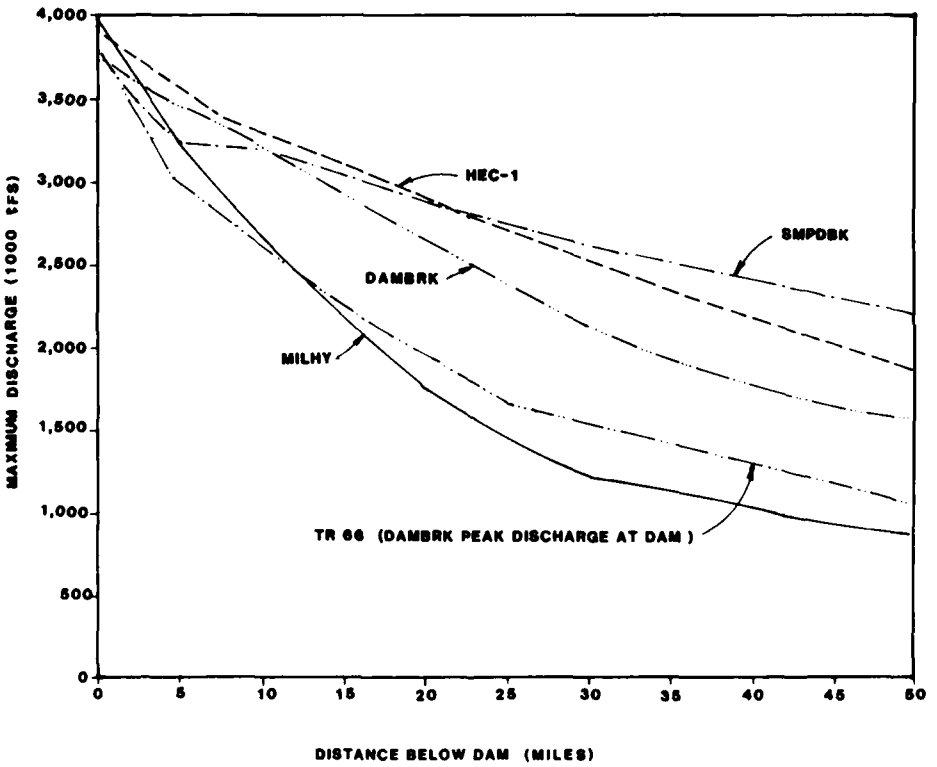

Figure 10. Peak discharges for prismatic channel

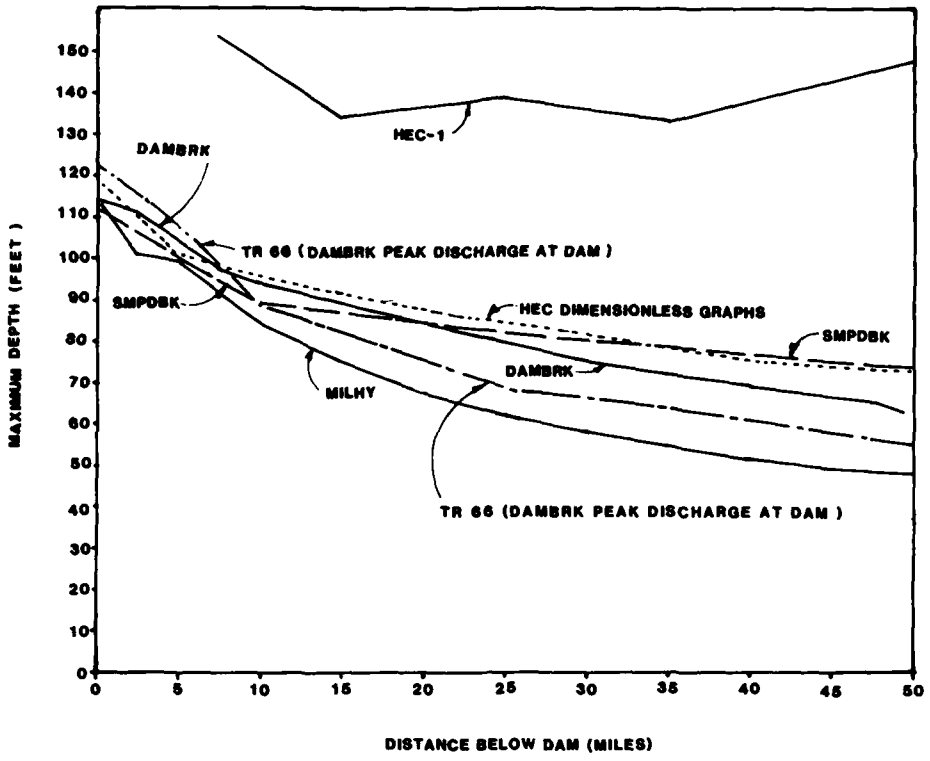

Figure 11. Peak flow depths for prismatic channel

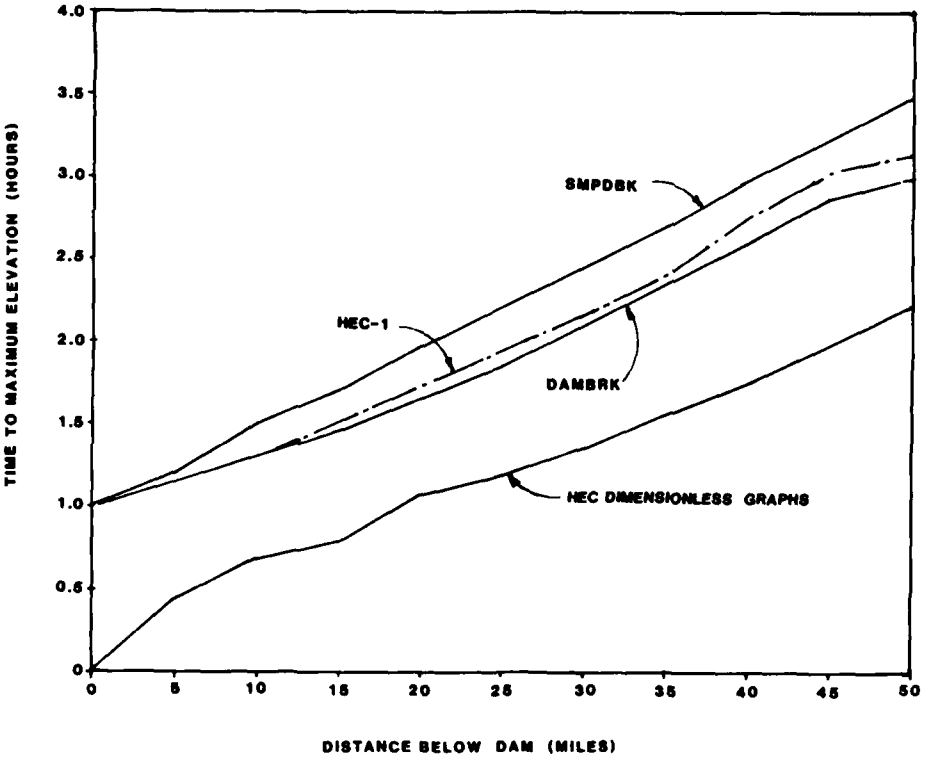

Figure 12. Time to peak depth for prismatic channel

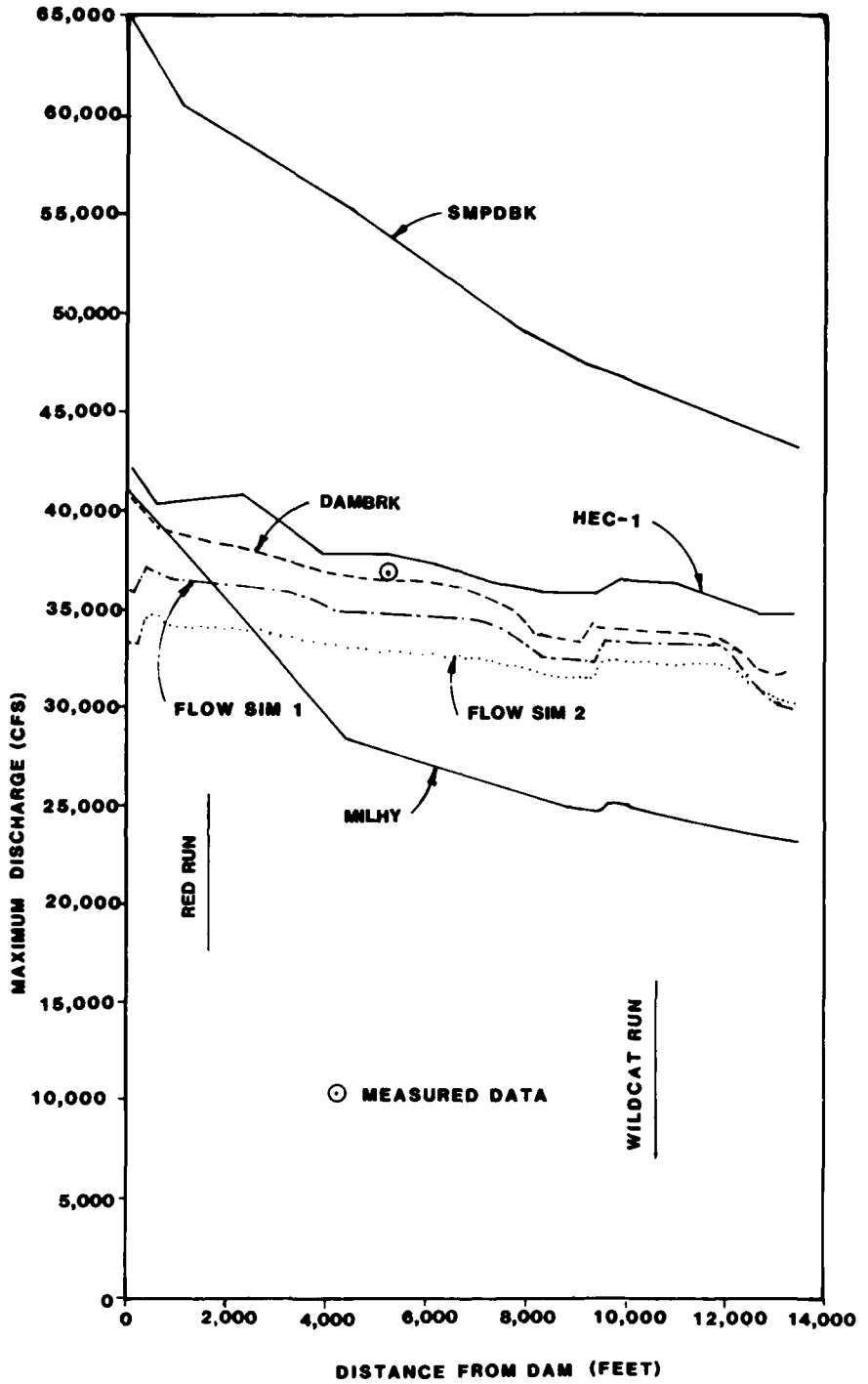

Figure 13. Peak discharges for Laurel Run

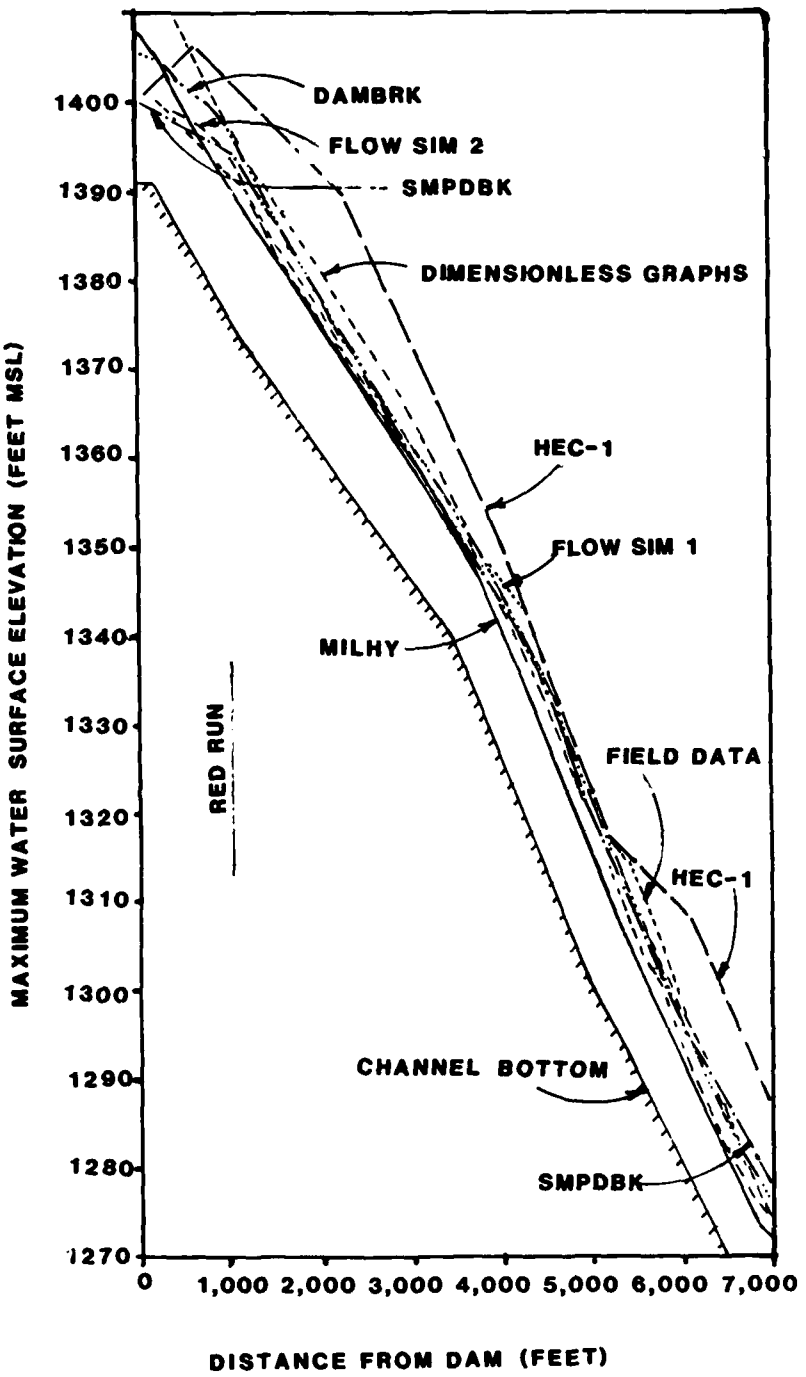

Figure 14. Peak water surface profiles for Laurel Run (Continued)

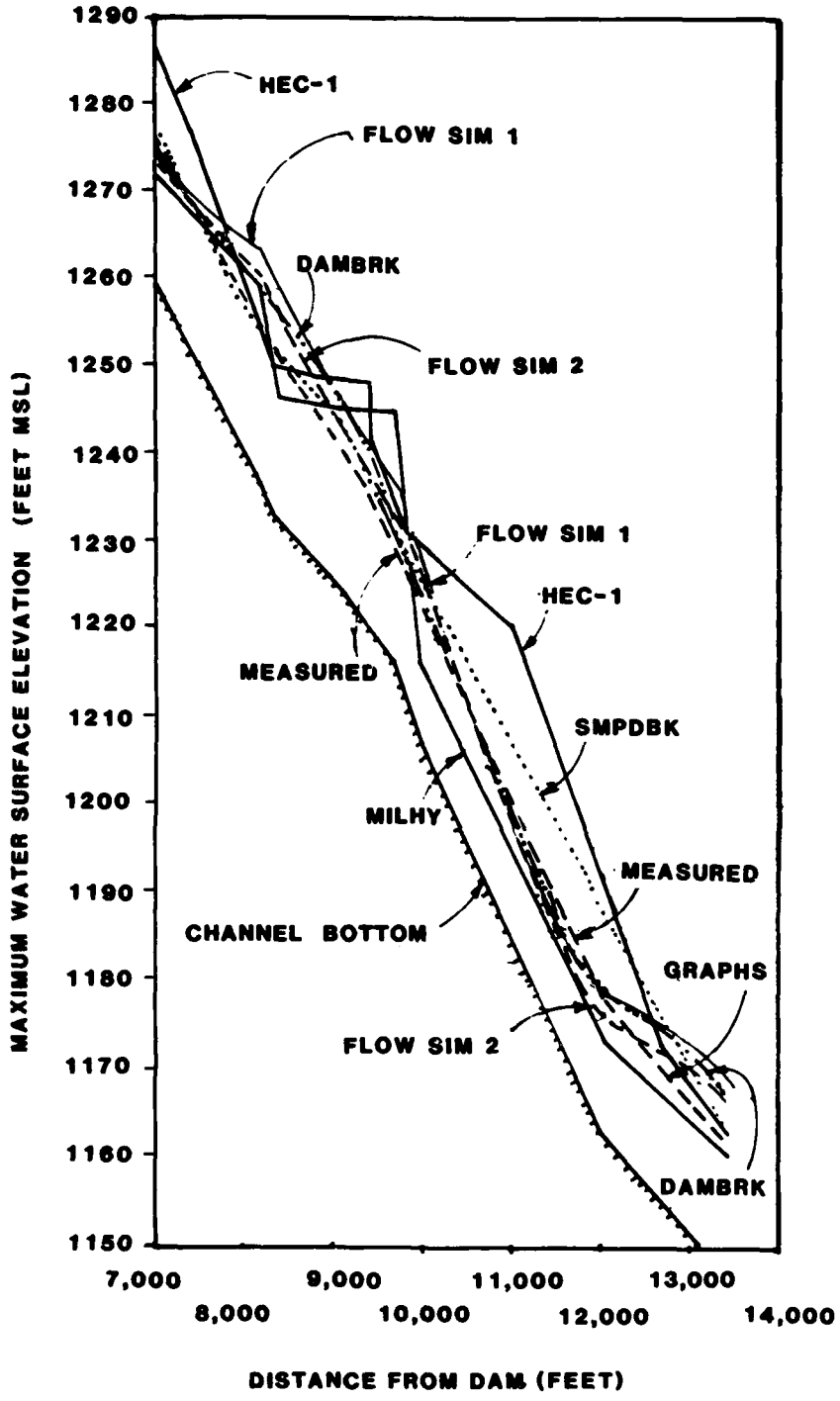

Figure 14. (Concluded)

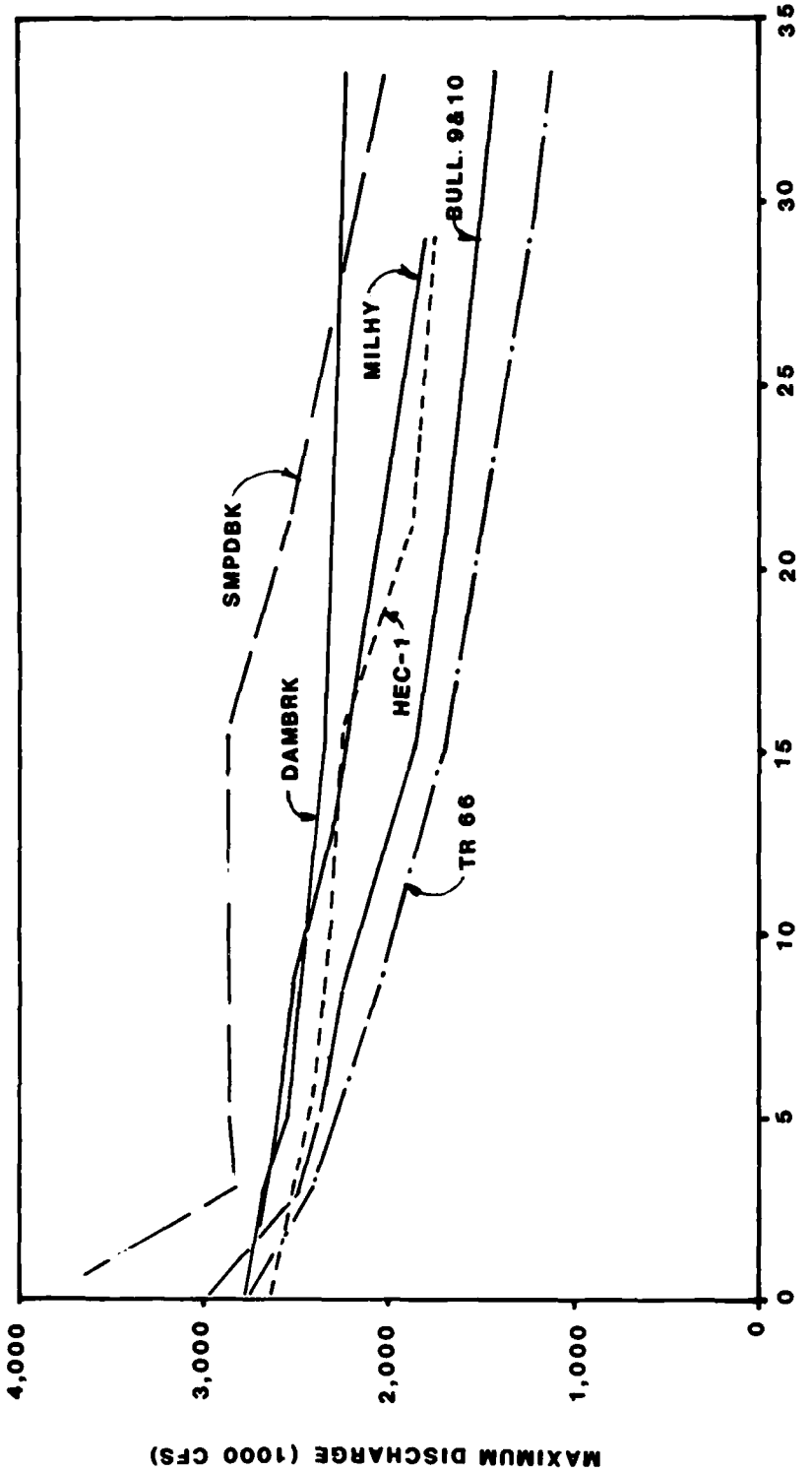

Figure 15. Peak discharges for Stillhouse Hollow

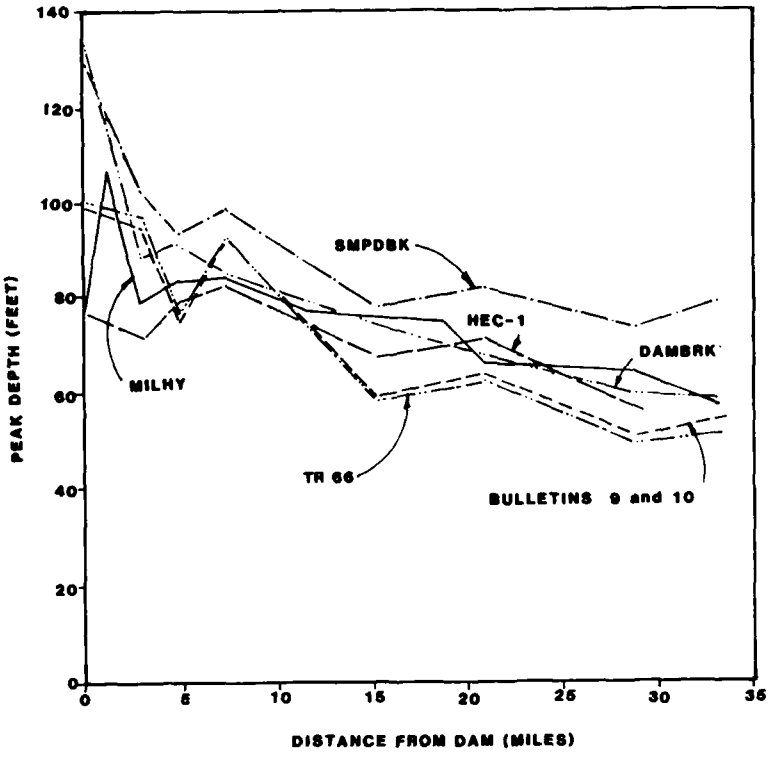

Figure 16. Peak flow depths for Stillhouse Hollow

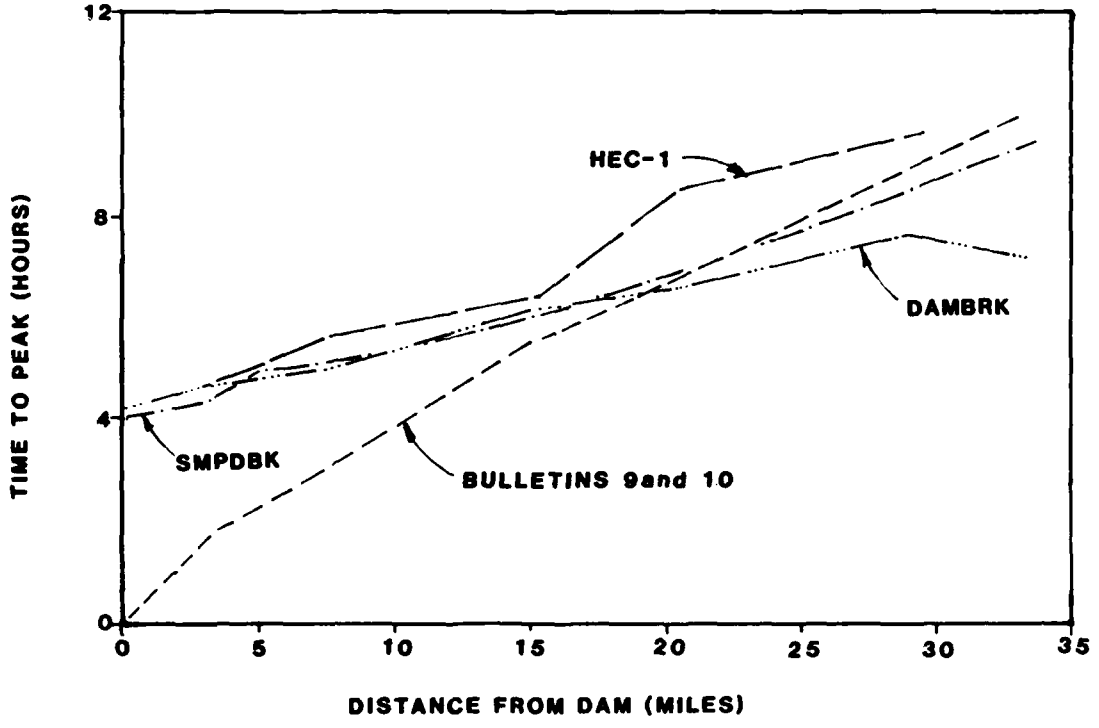

Figure 17. Time to peak flow depth for Stillhouse Hollow

channel locations at which results are printed. To facilitate comparison, model results were interpolated as necessary to obtain values for all the models at the same channel locations.

153. Table 18 represents an attempt to provide a concise quantitative measure of the performance of the models in each case study. Average deviation in peak flow depth is used to compare the models. The average deviation was computed by averaging the absolute values of the deviations shown in Tables 4, 7, 10, 13, and 16.

Teton case study

154. The Teton Dam case study actually consisted of two data sets. The DAMBRK computer program package obtained from the HEC included a set of test data for use in loading and checking the computer program. These test data are from the Teton flood but may not be completely representative of the flood in all respects. The cross sections are smoothed. The test data were run in the process of loading DAMBRK in the computer and provided a conveniently available data set for other purposes as well. This data set included 12 cross sections covering a 60-mile reach below the dam. HEC-1, SMPDBK, TR 66, and Military Hydrology Bulletins 9 and 10 were applied to the test data set as part of this study. However, an original data set was developed directly from topographic maps and data from the US Geological Survey report, independently of the test data. This data set had 21 cross sections covering 102 miles. DAMBRK, FLOW SIM 1 and 2, HEC-1, MILHY, and SMPDBK were applied to the original Teton data set.

155. In regard to the original data set, the valley geometry of the Teton and Snake Rivers below the Teton Canyon was significantly smoothed to obtain convergence to a solution with the dynamic wave models. The results shown were obtained assuming no volume losses. Otherwise, the input data were reasonably close to the best estimate of actual conditions. Since MILHY has no breach simulation capability, the reservoir outflow hydrograph computed with DAMBRK was provided as input data for MILHY.

156. Table 18 shows that, for the seven locations included in Table 4, the difference between computed and measured flood depths averaged 6.8, 5.5, 23.8, 19.4, and 8.5 ft for DAMBRK, FLOW SIM 1, HEC-1, SMPDBK, and MILHY, respectively. Thus, the differences between computed and measured peak water-surface profiles were large for all five models. FLOW SIM 1, DAMBRK, and MILHY were significantly more accurate than SMPDBK and HEC-1. Peak discharges

Table 18

Average Deviation in Peak Flow Depth

Model	Teton	Laurel Run	Teton Test Data	Prismatic Channel	Stillhouse Hollow
DAMBRK	6.8	2.9	0.0	0.0	0.0
FLOW SIM 1	5.5	4.0	--	no	no
FLOW SIM 2	no	2.8	--	no	no
HEC-1	23.8	9.7	7.6	65.5	15.2
SMPDBK	19.4	2.1	7.3	6.0	11.3
TR 66	--	--	13.2	6.3	13.5
Graphs	--	3.4	--	7.0	38.5
Bull. 9&10	--	--	18.2	--	12.6
MILHY	8.5	4.9	--	10.2	11.3

Notes:

The values given are average deviations in feet computed by averaging the absolute values of the deviations in Tables 4, 7, 10, 13, and 16.

For the Teton and Laurel Run case studies, the deviation is the maximum water-surface elevation computed with the model minus the measured high-water elevation.

For the Teton test data, prismatic channel, and Stillhouse Hollow Dam case studies, the deviation is the maximum water-surface elevation computed using a given model minus that computed using DAMBRK.

The MILHY and TR 66 analyses were limited to valley routing with the reservoir outflow hydrograph computed with DAMBRK provided as input data.

computed with DAMBRK were 82 to 297 percent of the measured peak discharges. FLOW SIM 1, MILHY, HEC-1, and SMPDBK had peak discharges of 73 to 223 percent, 92 to 238 percent, 76 to 327 percent, and 97 to 620 percent, respectively, of the measured values. Table 5 shows that the computed times to peak depth were significantly less than measured values. The FLOW SIM 1 times to peak shown in the table are actually not comparable to the other data because the breach began to form about 2 hr after time zero when the simulation began.

157. FLOW SIM 2 is not shown; because of computational instability, a solution was not obtained. The dimensionless graphs were considered to be almost meaningless for the extremely nonprismatic valley of the Teton and Snake Rivers.

158. For the Teton data furnished as test data with DAMBRK, the average deviations in peak flow depth shown in Table 18 are based on a comparison with

the DAMBRK values. SMPDBK, HEC-1, TR 66, and Military Hydrology Bulletins 9 and 10 resulted in peak flow depths averaging 7.3, 7.6, 13.2, and 18.2 ft, respectively, higher than those computed with DAMBRK. Peak discharge and time to peak depth variations are shown in Tables 6 and 8.

Hypothetical prismatic channel case study

159. Even with a prismatic channel, the results obtained with the different models varied significantly. The peak flow depths computed using the alternative models are compared in Tables 10 and 18 using the DAMBRK results as a base for comparison. The DAMBRK peak depths for the seven locations shown in Table 10 averaged 84.7 ft. Deviations from the DAMBRK peak depths averaged 6.0, 6.3, 7.0, 10.2, and 65.5 ft for SMPDBK, TR 66, dimensionless graphs, MILHY, and HEC-1, respectively. HEC-1 peak depths were from 155 to 278 percent of the DAMBRK peak depths. MILHY peak depths varied from 75 to 100 percent of the DAMBRK peak depths. The peak depths for SMPDBK, TR 66, and the dimensionless graphs are from 88 to 114 percent of the DAMBRK results for the first 40 miles. SMPDBK and the dimensionless graphs peak depths were 138 percent of the DAMBRK depth at mile 50.

160. HEC-1 peak discharges were from 102 to 123 percent of the DAMBRK values. SMPDBK peak discharges were from 93 to 141 percent of the DAMBRK values. As discussed below, the TR 66 peak discharge was set equal to 100 percent of the DAMBRK value at the dam. The TR 66 peak discharge decreased to 67 percent of the DAMBRK value 50 miles below the dam. The dimensionless graphs do not provide peak discharges.

161. Times to peak depth are shown in Table 11. HEC-1 and DAMBRK results varied by 6 percent or less. SMPDBK times to peak were within 20 percent of DAMBRK. The dimensionless graph times were significantly less than the other models due to the assumption of an instantaneous complete removal of the dam. TR 66 does not provide times to peak.

162. The base-run breach characteristics consisted of a 500-ft-wide rectangular overtopping breach formed over a 1-hr time period. Breach dimensions varied linearly with time. DAMBRK, HEC-1, and SMPDBK have the capability to model this type of breach. The dimensionless graphs are based on an instantaneous complete removal of the dam. The TR 66 breach outflow procedure is based on reservoir depth versus peak breach outflow data from actual past dam failures. This procedure resulted in a peak discharge at the dam of

1,931,000 cfs, which is about half the values computed with the other models. The TR 66 valley routing procedure is independent of the breach peak discharge computation procedure. Consequently, the DAMBRK peak discharge at the dam of 3,841,000 cfs was adopted for the TR 66 analysis shown in the tables, with all the other computations following the TR 66 procedure.

163. A solution could not be obtained for the base-run breach characteristics using FLOW SIM 1 and 2 due to difficulties with computational instability. Successful runs with FLOW SIM 1 and DAMBRK for a breach width of 100 ft were similar in terms of results. Peak discharges computed with FLOW SIM 1 were from 85 to 90 percent of those computed with DAMBRK. FLOW SIM 1 peak depths were 95 to 98 percent of the DAMBRK peak depths.

Laurel Run case study

164. The one indirect peak discharge measurement on Laurel Run was made at a location about a mile below the dam. The peak discharges computed with DAMBRK, FLOW SIM 1, FLOW SIM 2, HEC-1, and SMPDBK were 99, 94, 89, 102, and 145 percent of the measured value.

165. Deviations from the measured high-water elevations at seven locations evenly spaced along the channel averaged 2.1, 2.8, 2.9, 3.4, 4.0, 4.9, and 9.7 ft for SMPDBK, FLOW SIM 2, DAMBRK, dimensionless graphs, FLOW SIM 1, MILHY, and HEC-1, respectively. The average measured flow depth was 15.6 ft. The DAMBRK peak depths were from 85 to 141 percent of the measured values. FLOW SIM 1, FLOW SIM 2, MILHY, and HEC-1 peak depths were 83 to 159 percent, 78 to 139 percent, 61 to 138 percent, and 146 to 198 percent, respectively, of measured values. SMPDBK and the dimensionless graphs peak depths were 90 to 149 percent and 89 to 213 percent of measured.

166. The times to peak flow depth computed with the alternative models are shown in Table 14. Corresponding measured data are not available. The FLOW SIM 1 and FLOW SIM 2 times are not comparable to the DAMBRK times because DAMBRK started the breach at time zero and FLOW SIM 1 and FLOW SIM 2 started the breach several minutes after time zero. The assumption of an instantaneous breach with the dimensionless graph resulted in the times being less than those computed with the other models. A breach formation time of 15 min was used in the other models.

167. The Manning roughness coefficients were increased in the dynamic routing models to prevent supercritical flow from occurring. The values used in DAMBRK and FLOW SIM 1 were twice the actual estimated values. FLOW SIM 2

used roughness coefficient values 1.5 times the actual estimated values. As discussed in the later section on sensitivity analyses, doubling the Manning roughness coefficients raises the peak water-surface profile several feet. Thus, the flow depths shown for the three dynamic routing models should be significantly higher than those actually observed.

Stillhouse Hollow case study

168. The average deviations in peak depth between the values computed by DAMBRK and the other models at the seven locations indicated in Table 16 are shown in Table 18. The average deviations for MILHY, SMPDBK, Military Hydrology Bulletins 9 and 10, TR 66, HEC-1, and the dimensionless graphs were 11.3, 11.3, 12.6, 13.5, 15.2, and 38.5 ft. The average peak depth computed with DAMBRK was 82.8 ft (Table 16). Thus, the average deviation in peak depth between DAMBRK and either SMPDBK or MILHY was 13.6 percent of the DAMBRK average peak depth. Comparing the dimensionless graphs with DAMBRK, the difference is 66 percent.

169. The HEC-1 peak discharges (Table 15) ranged from 79 to 96 percent of the DAMBRK peak discharges. MILHY, SMPDBK, TR 66, and Military Hydrology Bulletins 9 and 10 peak discharges ranged from 76 to 102 percent, 91 to 138 percent, 50 to 100 percent, and 63 to 108 percent, respectively, of the corresponding DAMBRK results.

170. The times to peak flow depth (Table 16) computed with HEC-1, SMPDBK, dimensionless graphs, and Bulletins 9 and 10 ranged from 100 to 130 percent, 93 to 131 percent, 0 to 51 percent, and 0 to 139 percent, respectively, of the corresponding DAMBRK values. The dimensionless graphs and Military Hydrology Bulletins 9 and 10 are based on the assumption of an instantaneous failure. A breach time of 4 hr was used in the other models.

171. The peak discharge at the dam was computed to be 1,174,000 cfs using the TR 66 procedure, which is based on reservoir depth versus discharge data from actual past dam failures. Since the TR 66 peak discharge at the dam is much less than the values computed using the other models, the DAMBRK value of 2,783,000 cfs was adopted for the TR 66 analysis with all other computations following the TR 66 procedure.

Sensitivity Analyses

172. The comparative summary of results presented in the preceding paragraphs was limited to a single base run for each model applied to each case study. Numerous other runs were made with variations in the values of selected input data. Analyses were thus made of the sensitivity of model results to key input parameters. The sensitivity analyses also provided an additional test of model performance by verifying that results respond in a reasonable manner to changes in input data. Several of the key sensitivity analyses are summarized in the following paragraphs.

173. Quantifying breach characteristics is a major area of modeling uncertainty. Mathematically reproducing the actual Teton and Laurel Run breaches accurately is difficult even though information regarding the breaches is available. Predicting the breach characteristics of a dam that has not actually failed is necessarily highly uncertain. Consequently, a number of the sensitivity analyses focused on breach parameters. The effects of varying breach parameters are most pronounced near the dam, diminishing downstream. An analysis of the Teton flood using DAMBRK indicates that changing the breach time from 1 to 2 hr, with all other input data held constant, results in an 8.2-ft decrease in peak stage just below the dam, diminishing to a 0.4-ft decrease 9.5 miles below the dam and a few tenths of a foot or less change at locations further downstream. Changing the breach time from 1 to 0.5 hr increases the peak stage 1.8 ft at the dam, diminishing to essentially no change 9.5 miles below the dam. A DAMBRK analysis of the prismatic channel case study shows that widths of the rectangular breach of 100, 300, and 500 ft result in peak depths of 62.5, 99.2, and 114.6 ft just below the dam. Corresponding depths 50 miles downstream are 42.6, 50.9, and 53.0 ft. The results of this sensitivity analysis are plotted in Figures 18-20. A FLOW SIM 1 analysis of the Laurel Run data set indicates that doubling the breach time from 15 to 30 min results in a 3.0-ft decrease in peak stage just below the dam and a 0.5-ft decrease 2.5 miles downstream. Reducing the breach time from 15 to 5 min results in a 2.1-ft peak stage increase just below the dam and a 0.5-ft increase 2.5 miles downstream. Figure 21 shows the sensitivity of peak discharges to breach time for the Laurel Run data.

174. The DAMBRK analysis indicates that a 50-percent increase in the Manning roughness coefficient (n) values for Teton results in an increase in

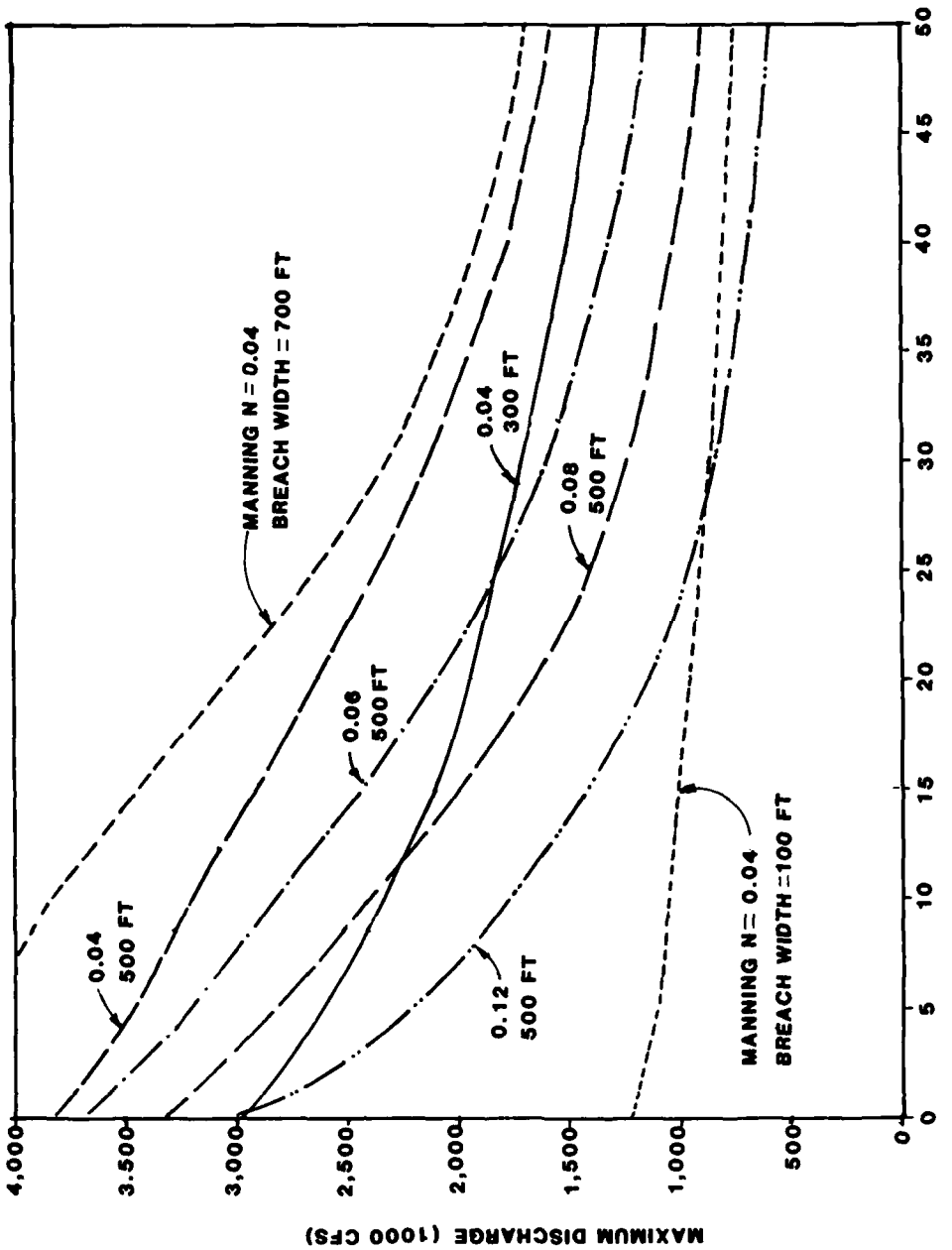

Figure 18. Sensitivity to Manning coefficient and breach width, peak discharge, prismatic channel, DAMBRK

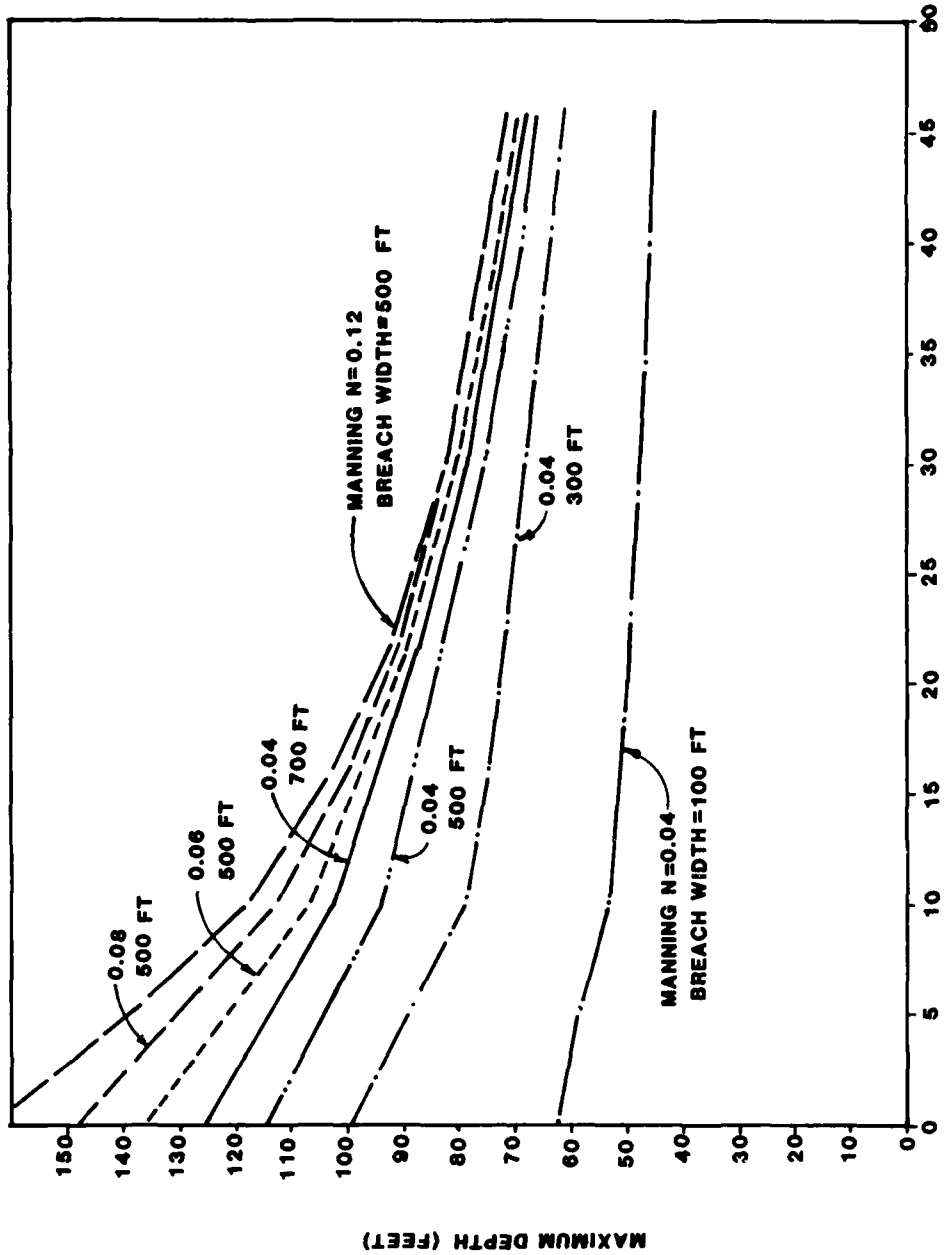

Figure 19. Sensitivity to Manning coefficient and breach width, peak depth, prismatic channel, DAMBRK

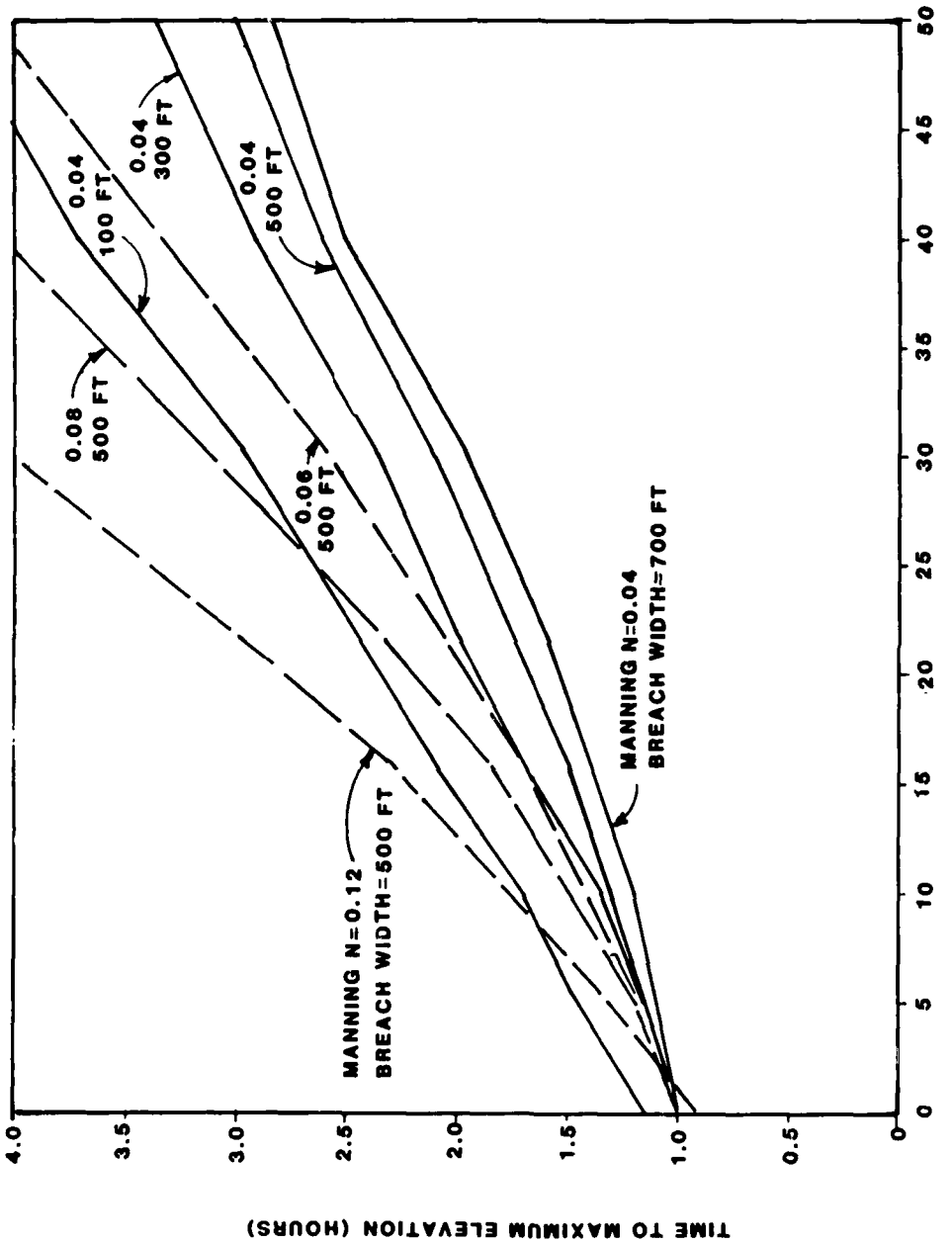

Figure 20. Sensitivity to Manning coefficient and breach width, time to peak depth, prismatic channel, DAMBRK

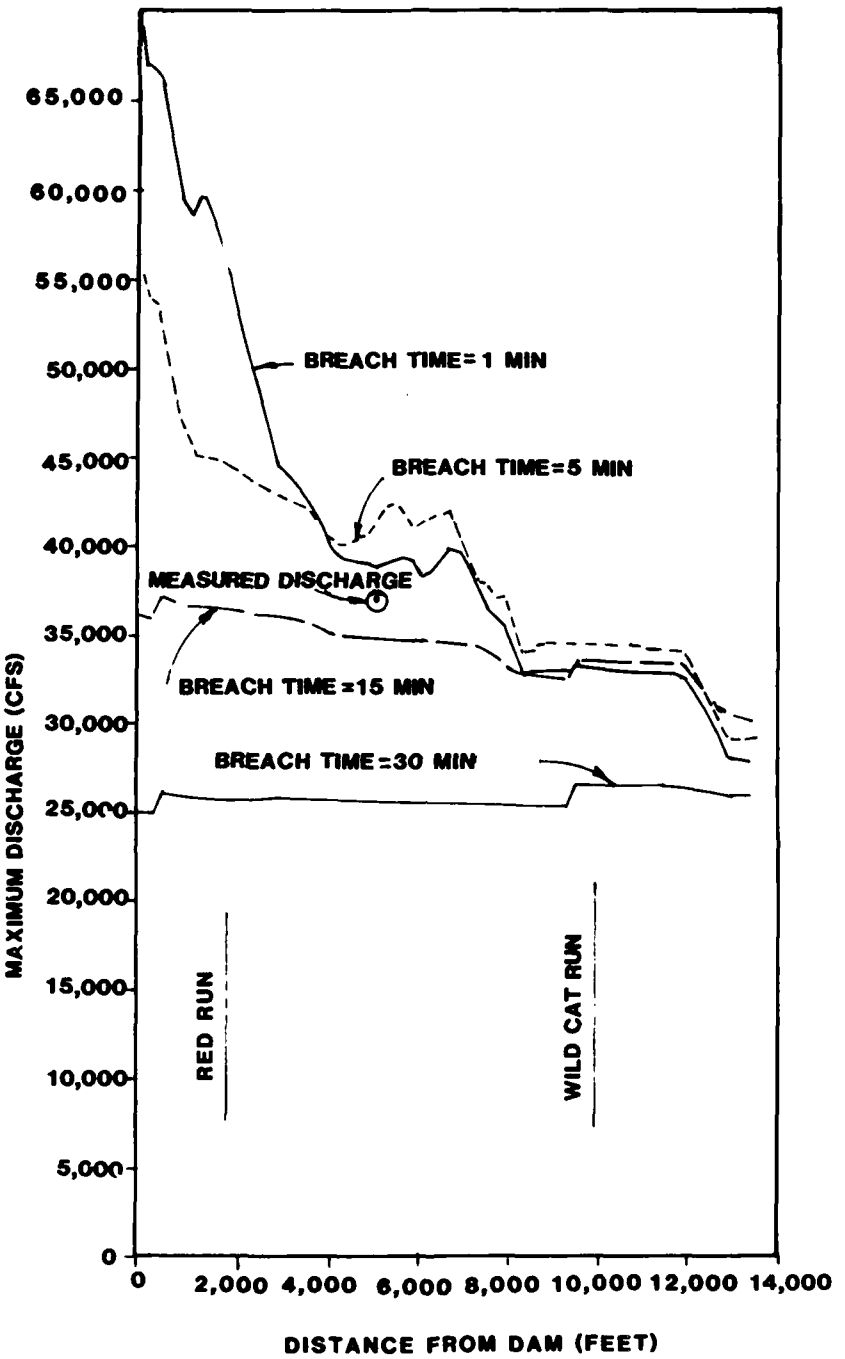

Figure 21. Sensitivity to breach times, peak discharge, Laurel Run, FLOW SIM 1

peak stage of 1 to 2 ft along most of the valley but up to almost 15 ft near the dam. For the prismatic channel case study, DAMBRK results indicate that a 50-percent increase in Manning n values results in a 22-ft increase in peak stage at the dam and a 4-ft increase 40 miles below the dam. The Manning n sensitivity analysis results for the prismatic channel are also shown in Figures 18-20. Doubling Manning n values in the FLOW SIM 2 analysis of Laurel Run increased peak stages from 3 to 6 ft.

175. With DAMBRK, FLOW SIM 1, and FLOW SIM 2, active and inactive flow areas can be differentiated. The inactive areas represent portions of the valley which provide significant storage with negligible conveyance. The dynamic routing models are the only models which can simulate this flow characteristic. The valley below Teton Dam was modeled with a significant portion of many of the cross sections designated inactive, containing storage but not conveying flow. Runs were also made in which the total area at each cross section was designated active, with no inactive areas. DAMBRK peak discharges computed using a best-estimate division between active and inactive areas, and discharges computed assuming the entire cross section to be active are shown in Figure 22. In the downstream reaches, flows depths were up to 8 ft higher for the run that did not consider inactive areas.

176. The Teton Dam failure resulted in a tremendous flood wave inundating a large area of dry ground. American Falls Reservoir, located 100 miles downstream, contained the entire inflow; however, about a third of the total volume released from Teton Reservoir was lost before reaching American Falls Reservoir. The DAMBRK analysis included runs with and without volume losses. Near the dam, volume losses have little effect on peak stage but decrease it by up to 10 ft further downstream. This means that near the downstream end of the study reach, peak flow depth determined without volume loss is over twice the depth with volume loss. The peak discharges with and without volume losses are shown in Figure 22.

177. The number of routing steps or subreaches in a reach (HEC-1 variable NSTPS) is a calibration parameter used in the modified Puls routing procedure. In the absence of observed hydrographs to use for model calibration, the number of routing steps associated with each reach is difficult to estimate precisely. Values of the NSTPS parameter are often approximated as the reach travel time divided by the computational routing time interval. The case study analyses showed that selection of NSTPS values for each routing

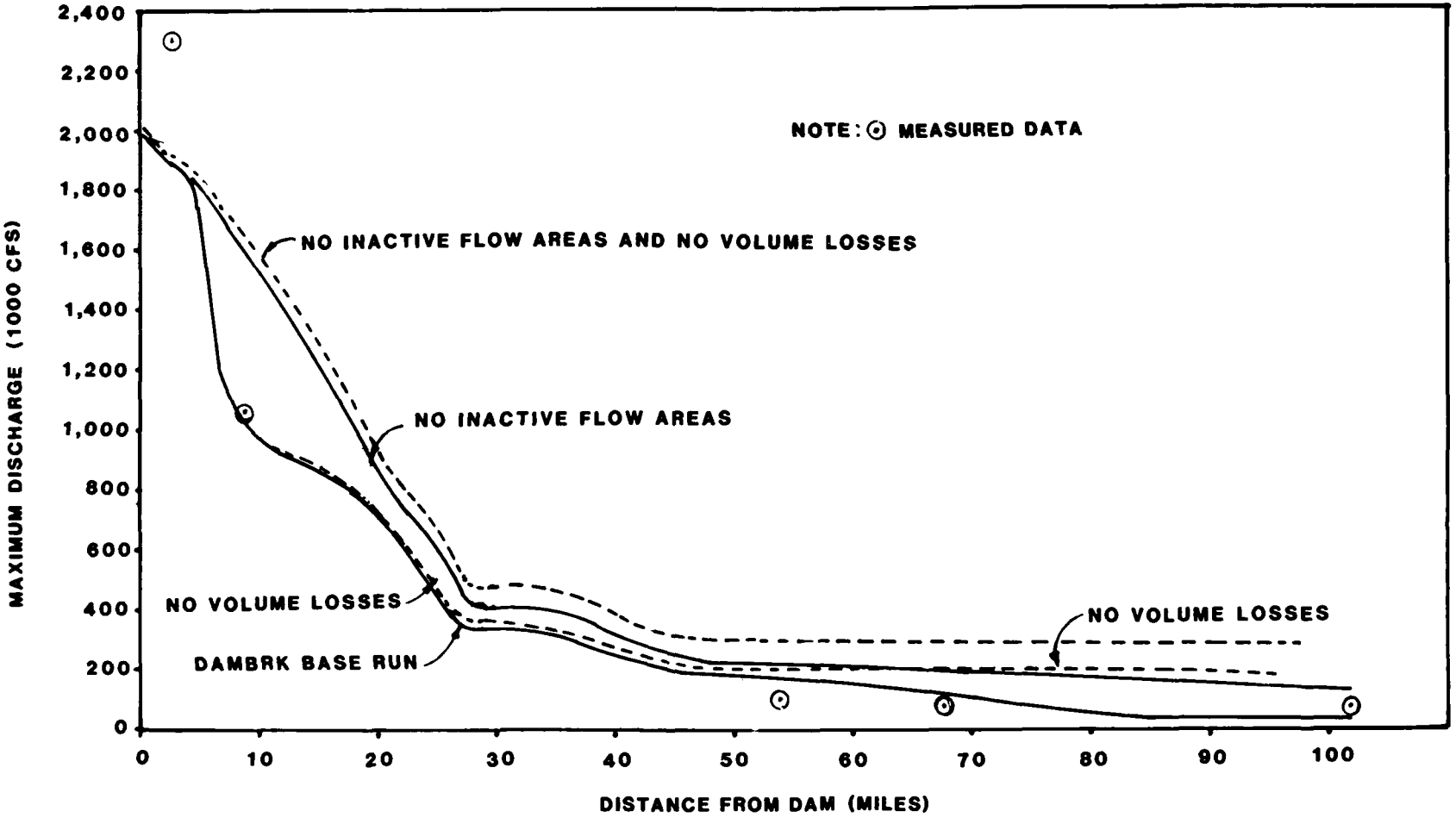

Figure 22. Sensitivity to volume losses and inactive areas, peak discharge, Teton, DAMBRK

reach significantly affected the results obtained with HEC-1. Figure 23 compares runs with different NSTPS values for the hypothetical prismatic channel case study. NSTPS values of 4, 5, 7, 8, and 13 were estimated for each of five reaches using the rule-of-thumb that the number of subreaches should be approximately the travel time divided by the routing interval (HEC 1981). Alternative runs made with NSTPS values of 1 for all reaches and also with constant values of 5 and 10 for all reaches are also included in Figure 23.

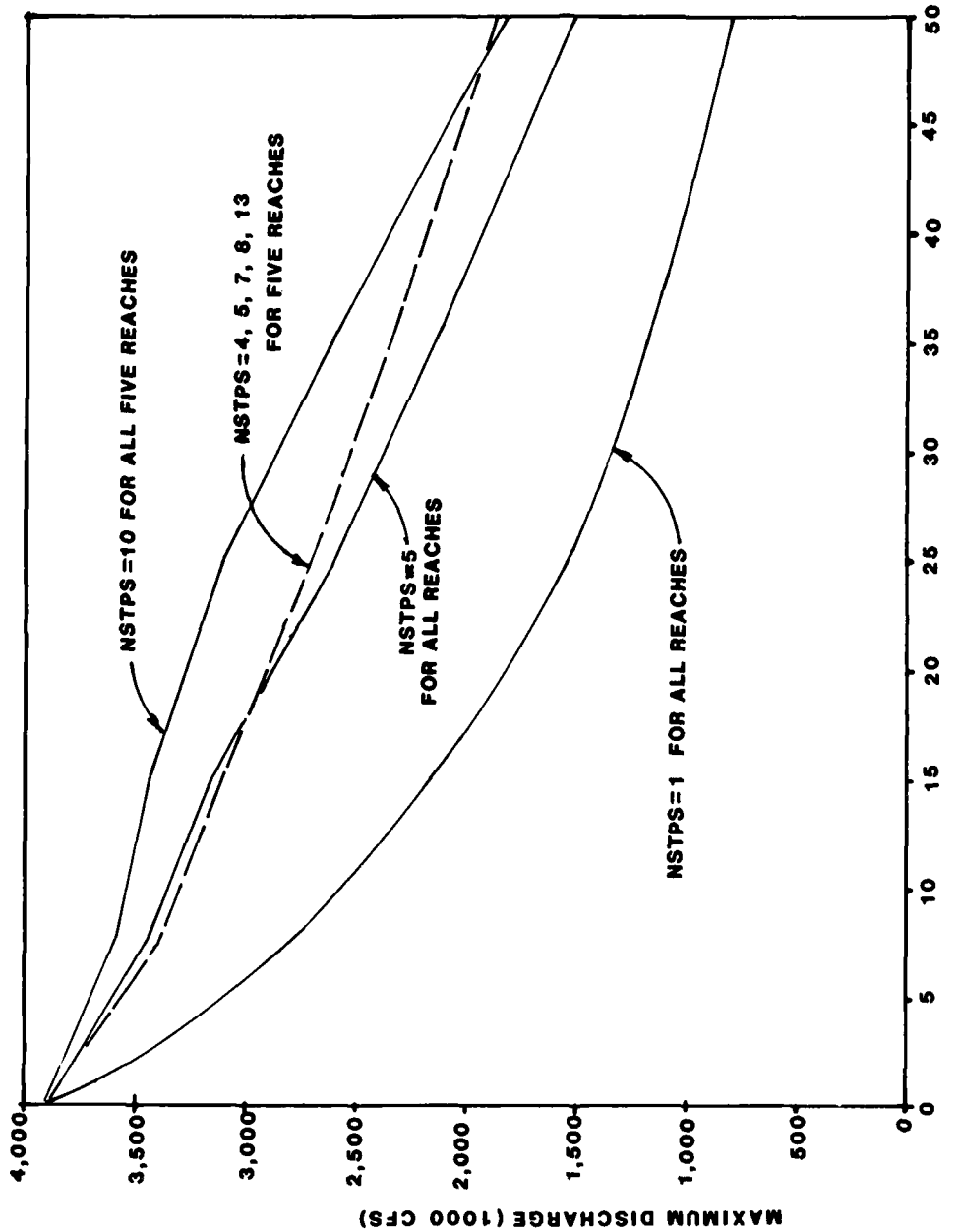

Figure 23. Sensitivity to number of routing steps, peak discharge, prismatic channel, HEC-1

PART IV: MODEL EVALUATION AND COMPARISON

178. The following comparative evaluation of dam-breach flood forecasting models extends and elaborates upon the material addressed in the preceding two parts of this report. Conclusions are reached based upon: (a) consideration of the underlying concepts and theory incorporated into the models and analysis capabilities provided by the models, (b) findings reported in the published and unpublished literature with respect to application, testing, evaluation, and comparison of various models, and (c) experience gained in the case study analyses reported in Part III. The objective is to provide an overall assessment of the state of the art of dam-breach flood wave analysis which can serve as a basis for selecting and adapting specific models for military use. The approach taken is to focus on a select group of leading models which are representative of the current state of the art.

Comparative Evaluations Reported in the Literature

179. The currently available dam-breach flood forecasting models have been tested and evaluated to various extents by the model developers and users. A typical approach for testing the models has been to analyze past dam failures and compare the model results with actual measured field data. Significant experience has been acquired in applying several of the models in dam safety studies. However, few investigations have been made of the trade-offs and merits of the models relative to each other. Military Hydrology Report 9 (Wurbs 1985a) addresses the availability of reported studies which test, evaluate, and compare available dam-breach flood forecasting models. Several studies similar to or particularly pertinent to the comparative evaluation reported herein are cited below.

US Geological Survey

180. An evaluation of four dam-break flood wave computer programs was made by Larry F. Land of the USGS Gulf Coast Hydroscience Center. using three data sets and selected criteria of desirable model features. The investigation is documented in detail in a USGS report (Land 1980a) and is also discussed in a journal article (Land 1980b).

181. The models evaluated were the NWS Dam-Break Flood Forecasting Model (DAMBRK), the HEC Gradually Varied Unsteady Flow Profile Model (USTFLO),

the USGS coupled method of characteristics and general-purpose linear implicit finite difference models (MOC-LIF), and the USGS modified Puls model (MP). The data sets were from failures of Teton Dam, Idaho, in 1976; Laurel Run Dam, Pennsylvania, in 1977; and Kelly Barnes Dam, Georgia, in 1977. The criteria for model evaluation were several desirable dam-break model features and the models' ability to accurately simulate field occurrences. The desirable features included such items as requiring only readily available data; having numerical stability and accuracy; simulating flow on hydraulically mild or steep slopes; and having simplicity, flexibility, and economy.

182. Land's results and conclusions are summarized as follows. Model results were compared with field data. Except for the Teton Dam analysis, computed peak discharges were often within 20 percent of the values obtained by indirect methods based on the field data. Computed crest elevations were usually within 2 ft of high-water marks. Results for the Teton Dam showed greater deviations between computed and measured values than for the other two dams. (The Teton and Laurel Run dam failures are included in the case study analysis performed as a part of the investigation reported herein, except that 102 miles of the valley below Teton Dam was modeled rather than the 9 miles included in Land's studies.)

183. Although no error analysis between the computed and observed data was made, it appeared that the DAMBRK model achieved the best results. The MP model appeared to be second best. The MOC-LIF tended to compute high discharges and stages in the stream reach immediately below the dam and also had relatively high mass-balance errors.

184. The MP model was most stable, followed by DAMBRK, MOC-LIF, and USTFLO. The MOC-LIF model often required minor time step and data alterations to achieve stability. The results from the MOC-LIF simulations showed some irregularities. Occasionally, the USTFLO model would not stabilize.

185. Another feature evaluated was the ease of getting the model operational, making minor adjustments for subsequent runs, and making calibrations and production runs. The MP model was easiest to get running. The most difficult were the MOC-LIF and the USTFLO. Major data alterations are likely to be required for the LIF model. To prevent failure, the USTFLO model may also require major data alterations. The MP and DAMBRK models were easiest to run because they are one-step operations. The USTFLO model usually requires four steps but may require more if a separate model is used to determine the

AD-A170 641 MILITARY HYDROLOGY; REPORT 13: COMPARATIVE EVALUATION OF DAM-BREACH FLOOD.. (U) ARMY ENGINEER WATERWAYS EXPERIMENT STATION VICKSBURG MS ENVIR.. R A WURBS

2/2

UNCLASSIFIED JUN 86 WES/MP/EL/79-6 F/G 13/2 NL

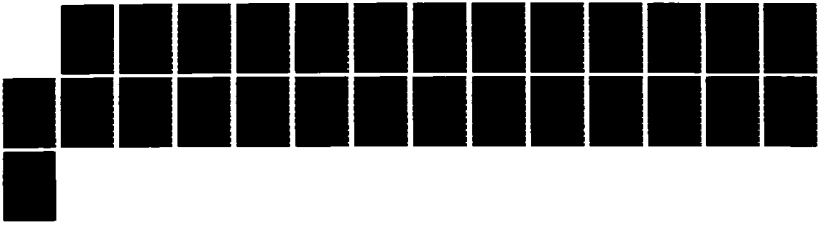

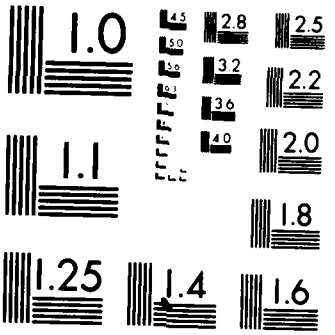

initial conditions. The MOC-LIF models require the user to perform several lengthy tasks when transferring the necessary information during the coupling step. The MOC model requires unusual data that are not needed in the other models. The printout from all the models is fairly easy to read.

186. The USTFLO and LIF models are not programmed to simulate supercritical flow. As programmed, the MOC model is unable to represent complex channel geometry, such as irregular shapes, variable roughness with depth, or overbank storage.

187. In terms of computer costs, the MP model was the least expensive. Compared to the MP model, the DAMBRK and USTFLO models seemed to be about 5 times more expensive and the MOC-LIF about 50 times more expensive. The MOC-LIF model has the potential of being extremely expensive.

188. A primary objective of the investigation was to identify the dam-break flood wave model that would be expected to perform best for most applications. The NWS Dam-Break Flood Forecasting Model (DAMBRK) was selected as the best general-purpose dam-break model. Based on the results of this investigation, the USGS made minor modifications to DAMBRK to emphasize general-purpose dam-break applications and developed a user's manual for their version of the model (Land 1981).

Georgia Safe Dams Task Force

189. A journal paper by George F. McMahon of the USAED, Savannah, describes the work of an interagency task force in developing a model dam-break flood hazard ordinance for counties and municipalities and adapting the ordinance to Gwinnett County, Ga. (McMahon 1981). The task force developed guidelines to establish criteria for reasonably accurate determinations of inundated areas due to dam failures. Efforts were made while developing the guidelines to recommend dam-break flood forecasting methods that are theoretically applicable, are reasonably easy to apply to large numbers of dams, and will withstand legal and technical scrutiny for purposes of amending dam-break flood hazard zones determined by the State.

190. In order to select a model for general application, the following four alternative models were considered in detail: HEC-1, DAMBRK, USTFLO, and MOC-LIF. These four models were considered to be well documented and tested. The many other models for unsteady flow simulation were believed to offer no significant advantage over these four, are generally proprietary, and are neither documented nor readily available. (Note that these are the same

models evaluated by Land (1980a), except HEC-1 is included instead of the USGS modified Puls model.) The kinematic wave option in HEC-1 was used for the downstream routing.

191. McMahon (1981) outlines the use of each of the four models and presents the following summary remarks.

a. HEC-1 is well documented, easily applied, and incorporates variation in breach geometry and time rate of breach formation. It is presently limited to single-dam applications with dry downstream channels.

b. DAMBRK is designed specifically for dam-break floods and is easily applied and extremely versatile. It handles variable breach and time rate of breach formation, using storage or dynamic routing in the reservoir. Cross sections may be irregularly spaced. Multiple domino-type dam failures can be handled. It will route supercritical or subcritical flow.

c. USTFLO was designed for river routing, and usage for dam-break floods is difficult. It requires relatively small time steps and fixed distance steps.

d. MOC-LIF is not widely used. The dam is treated as an internal node. A single bore is propagated. Only subcritical flow can be handled. Analysis is limited to single dams. Trapezoidal cross sections, evenly spaced distance steps, and small time steps are required. Computational cost is relatively expensive.

192. The four models were compared by use of a weighted decision matrix. Criteria for acceptance were established and assigned weighting factors that reflect the opinions of the investigator developed during the study. Each model was assigned a number between 1 and 10 for each acceptance criterion, with 10 signifying "best." The selection matrix is reproduced below.

Criteria (Weighting Factor)	Model			
	HEC-1	DAMBRK	USTFLO	MOC-LIF
Theoretical applicability (0.30)	5	8	7	8
Ease of usage, input data requirements (0.25)	9	8	3	5
Total usage cost (0.15)	9	8	6	5
Versatility (0.2)	6	9	6	5
Availability, documentation, and user experience (0.1)	10	9	8	4
Total	7.3	8.3	5.75	5.80

193. Based on the decision matrix, DAMBRK is the best model, followed by HEC-1. DAMBRK was the model recommended and included in the guidelines developed by the task force.

Tennessee Water Resources Research Center

194. An investigation conducted by Bruce A. Tschantz, Professor of Civil Engineering, and Reza M. Mojib, Graduate Research Assistant, University of Tennessee, under the sponsorship of the Office of Water Research and Technology, is documented by the report "Application of and Guidelines for Using Available Dam Break Models" (Tschantz and Mojib 1981). The report states that, based on a literature review and informal survey of model users and potential users, it is evident that few models are ready for immediate general application. The DAMBRK and HEC-1 computer programs and the SCS Simplified Dam Breach Routing Procedure given in SCS TR 66 were chosen for testing and evaluation. The three models were tested by application to a 36-ft-high earthen dam impounding a 1.1-mile-long, 3,900-acre-ft reservoir.

195. For the test dam, DAMBRK was found to produce 1.3 to 8.9 percent lower peak flows than HEC-1, depending on the location along the stream. DAMBRK and HEC-1 produced consistently close times to peak. The maximum flow profiles were similar for all three models, with the greatest variation being between the SCS method and the other two models. DAMBRK required significantly more computer time and manpower than the other two methods.

Illinois State Water Survey

196. Krishan P. Singh and Arni Snorrason of the University of Illinois conducted a study for the Illinois State Water Survey which included a comparison of DAMBRK and HEC-1 (Singh and Snorrason 1982). The study focused on peak discharges and stages occurring at short distances below the breached dam. DAMBRK and HEC-1 were applied to assumed failures of eight selected earthen dams located in Illinois.

197. The report presents results of the various simulations. The following general remarks were made regarding the experience gained in applying DAMBRK and HEC-1. In general, the flood stage profiles predicted by DAMBRK were smoother and more reasonable than those predicted by HEC-1. For channels with relatively steep slopes, results for the various methods were similar, whereas, for channels with mild slopes, HEC-1 often predicted oscillating, erratic flood stages. No problems were posed in obtaining solutions with HEC-1. Nonconvergence problems were experienced in applying DAMBRK. The problems were solved by adjusting the initial flow and the time and distance steps. In one case, Manning's roughness coefficient was adjusted to prevent

flow from changing from subcritical to supercritical as the discharge increased.

Soil Conservation Service

198. Keefer and Peck (1982) document the results of an evaluation of one-dimensional unsteady flow models for use in SCS programs. The study consisted of interviews with researchers in universities, private organizations, and Federal agencies throughout the United States, supplemented by information in research publications. A number of unsteady flow models were investigated. Of the conclusions reached in this study, the following are most pertinent to the present discussion.

a. The National Weather Service DWOPER and DAMBRK models are the most highly developed and widely accepted channel and dam-break routing models currently available.

b. The weighted nonlinear, four-point implicit finite difference solution of the full St. Venant equations is the best available.

Overview Assessment of Modeling Capabilities

199. DAMBRK, FLOW SIM 1, FLOW SIM 2, HEC-1, SMPDBK, TR 66, and the dimensionless graphs are representative of the current state of the art of dam-breach flood forecasting. MILHY is a state-of-the-art model developed specifically for military use in forecasting streamflow conditions resulting from precipitation events. MILHY could be modified to include dam-breach flood forecasting. All of the above models were developed within the last 10 years and are readily available from Federal agencies in the United States. Model development generally tends to be a process of continual evolution. Several of the models have recently undergone significant revisions, and further improvements and modifications are likely. The numerous other dam-breach flood forecasting models reported in the literature are not considered to offer significant advantages over these selected models from the perspective of military application.

200. Military Hydrology Bulletins 9 and 10 provide a step-by-step manual computation method for developing the outflow hydrograph from a dam breach and routing it downstream. The Defense Intelligence Agency outflow hydrograph procedure improved upon the outflow hydrograph portion of the Military Hydrology Bulletins 9 and 10. These dam-breach flood forecasting procedures

were developed during the 1950's and early 1960's and were representative of the state of the art at that time. The computations are rather tedious, involving development of a number of graphs. The outflow hydrograph modeling capability is somewhat limited by the assumption of an instantaneous breach. The Muskingum valley routing method is significantly less accurate than the more recently developed routing models, particularly for a dam-breach flood wave. The old military hydrology procedures have become obsolete with the development of improved methods during the past decade.

201. The selected models were developed to provide improved modeling capabilities necessitated by dam safety programs being conducted by the various water resources development agencies and/or flood warning activities conducted by the National Weather Service. The primary application of dam-breach flood forecasting models in dam safety studies is preparation of flood inundation maps for postulated dam failures. The NWS is responsible for real-time issuance of flood warnings in the event of an actual dam failure. Modeling uncertainties can be handled to some extent in civilian application by assuming conservative or worst-case conditions.

202. Military applications are similar to civilian sector applications but, in many respects, are more demanding. Military applications may require "actual" rather than "conservative" predictions of flooding conditions. Floodplain trafficability for military purposes involves flood durations and velocities under low-flow conditions as well as the peak flow depths, which are of primary concern in preparing floodplain inundation maps in civilian dam safety studies. In certain military applications, modeling expertise, computer resources, and time will be available to perform an analysis at the level of sophistication required to maximize accuracy. In other situations, though, a terrain team will be required to perform an expeditious analysis under adverse working conditions.

203. Dam-breach flood wave modeling capabilities to provide meaningful and useful information for practical military and civilian applications are definitely available. Significant advancements in the state of the art have been achieved during the past 10 years. The various dam-breach flood forecasting models provide a wide range of trade-offs between accuracy and ease of use. However, mathematical models always have accuracy limitations, regardless of the type of model or application. Model users should always be aware of accuracy limitations. The dam-breach flood wave is extremely difficult to

model mathematically. Consequently, achieving a high level of accuracy for all situations is particularly difficult.

204. The case study results presented in Part III show a large variation between computed and measured flood wave characteristics. The accuracies achieved in this study are consistent with those reported by others in the literature. Even with the significantly improved modeling capabilities developed in recent years, dam-breach flood wave modeling is still not highly accurate.

205. Numerous factors determine model accuracy. The significance of each factor depends upon the particular dam and application. For example, the measured high-water elevations for a reach of the Teton Valley just below the canyon mouth varied by 20 ft between the right and left sides of the valley. The flow was clearly not one-dimensional at this location. However, all of the models are based on the assumption of one-dimensional flow. About a third of the volume of water from the Teton was lost before reaching the downstream American Falls Reservoir. Little information is available to predict the loss of flow volume through infiltration and pondage. Irregularity in valley topography is a major complicating factor in modeling which will vary significantly between dams. Some river valleys are relatively uniform while others have abrupt variation in geometry. Likewise, tributaries, levees, bridges, downstream dams, and split channels complicate modeling. Capabilities for handling valley geometry and other complexities vary between the models. Predicting breach characteristics will typically involve a high level of uncertainty. Even with detailed eye-witness accounts of the breaching of Teton Dam, the breach is difficult to model accurately. In the case of both Teton and Laurel Run, the breach did not form instantaneously nor did the breach dimensions vary linearly with time.

206. In general, the accuracy achieved in modeling flows in rivers and reservoirs and in similar types of modeling is highly dependent upon how well the model is calibrated. Parameters are adjusted until the model reproduces results known to be correct from actual observation. However, field measurements of the characteristics of an actual flood wave similar to that being modeled must be available if a flood-routing model is to be calibrated. Since a dam-breach flood will usually be much larger than the flood of record for a river, calibration of a dam-breach flood wave model is difficult. In most applications, the dam-breach flood wave analysis will be performed without parameter calibration.

Breach Simulation and Outflow Hydrograph Computations

207. Breach characteristics, such as size, shape, elevation, and formation as a function of time, are major factors in determining flood wave characteristics. The effect of breach characteristics will be most pronounced near the dam, diminishing as the flood wave propagates downstream.

208. The simplifying assumption of an instantaneous complete removal of the dam severely limits model applicability. The assumption of an instantaneous partial breach is less severe but still a significant limitation. In addition to not necessarily representing actual breach characteristics, an instantaneously peaking outflow hydrograph is very difficult to route downstream using dynamic routing due to computational problems.

209. From a military applications perspective, the breach simulation routine incorporated in DAMBRK, FLOW SIM 1 and 2, and HEC-1, in which breach dimensions grow linearly with time, is probably the most practical general approach. Predicting the response of the dam to an attack or damaging action is essentially accomplished independently of the model. The breach routine provides a flexible framework in which breach characteristics can be provided as input data to the model.

210. FLOW SIM 1 and 2 contain an option for using a sediment transport equation to simulate the erosion of a breach in an earthen embankment. The erosion model for computing the breach outflow hydrograph recently developed by the NWS (Fread 1985) is a separate computer program that can be used in conjunction with DAMBRK or some other model with the capability of routing the outflow hydrograph on downstream. The general approach of using sediment transport algorithms to model the erosion of a breach in an earthen embankment provides a more realistic representation of the erosion process than assuming the breach dimensions grow linearly with time. However, this approach is limited to breaches caused by the erosive action of an overtopping flood or piping in an earthen embankment.

211. The TR 66 relationship between peak breach outflow and reservoir depth was developed from actual dam failure data. Since military applications may involve intentionally caused dam breaches, breaches significantly different from the actual past dam failures used to develop the relationship, the usefulness of TR 66 for military purposes is limited. The TR 66

relationship produced peak outflows significantly different from the other models and the measured data in the case studies.

212. DAMBRK, FLOW SIM 1 and 2, HEC-1, and MILHY use variations of the modified Puls technique for reservoir routing. DAMBRK and FLOW SIM 1 and 2 also have options for using dynamic routing to develop the reservoir outflow hydrograph. Dynamic routing is theoretically more accurate than storage routing for a long, narrow reservoir with a significantly sloping water surface. However, the modified Puls method is also considered to provide a high level of accuracy for reservoir routing. In most applications, dynamic routing is not considered to be particularly advantageous over storage routing for computing a reservoir outflow hydrograph. Dynamic routing is significantly more accurate in developing water-surface profiles through and upstream of a reservoir.

Valley Routing

213. The key difference between the various dam-breach flood forecasting models considered is the procedure used for routing the flood wave through the valley below the dam. The models can be divided into three categories based on valley routing techniques as follows:

a. Dynamic routing models (DAMBRK, FLOW SIM 1 and 2).

b. Generalized dynamic routing relationships (SMPDBK and dimensionless graph procedure).

c. Storage routing models (HEC-1, TR 66, MILHY).

Dynamic routing models are based on a numerical solution of the St. Venant equations. The dynamic routing models are generally the most accurate, but they are also the most difficult of the models to use. The other two categories consist of models which are simpler to use but are also less accurate. The simplified dynamic routing models are based on generalized relationships between selected input parameters and selected routing output quantities which were predeveloped using a dynamic routing model. The third category consists of models which use techniques other than dynamic routing.

Dynamic routing models

214. A dynamic routing model should be used for military or civilian applications whenever obtaining a maximum practical level of accuracy is important and adequate manpower, time, and computer resources are available.

Although dynamic routing is based on simplifying assumptions including one-dimensional flow, it is the most theoretically correct of the state-of-the-art routing techniques. The case study analyses confirmed that the dynamic routing models are the most versatile and accurate of the models tested.

215. DAMBRK, FLOW SIM 1, and FLOW SIM 2 were the three dynamic wave models investigated. FLOW SIM 1 and 2 require the same input data. The numerical solution technique used in the dynamic routing is the only difference between these two models. FLOW SIM 1 employs an explicit solution and FLOW SIM 2 an implicit finite difference solution of the St. Venant equations. DAMBRK employs an implicit four-point finite difference solution of the St. Venant equations similar to that contained in FLOW SIM 2.

216. The dynamic routing models can reflect a significantly broader range of conditions than the other models, including backwater effects and inactive versus active flow areas. The dynamic routing models are generally more accurate than the other models. However, numerical computation problems may require significant modification of input data to obtain solutions. Smoothing the valley geometry and modifying other input data can significantly reduce the accuracy of the results. Computational problems also make the dynamic routing models much more complicated to use than the other models.

217. Results obtained with DAMBRK, FLOW SIM 1, and FLOW SIM 2 were found to be very close in the case studies whenever solutions were obtained with comparable input data. The results were too close to conclude that one of the three models is more or less accurate than the others. FLOW SIM 1 and 2, in particular, yield extremely close results for the same input data, if solutions are obtained. The primary factor in differentiating between the models is how much the input data had to be modified to obtain a solution. Stated another way, model performance is measured in terms of the range of input data values for which a solution is obtained versus a termination of the calculations due to nonconvergence or instability. DAMBRK performed significantly better in the case studies than FLOW SIM 1 and 2 in this regard. FLOW SIM 1 performed better than FLOW SIM 2.

Generalized dynamic routing relationships

218. Significant expertise and time and a mainframe computer are required to use a dynamic wave model. Some military applications require the capability to perform an analysis expeditiously without access to a mainframe computer. Further, personnel performing the analysis may have limited

training and experience in numerical hydraulic modeling. Consequently, simplified routing methods are needed for those situations in which using a dynamic routing model is not practical.

219. SMPDBK and the HEC dimensionless graphs procedure are based on generalized relationships between dimensionless parameters that have been precomputed using dynamic routing models. Relative to dynamic routing models, the simplified dynamic routing procedures are extremely easy to use. The results of the simplified routing models were reasonably close to the dynamic routing models in the case studies.

220. SMPDBK was somewhat more accurate in the case studies than the dimensionless graphs procedure. The dimensionless graphs procedure is carried out with manual computations; with a microcomputer, SMPDBK is quicker to use. The dimensionless graphs procedure is somewhat easier to use than the manual version of SMPDBK.

221. The prismatic channel assumption is a significant limitation of both models, which was particularly evident in the Teton case study. For the general case where not valid, the assumption of an instantaneous complete removal of the dam limits the accuracy of the dimensionless graphs, particularly near the dam.

222. SMPDBK was generally more accurate than HEC-1 and TR 66 in the case studies. SMPDBK is much easier to use than HEC-1 and TR 66.

Storage routing models

223. Computational instability was not a problem with HEC-1 in the case studies. Although warnings that the modified Puls routing may be numerically unstable for certain ranges of outflow were often obtained, the computed hydrographs were generally reasonable. Consequently, HEC-1 was found to be much simpler to use than DAMBRK and FLOW SIM 1 and 2. The peak discharges and times to peak computed with HEC-1 were reasonably close to the measured data and DAMBRK results. However, the peak depths were highly inaccurate. The program option in which the Manning equation and an assumption of uniform flow are used to compute the outflow versus storage functions and the discharge versus stage functions. Although not investigated, the results could be somewhat improved by developing outflow versus storage functions with HEC-2; however, this would more than double the effort required.

224. HEC-1 performed as well or better than SMPDBK in regard to peak discharges and time to peak stage. Also, HEC-1 provides an entire hydrograph

while SMPDBK is limited to peak discharge. However, peak water-surface elevation is the most important model result in most applications, and for the case studies, water-surface elevation profiles computed with HEC-1 are less accurate than those computed with SMPDBK.

225. The HEC-1 computer program used in this study requires a mainframe computer. However, the Hydrologic Engineering Center has recently coded the model for microcomputer use. The HEC-1 program is actually an assemblage of computational packages. The computational options available for dam-breach flood wave modeling are a relatively small portion of the total program.

226. MILHY is very easy to use; another advantage is that it is already being used by Army personnel for precipitation-runoff modeling. With respect to peak discharges, MILHY and HEC-1 were comparable in accuracy in the case studies. MILHY performed significantly better than HEC-1 in computing peak water-surface profiles.

227. The manual TR 66 procedure is time-consuming, due primarily to the requirement for developing stage versus discharge and storage versus discharge relationships for the valley routing. HEC-1 and MILHY are much easier to apply than the manual TR 66 computations. However, TR 66 could be easily programmed for a microcomputer.

228. HEC-1 has a breach routine not presently available in TR 66 and MILHY. However, the channel routing methods can be compared independently of the development of the reservoir outflow hydrograph. The TR 66 attenuation-kinematic and MILHY variable storage coefficient channel routing procedures could be easily combined with a breach simulation and reservoir routing algorithm.

Model Comparison Matrix

229. The model comparison matrix, presented in Tables 19 and 20, provides a means to systematically organize and communicate an essentially subjective evaluation of the various models. The matrix includes scores for each of several criteria. Scores vary from 0 to 10, with 10 indicating the strongest model and 0 the weakest with reference to a particular criterion. Weighting factors are assigned to indicate the relative importance of each criterion. The relative merit of each model is indicated by a weighted average score. The scores and weighting factors are valid only for a specifically

Table 19

Model Comparison Matrix, Scenario 1*

Criteria	Weighting Factor	DAMBRK	FLOW SIM 1	FLOW SIM 2	HEC-1	SMPDBK	GRAPHS	TR66	MILHY
MILHY									
Computer requirements	0.05	0	0	0	5	10	10	10	10
Documentation and maintenance	0.10	10	0	0	10	7	6	7	9
User experience	0.10	10	6	6	10	4	0	5	5
Versatility	0.10	10	10	10	6	4	0	0	5
Ease of use	0.05	2	0	0	8	10	9	4	8
Robustness	0.10	4	2	0	9	9	9	10	9
Theoretical accuracy	0.25	10	10	10	0	5	3	3	3
Observed accuracy	0.25	10	10	10	0	6	4	4	3
Weighted average	1.00	8.5	6.8	6.6	4.2	6.2	4.2	4.7	5.2

* Scenario description: A model is being selected for use in preparing flood inundation maps and other data for hypothetical failures of various major dams to provide a data base for future reference. The modeling will be accomplished in an office with mainframe computer capabilities. Adequate time and manpower resources are available for a fairly in-depth modeling effort.

Table 20

Model Comparison Matrix, Scenario 2*

Criteria	Weighting Factor	DAMBRK	FLOW SIM 1	FLOW SIM 2	HEC-1	SMPDBK	GRAPHS	TR66	MILHY
Computer requirements	0.25	0	0	0	5	10	10	10	10
Documentation and maintenance	0.05	10	0	0	10	7	6	7	9
User experience	0.05	10	6	6	10	4	0	5	5
Versatility	0.05	10	10	10	6	4	0	0	5
Ease of use	0.25	2	0	0	8	10	9	4	8
Robustness	0.05	4	2	0	9	9	9	10	9
Theoretical accuracy	0.15	10	10	10	0	5	3	3	3
Observed accuracy	0.15	10	10	10	0	6	4	4	3
Weighted average	1.00	5.2	3.9	3.8	5.0	7.9	6.6	5.7	6.8

* Scenario description: A model is being selected for use by terrain teams who will need to be able to analyze a postulated dam breach quickly under adverse working conditions.

defined scenario. A scenario encompasses the purpose for performing a dam-breach analysis and the conditions under which the analysis will be performed.

230. Weighted average scores associated with two scenarios are provided in Tables 19 and 20. The first scenario (Table 19) consists of using a dam-breach flood wave model to prepare a set of inundation maps and other data on flood wave characteristics for hypothetical failures of various major dams throughout the world. The information will be kept on file so as to be readily available if needed at some time in the future. The modeling will be performed by trained hydraulic engineers in an office with mainframe computer capabilities. Adequate manpower and time resources are available for a fairly in-depth modeling effort. The second scenario (Table 20) involves selecting a dam-breach flood wave model for use by terrain teams who will need to be able to analyze a postulated dam breach quickly under significant time and data constraints. Access to a mainframe computer is possible, but a microcomputer or manual procedure would be advantageous. The same scores are used for both scenarios, but the criteria weighting factors are varied. The models are discussed below with respect to each criterion.

Computer requirements

231. DAMBRK and FLOW SIM 1 and 2 require a mainframe computer. The three alternative dynamic routing models have comparable memory and processing time requirements. HEC-1 memory requirements are comparable to the dynamic routing models. However, the dynamic routing models require much more computer time than HEC-1. If an adequate mainframe computer is available, none of the models requires excessive or unusual resources. Although not true at the time the case study analyses were performed, DAMBRK and HEC-1 have recently been coded to run on an IBM PC microcomputer with 640K bytes of memory. Microcomputer, calculator, and manual versions of SMPDBK are available. MILHY is also programmed for a microcomputer. Memory requirements are much less for SMPDBK and MILHY than the HEC-1 and DAMBRK microcomputer programs. The dimensionless graphs and TR 66 are manual procedures.

Documentation and maintenance

232. The models continue to be improved and expanded. Model development is a process of evolution in which improved versions of the models are released fairly frequently. All the models are readily available from Federal agencies. DAMBRK has very good documentation and is maintained by both the NWS and HEC. The NWS continues an active interest in improving and refining

the program. HEC-1 has excellent documentation, probably the best of all the models. With the numerous options and broad applicability, detailed user instructions are particularly important for HEC-1. MILHY is maintained by WES as a part of the Military Hydrology Program. The model is documented specifically for military use. The FLOW SIM 1 and 2 user manual is relatively informal and is not documented to the same level of detail as the other models. SMPDBK, TR 66, and the dimensionless graphs are simpler to use and require less documentation than the other models. These simplified models are fairly well documented. The NWS is still actively expanding and refining SMPDBK.

User experience

233. User experience is important for testing, improving, and developing confidence in a model. DAMBRK and HEC-1 are, by far, the most extensively used of the models. FLOW SIM 1 and 2 have been applied in a significant number of dam safety studies in the USAE Division, Southwestern. The SCS is using TR 66 in dam safety studies. SMPDBK is undergoing significant testing by the NWS and others. Little actual use of the HEC dimensionless graphs has been reported. MILHY was not developed for and has not been used for dam-breach flood forecasting. The precipitation-runoff model is presently being integrated into the Army's hydrologic engineering capability.

Versatility

234. A wide range of conditions can be encountered in dam-breach flood forecasting applications. DAMBRK and FLOW SIM 1 and 2 are the most flexible or versatile of the models in regard to simulating various field conditions. Numerous options are available in the programs. However, the versatility of the models is sacrificed significantly when input data have to be altered from the desired values to obtain convergence to a solution. FLOW SIM 1 and 2 are the only models which can directly simulate multiple dam failures with the dams located on different tributaries. HEC-1 is also relatively versatile. SMPDBK, dimensionless graphs, and TR 66 cannot simulate lateral inflows, inactive flow areas, bridges, abrupt contractions, and other conditions that can be modeled with DAMBRK and FLOW SIM 1 and 2. SMPDBK and the dimensionless graphs are particularly limited in regard to modeling complex valley geometry. MILHY is evaluated on the premise that a breach simulation routine could be easily added to the model.

235. The dynamic routing models are the most versatile in regard to providing a broad range of output data. HEC-1 and MILHY provide complete

hydrographs and peak water-surface elevations at selected locations. MILHY also provides water-surface profiles at selected points in time. SMPDBK provides peak discharges and depths, time to peak depth, and the time at which a specified discharge is exceeded at each cross section. The dimensionless graphs provide only peak depth and time to peak. TR 66 provides only peak discharges and depths.

Ease of use

236. SMPDBK and the dimensionless graphs are the simplest and quickest models to use. The SMPDBK microcomputer program is more convenient to use than the manual dimensionless graphs procedure, assuming an appropriate microcomputer is available. The dimensionless graphs procedure is easier to use than the manual version of SMPDBK. MILHY is also very easy to use and has the additional advantage of already being used for similar military applications. TR 66 requires storage versus outflow and stage versus discharge relationships, which are very time-consuming to develop. The TR 66 procedure is significantly more difficult than SMPDBK, dimensionless graphs, and HEC-1. HEC-1 requires about the same effort to develop the input data as DAMBRK and FLOW SIM 1 and 2. However, in the case studies, HEC-1 required only a small fraction of the time and effort spent on DAMBRK and FLOW SIM 1 and 2 because HEC-1 did not have the computational problems associated with the dynamic routing models. DAMBRK and FLOW SIM 1 and 2 were much more difficult to use than the other models due primarily to difficulties in achieving convergence to a solution. DAMBRK performed better than FLOW SIM 1 and 2 in this regard. FLOW SIM 1 performed better than FLOW SIM 2. DAMBRK also has a little more convenient input and output data structure than FLOW SIM 1 and 2.

237. Collecting and organizing the input data is, of course, an extremely important aspect of dam-breach flood wave modeling. However, input data requirements are not considered a major factor in differentiating between models. Although additional input data are required to fully utilize the capabilities of the more sophisticated models, these models can be used with less input data if a corresponding decrease in accuracy is acceptable. All the models use essentially the same types of valley geometry data. SMPDBK and the dimensionless graphs procedure require less data than the other models to describe the reservoir. SMPDBK automatically provides default values if certain items of input data are not provided.

Robustness

238. This criterion refers to the likelihood of obtaining a solution for a reasonable range of values for the input parameters. HEC-1, SMPDBK, TR 66, the dimensionless graphs procedure, and MILHY can be expected to yield a solution for a given set of input data. Highly nonprismatic channel geometry may render the SMPDBK and dimensionless graphs solutions extremely questionable. As discussed above in regard to the ease-of-use criterion, computational instability and nonconvergence of the iterative solution algorithm can prevent obtaining a solution with the dynamic wave models. DAMBRK performed better than FLOW SIM 1 and 2 in the case studies in regard to obtaining solutions. FLOW SIM 1 performed better than FLOW SIM 2.

Theoretical accuracy

239. All of the models are based on simplifying assumptions such as one-dimensional flow. Dynamic routing has fewer assumptions than the other models and essentially no significant assumptions which are not also applicable to the other models. The dynamic routing models are theoretically the most accurate of the alternative models. Since SMPDBK and the dimensionless graphs procedure are based on functions precomputed using dynamic routing, these models should be fairly accurate whenever the conditions for which the functions were developed are met. The most important assumption is that of a prismatic channel. HEC-1 and TR 66 use simplified routing methods that should be significantly less accurate than dynamic routing, particularly for a dam-breach flood wave. The attenuation-kinematic routing used in TR 66 and the variable storage coefficient routing used in MILHY theoretically should be improvements over the HEC-1 modified Puls routing.

Observed accuracy

240. The results of the case study analyses support the conclusion that dynamic routing is the most accurate. All three dynamic routing models performed at a comparable level of accuracy for those sets of input data for which a solution was obtained. The degree to which input data has to be altered to overcome computational instability and convergence problems is a key factor in determining the accuracy of the final solution. However, for purposes of the comparison matrix, this aspect of the modeling is reflected in the scores shown for the ease-of-use and robustness criteria. The scores for the observed accuracy criterion assume that a set of input data is used which yields a solution with all the models. HEC-1 performed reasonably well in

computing discharges, but peak water-surface profiles were significantly less accurate than the other models. The HEC-1 option of computing flow depths assuming uniform flow was used. The results possibly could have been improved by using a gradually varied water-surface profile model in combination with HEC-1, but the required effort would have significantly increased as well. SMPDBK had trouble with peak discharges but performed well in regard to computing peak water-surface profiles. The scores in the comparison matrix are based on the assumption that peak water-surface elevations are usually the most important of the flow characteristics computed. MILHY tended to yield discharge and water-surface profiles that were significantly low.

Weighted average scores

241. Tables 19 and 20 show the weighted average scores for each of the models for the two scenarios. The numbers are not intended to imply a quantitative measurement of model performance. Rather, the scoring system is simply a way to help organize and communicate a largely subjective model comparison involving many complex considerations. DAMBRK is the preferred model when adequate manpower, time, and computer resources are available. SMPDBK is the preferred method for obtaining a solution quickly under adverse working conditions.

Model Selection

242. Selection of a single dam-breach flood wave model for all military applications would be desirable. However, the broad range of applications and model characteristics necessitates adoption of at least two models. A dynamic routing model should be used whenever sufficient manpower, time, and computer resources are available. A simpler model is also needed to provide the capability to obtain solutions quickly with limited resources.

243. Based on the study reported herein, DAMBRK and SMPDBK are concluded to be the models that should be adopted for military use.

244. A breach simulation routine could also be added to MILHY. MILHY is already being used for forecasting streamflow resulting from precipitation. MILHY could provide a useful supplement to DAMBRK and SMPDBK. A storage routing model could serve as an easy-to-use check on the degree of confidence to be placed in the results of SMPDBK, particularly in applications involving highly nonprismatic valley geometry.

PART V: CONCLUSIONS AND RECOMMENDATIONS

Conclusions

245. The purpose of this comparative evaluation of models is to provide a sound basis for selecting and adapting one or more models for military use and otherwise improving the dam-breach flood forecasting capabilities of the Armed Forces. Recent dam safety programs conducted by Federal and State water resources development agencies and the flash flood warning program of the National Weather Service have provided the impetus for civilian sector development of models; these models have greatly expanded dam-breach flood forecasting capabilities during the past decade. Based on the state-of-the-art review documented by Military Hydrology Report 9 (Wurbs 1985a), the following dam-breach flood wave models were selected for detailed evaluation and comparison: NWS Dam-Break Flood Forecasting Model (DAMBRK), SWD Flow Simulation Models (FLOW SIM 1 and 2), HEC Flood Hydrograph Package (HEC-1), SCS Simplified Dam-Breach Routing Procedure (TR 66), NWS Simplified Dam-Break Model (SMPDBK), and the HEC dimensionless graphs procedure. These leading models are representative of the current state of the art of dam-breach flood wave modeling. A set of dam-breach flood forecasting methods developed for military use during the 1950's and early 1960's were also reviewed. The recently developed Military Hydrology (MILHY) model was also included in the evaluation. Although MILHY is a runfall-rainfall model with no special features for dam-breach modeling, a breach simulation routine could be added.

246. The models were evaluated on the basis of: (a) underlying concepts and theory incorporated into the models and analysis capabilities provided by the models, (b) findings reported in the published and unpublished literature with respect to application, testing, evaluation, and comparison of various models, and (c) results obtained and experience gained in the case study analyses performed as a part of the investigation. Key conclusions derived from the study are as follows.

247. Significant advances in the state of the art of dam-breach flood wave modeling have occurred during the last 10 years and are readily available for incorporation into the Military Hydrology Program.

248. Although modeling capabilities are available to provide meaningful and useful information for practical military application, dam-breach flood

wave modeling is not highly accurate. Model users should be aware of limitations in accuracy.

249. Although the dynamic wave models are significantly more accurate and versatile than the other models, numerical computation problems are a major concern in their application. Training and experience in numerical computer modeling are needed to use the dynamic routing models.

250. A dynamic wave model should be used when accuracy is very important and adequate manpower, time, and computer resources are available. A simpler model is needed for obtaining solutions expeditiously with limited resources.

251. The NWS DAMBRK and SMPDBK are the optimal models for adoption by the Military Hydrology Program.

Additional Research and Development Needs

252. Although dam-breach flood forecasting capabilities have been greatly expanded during the past decade, significant potential exists for continued improvements. Several general areas of research and development needs of dam-breach flood forecasting that are particularly pertinent to military applications are cited below.

253. Dam-breach flood forecasting actually involves four major areas of concern: (a) predicting the occurrence of a condition or event (such as seepage, an overtopping flood, an earthquake, or various acts of war) that could cause a dam to fail, (b) predicting the response of a dam to a damaging condition or event (analyzing the mechanics of breaching), (c) predicting the response of the water to a dam breach (analyzing the flood wave), and (d) predicting the impact of the flood wave on facilities and activities located in the downstream floodplain. The scope of this investigation and the research and development needs cited below are limited to the third concern, flood wave analysis. However, the other three major areas of concern have associated research and development needs. In addition, the interfacing of the major areas of concern involves research and development needs.

254. Breach simulation is the interface between areas of concern (b) and (c) above. Predicting the response of a dam to an explosion or other damaging event is well outside the scope of flood wave analysis. However, since the reservoir outflow hydrograph is governed largely by breach

characteristics, breach simulation is necessarily an integral part of dam-breach flood wave analysis. As previously discussed, breach simulation is highly uncertain. Modeling the erosion rate of a breach in an earthen dam has already received some attention and has potential for further development. Other improvements in breach simulation methods incorporated in the flood wave models will depend largely on developing a better understanding of breach mechanics from a structural and geotechnical engineering perspective.

255. Areas of concern (c) and (d) above are also closely interrelated. One of the primary reasons for military interest in induced flood waves is the potential for rapid barrier creation. Predicting the extent and duration of the military barrier created and the damage inflicted on downstream facilities is a major research area. Methods are needed to predict the trafficability of soil following inundation by a dam-breach flood. Additional research is also required in predicting the impact of the flood wave on downstream structures. Capabilities are needed to predict whether a bridge will fail and how other downstream facilities will be affected by the flood wave.

256. The major difficulties encountered in the case study analyses were in overcoming dynamic routing computational problems associated with numerical instabilities and in the iterative solution algorithm terminating without converging to a solution. Nonlinear instabilities in dynamic routing are caused by rapid variations in cross-sectional geometry with elevation and distance along the channel. Development of more robust computational algorithms and improved manual and/or automatic valley smoothing methods are key research needs.

257. Another related major research need illustrated by the case studies is the development of dynamic routing capabilities for simulating supercritical as well as subcritical flow under all situations likely to be encountered in practical applications. DAMBRK is presently being modified by the NWS to handle changes between supercritical and subcritical flows, with both time and distance.

258. The dam-breach flood wave represents a particularly pertinent application for two-dimensional unsteady flow modeling. The state-of-the-art models addressed by this investigation are all one-dimensional. Studies are needed to evaluate the significance of the one-dimensional assumption in dam-breach flood forecasting.

259. Another broad group of research and development needs involves

expanding the capabilities of existing models to handle flow complexities such as: volume losses due to infiltration and pondage; multiple breaches of dams on different tributaries; dendritic and bifurcated stream networks; meandering streams with large differences between main channel and floodplain flow characteristics; downstream dams, bridges, and levees, which may or may not fail; and natural obstructions to flow such as ice or debris accumulations. Capabilities for handling these complications are incorporated to various extents in the available models.

260. Dam-breach flood forecasting is presently based on the assumption of a fixed streambed without erosion or sedimentation. Channel geometry and roughness can be drastically changed by a dam-breach flood wave. The impacts of erosion and sedimentation on the flood wave, and vice versa, need to be assessed. Erosion and sedimentation simulation is a major feature to be added to dam-breach flood forecasting models.

261. The dam breach work now needs to be extended to include predicting the characteristics of induced flood waves caused by repeated opening and closing of spillway and outlet works gates.

262. The capabilities provided by the selected models, DAMBRK and SMPDBK, for military applications should be further evaluated through case studies of militarily significant dams located outside the United States. The studies should focus on defining and meeting military requirements for dam-breach flood forecasting information under realistic conditions representative of military applications.

REFERENCES

Abbott, M. B. 1979. Computational Hydraulics, Elements of the Theory of Free Surface Flows, Pitman Publishers, London, England.

Bodine, B. R. Undated. "User's Manual for FLOW SIM 1, Numerical Method for Simulating Unsteady and Spatially Varied Flow in Rivers and Dam Failures," US Army Engineer Division, Southwestern, Dallas, Tex.

Bureau of Reclamation, Division of Dam Safety, US Department of the Interior. 1983 (Oct). "Dam Safety Hazard Classification Guidelines."

Buttery, David N. 1984. "A Military Applications Comparative Analysis of Dam-Break Flood Routing Techniques," Master of Engineering Technical Report, Civil Engineering Department, Texas A&M University, College Station, Tex.

Chen, Cheng-Lung, and Armbruster, Jeffrey T. 1980 (May). "Dam-Break Wave Model: Formulation and Verification," Journal of the Hydraulics Division, American Society of Civil Engineers, Vol 106, No. HY5, pp 747-767.

Chow, Ven Te. 1959. Open-Channel Hydraulics, McGraw-Hill, New York.

Comer, George H., Theurer, Fred D., and Richardson, Harvey H. 1982. "The Modified Attenuation-Kinematic (Att-Kin) Routing Model," Rainfall-Runoff Relationship, V. P. Singh, ed., Water Resources Publications, Littleton, Colo.

Cunge, J. A. 1969. "On the Subject of a Flood Propagation Computation Method (Muskingum Method)," Journal of Hydraulic Research, Vol 7, No. 2, pp 205-230.

Cunge, J. A., Holley, F. M., and Verway, A. 1980. Practical Aspects of Computational River Hydraulics, Pitman Publishers, London, England.

Defense Intelligence Agency. 1963 (Jun). "Computation of Outflow from Breached Dams," Washington, DC.

Fread, Danny L. 1971. "Discussion of Implicit Flood Routing in Natural Channels by Amein and Fang," Journal of the Hydraulics Division, American Society of Civil Engineers, Vol 97, No. HY7, pp 1156-1159.

_____. 1974. "Numerical Properties of Implicit Four-Point Finite Difference Equations of Unsteady Flow," National Oceanic and Atmospheric Administration Technical Memorandum NWS HYDRO-18, Office of Hydrology, Washington, DC.

_____. 1977. "The Development and Testing of a Dam-Break Flood Forecasting Model," Proceedings of Dam-Break Flood Routing Model Workshop Held in Bethesda, Maryland, on October 18-20, 1977.

_____. 1978 (Apr). "National Weather Service Operational Dynamic Wave Model," Hydrologic Research Laboratory, National Weather Service, Silver Spring, Md. (reprinted June 1982).

_____. 1982. "Flood Routing: A Synopsis of Past, Present, and Future Capability," Rainfall-Runoff Relationship, V. P. Singh, ed., Water Resources Publications, Littleton, Colo.

_____. 1983 (Jul). "DAMBRK: The NWS Dam-Break Flood Forecasting Model," Office of Hydrology, National Weather Service, Silver Spring, Md.

Fread, Danny L. 1984 (Jul). "DAMBRK: The NWS Dam-Break Flood Forecasting Model," Office of Hydrology, National Weather Service, Silver Spring, Md.

_____. 1985 (Jan). "BREACH: An Erosion Model for Earthen Dam Failures," Office of Hydrology, National Weather Service, Silver Spring, Md.

Hydrologic Engineering Center. 1981 (Sep). "HEC-1 Flood Hydrograph Package, User's Manual," Davis, Calif.

_____. 1982 (Sep). "HEC-2 Water Surface Profiles, User's Manual," Davis, Calif.

Keefer, T. N., and Peck, E. L. 1982 (Feb). "Evaluation and Classification of One-Dimensional Unsteady Flow Models for Use in SCS Programs," Final Report by Sutron Corp. for US Department of Agriculture, SCS-NES-Hydrology Unit, Lanham, Md.

Land, Larry F. 1980a. "Evaluation of Selected Dam-Break Flood-Wave Models by Using Field Data," US Geological Survey, Washington, DC (NTIS, PB 81-115776).

_____. 1980b. "Mathematical Simulation of the Toccoa Falls, Georgia, Dam-Break Flood," Water Resources Bulletin, American Water Resources Association, Vol 16, No. 6, pp 1041-1048.

_____. 1981. "User's Guide for a General Purpose Dam-Break Flood Simulation Model (K-634)," US Geological Survey Water Resources Investigations 80-116, Gulf Coast Hydroscience Center, NSTL Station, Bay St. Louis, Miss.

Liggett, James A., and Cunge, Jean A. 1975. "Numerical Methods of Solution of the Unsteady Flow Equations," Chap. 4, Unsteady Flow in Open Channels, K. Mahmood and V. Yevjevich, eds., Water Resources Publications, Littleton, Colo.

McMahon, George F. 1981. "Developing Dam-Break Flood Zone Ordinance," Journal of the Water Resources Planning and Management Division, American Society of Civil Engineers, Vol 107, No. WR2, pp 461-476.

Miller, William A., Jr. 1971. "Numerical Solution of the Equations for Steady Open-Channel Flow," Ph. D. Thesis, Georgia Institute of Technology, Atlanta, Ga.

Preissmann, A. 1961. "Propagation of Translatory Waves in Channels and Rivers," Proceedings, First Congress of the French Association for Computation, Grenoble, France, pp 433-442.

Price, Roland K. 1974. "Comparison of Four Numerical Methods for Flood Routing," Journal of the Hydraulics Division, American Society of Civil Engineers, Vol 100, No. HY7, pp 879-899.

Ray, H. A., and Kjelstrom, L. C. 1978. "The Flood in Southeastern Idaho from the Teton Dam Failure of June 5, 1976," US Geological Survey, Open File Report 77-765, Washington, DC.

Sakkas, J. G. 1980. "Dimensionless Graphs of Floods from Ruptured Dams," Research Note No. 8, US Army Engineer Hydrologic Engineering Center, Davis, Calif.

Singh, Krishan P., and Snorrason, Arni. 1982. "Sensitivity of Outflow Peaks and Flood Stages to the Selection of Dam Breach Parameters and Simulation Models," SWS Contract Report 289, State Water Survey Division, University of Illinois, Urbana, Ill.

Soil Conservation Service, US Department of Agriculture. 1979 (revised December 1981). "Simplified Dam-Breach Routing Procedure," Technical Release No. 66, Engineering Division, Glenn Dale, Md.

Tschantz, Bruce A., and Mojib, Reza M. 1981. "Application of and Guidelines for Using Available Dam Break Models," Tennessee Water Resources Center Report 83 (NTIS, PB 82-224577).

US Army Engineer District, Washington. 1957a (Jun). "Flow Through a Breached Dam," Military Hydrology Bulletin 9, Washington, DC.

_____. 1957b (Jun). "Artificial Flood Waves," Military Hydrology Bulletin 10, Washington, DC.

US Army Engineer Waterways Experiment Station. 1985. "MILHY User's Manual" (draft), Vicksburg, Miss.

Wetmore, Jonathan N., and Fread, Danny L. 1981. "The NWS Simplified Dam-Breach Flood Forecasting Model," Proceedings of the 5th Canadian Hydrotechnical Conference, 26-27 May 1981, Fredericton, New Brunswick, Canada.

_____. 1983. "The NWS Simplified Dam-Break Model Executive Brief," Hydrologic Research Laboratory, National Weather Service, Silver Spring, Md., paper distributed at the Dam-Break Modeling Symposium sponsored by the NWS Tulsa River Forecast Center, 27-30 June 1983.

Williams, Jimmy R. 1969. "Flood Routing with Variable Travel Time or Variable Storage Coefficients," Transactions of the American Society of Agricultural Engineers, Vol 12, No. 1, pp 100-103.

Wurbs, Ralph A. 1985a. "Military Hydrology; Report 9: State-of-the-Art Review and Annotated Bibliography of Dam-Breach Flood Forecasting," Miscellaneous Paper EL-79-6, US Army Engineer Waterways Experiment Station, Vicksburg, Miss.

_____. 1985b. "Military Hydrology; Report 12: Case Study Evaluation of Alternative Dam-Breach Flood Wave Models," Miscellareous Paper EL-79-6, US Army Engineer Waterways Experiment Station, Vicksburg, Miss.

Yevjevich, Y. 1975. "Sudden Water Releases," Chap. 15, Unsteady Flow in Open Channels, K. Mahmood and V. Yevjevich, eds., Water Resources Publications, Littleton, Colo.

END

DTIC

9-86